UNIVERSITY OF BIRMINGHAM

Simple Metal Halide-Organobase Lewis Pair Catalysts for the Ring-Opening Copolymerisation of Cyclic Anhydrides and Epoxides

by

Edward James Maynard

A thesis submitted to the University of Birmingham for the degree of DOCTOR OF PHILOSOPHY

School of Chemistry
College of Engineering and Physical Sciences
University of Birmingham
September 2023

Abstract

Polyesters offer promise as a sustainable replacement for single-use petrochemical plastics due to their ability to synthesised from bio-sourced building blocks and ease of degradation. Yet, challenges exist in energy-efficient, low-cost synthesis of polyesters with versatile functionalities and thermomechanical properties. The ring-opening copolymerisation (ROCOP) of anhydrides and epoxides provides a route from biomass to a range of structurally-diverse polyesters with effective control of molecular weights and polymer microstructures. Previous research has mainly employed complex and expensive catalysts for precise copolymerisation control. However, recent interest has shifted towards affordable, simple catalysts to reduce costs and energy consumption. The scope for these simple catalysts is still limited and a challenge remains to combine their simplicity with competitively efficient and controlled copolymerisation.

This thesis explored using commercially-available simple metal halide salts and organic Lewis bases as simple Lewis pair catalysts for the ROCOP of anhydrides and epoxides. Simple metal halide salts, although employed in other polymerisation systems, represent a novel approach for the ROCOP of anhydrides and epoxides and offer potential for a highly tuneable range of catalytic activities by simply replacing the metal centre or halide ligand. Efficient copolymerisation (93% monomer conversion in 5 h) of PA and CHO was achieved using a $ZnCl_2$/DMAP Lewis pair and an alcohol chain transfer agent in toluene resulting in highly alternating (95% ester linkages) polyesters with some end-group control. Screening metal halides and organobases for higher catalytic activities revealed three Lewis pairs (YCl_3/PPNCl, $PdCl_2$/PPNCl,

$MgCl_2$/PPNCl) which when employed without a solvent afforded highly alternating (≤94% ester linkages) polyesters at faster rates (99% monomer conversion in 10 min) than PPNCl employed alone. The most active and selective pair, $PdCl_2$/PPNCl, successfully copolymerised a range of anhydrides and epoxides to afford 12 varied polyesters (M_n ≤ 6029 $g \cdot mol^{-1}$). While precise polymerisation control could not be demonstrated due to metal halide solubility issues, the metal halide-based Lewis pair system was found to be a highly-tuneable, efficient and versatile catalyst system.

Acknowledgements

I would like to thank Professor Andrew Dove for providing me with the opportunity to conduct a PhD in the research group and the mentorship, guidance and care that has fuelled my efforts. I would especially like to thank him for giving me the confidence to pursue my research through particularly tough moments. I would also like to thank Professor Rachel O'Reilly for supporting my research efforts as an ever-friendly supporting supervisor.

I am indebted to the University of Birmingham for funding my studies and to the School of Chemistry for providing the facilities and support needed to undertake them.

I would like to extend my thanks to all the Dove and O'Reilly Group members. I have never encountered such a friendly and encouraging group before, and I will miss being surrounded by such talented individuals. A particular mention must go to Dr. Kayla Delle Chiaie and Dr. Natalia Reis, who have given me indispensable support in the labs and in report writing. Both have been immense inspirations to me. I am also indebted to the three Dove Group Leaders during my time in the group: Dr. Chiara Arno, Dr. Josh Worch, Dr. Arianna Brandolese, for their wisdom, time, and welcoming attitudes. Thanks to Matt Price who I met on my very first day and instantly became a lifelong friend, for his wonderful energy and sense of humour.

I am grateful to my family for their continued support, and their sacrifice to give me many opportunities to expand my horizons.

Finally, I want to thank Zara, who I was extremely lucky to meet during my studies, for her unwavering support, kindness, and patience.

Table of Contents

Table of Figures

Table of Tables

Table of Schemes

Abbreviations

Å – Angstrom

AGE – Allyl glycidyl ether

AMC – Alkali metal carboxylate

BDI – β-diiminate

BO – Butylene oxide

CA – Carbic anhydride

CHO – Cyclohexene oxide

CTA – Chain transfer agent

CTPB – Cyclic trimer phosphazene base

°C – Degrees Celsius

DABCO – 1,4-Diazabicyclo[2.2.2]octane

DBU – 1,8-Diazabicyclo(5.4.0)undec-7-ene

DCM – Dichloromethane

DCTB – *Trans*-2-[3-(4-*tert*-butylphenyl)-2- methyl-2-propenylidene] malononitrile

DFT – Density functional theory

DGA – Diglycolic anhydride

DHB – 2,5-dihydroxybenzoic acid

DMAP – 4-Dimethylaminopyridine

DPP – Diphenyl phosphate

$Đ_M$ – Dispersity

ECH – Epichlorohydrin

g – Grams

h – Hours

HOMO – Highest occupied molecular orbital

HPLC – High performance liquid chromatography

IA – Itaconic anhydride

k – Rate constant

K – Kelvin

LO – Limonene oxide

LPP – Lewis pair polymerisation

MA – Maleic anhydride

min - Minutes

L – Litres

LUMO – Lowest unoccupied molecular orbital

[M] – Concentration of monomer

MALDI-ToF MS – Matrix-assisted laser desorption/ionisation time of flight mass spectrometry

4-MBA – 4-Methoxybenzyl alcohol

M_n – Number average molecular weight

mol – Moles

m – Metre

M_w – Weight average molecular weight

MSA – Methanesulfonic acid

MTBD – 7- Methyl-1,5,7-triazabicyclo[4.4.0]dec-5-ene

NBGE – *n*-Butyl glycidyl ether

N-MeIm – *N*-methylimidazole

NMR – Nuclear magnetic resonance

PA – Phthalic anhydride

PHA – Polyhydroxyalkanoate

PLA – Poly(lactic acid)

PO – Propylene oxide

ppm – Parts per million

PPN – Bis(triphenylphosphine)iminium

ROCOP – Ring-opening copolymerisation

ROP – Ring-opening polymerisation

SA – Succinic anhydride

SEC – Size exclusion chromatography

SO – Styrene oxide

t – Time

T – Temperature

TBD – Triazabicyclo[4.4.0]dec-5-ene

T_g – Glass transition temperature

THF – Tetrahydrofuran

TMPP – Tris(2,4,6-trimethoxyphenyl)phosphine

TOF – Turnover frequency

TON – Turnover number

TTP – Tetraphenylporphyrin

VCHO – Vinyl-cyclohexene oxide

Declaration of Authorship

This thesis is submitted to the University of Birmingham in support of my application for a Doctor of Philosophy award. The work presented here was carried out by myself between October 2019 and April 2023 and the thesis has been composed by myself subsequently. None of the material here has been submitted for any previous application for any other degree or at any other institution.

Chapter 1 – Introduction

1.1 Sustainable polymers

How we produce, consume and dispose of plastics has become a pressing issue of our time. Plastics dominate modern materials due to their diverse range of material applications, thanks to their easy-to-manipulate properties, and demand for them continues to increase.[1] However, currently the vast majority of plastics are derived from petrochemicals and disposed of into the environment after use.[2] This system presents issues such as the limited nature of fossil-fuel reserves and the environmental destruction of plastic waste.[3-5] While no simple solution exists to this problem, one contribution to tackle it has been the development of sustainable plastics. Ideally, sustainable plastics are those which are renewably sourced from biomass, synthesised *via* green chemistry methods and are able to degrade in the environment to environmentally benign products and/or can be recycled back into useful plastic materials.[6, 7]

Despite research interest over the last twenty years, today the commercial production of bio-derived plastics (single-use and degradable) remains limited relative to their petrochemical-based counterparts – the global capacity for their plastic production in 2022 stood at only 2.3 million tonnes (representing 1% that of fossil-fuel derived plastics).[8] One of the main factors recognised as impeding their widespread use is the high cost of production when compared to petrochemical analogues.[9] Thus the task for research going forwards is to develop sustainable plastics which show competitive properties and competitive economic viability with current commercial plastics. This includes research into effective yet low-cost synthetic routes with simple, green synthetic pathways that afford polymers with sought after properties.

1.2 Polyesters

1.2.1 A potential sustainable plastic

The polyester class of plastics lends itself well to the development of sustainable plastics. They can easily be modified to produce a diverse range of material properties, undergo facile degradation due to the presence of ester linkages in their backbone which can be broken down through mechanical or chemical recycling, biodegradation and composting, and they can be derived from renewable sources.[10-13] Additionally, a substantial amount of research already exists in their synthesis and application, including established commercial production.[8] Further optimisation therefore has a basis in existing research and production infrastructure providing one of the most viable and rapid routes to mass-produced, commercial, sustainable plastics.

In 2022, the sustainable plastic with the highest global production capacity was reported to be the aliphatic polyester poly(lactic acid) (PLA).[8] PLA is bio-based and biodegradable and is used as a sustainable alternative material for packaging, fibres and biomedical applications.[14-17] Polyhydroxyalkanoates (PHAs) are another class of polyester which is produced as a commercial, sustainable plastic.[8] However, PLA and PHAs together provide only a narrow range of applications due to their specific thermal and mechanical properties such as PLA's brittleness.[18] They also lack reactive functionalities accessible for further modifications to enhance their properties.[19] To incorporate a wider range of thermal and mechanical properties and reactive functional groups, the challenge of synthesising such polyesters in a controlled and effective manner must be overcome.

1.2.2 Synthesis of polyesters

Three main synthetic routes exist for the preparation of polyesters: the condensation polymerisation of a diol with a carboxylic acid or of hydroxy-acid, the ring-opening polymerisation (ROP) of cyclic esters and the ring-opening copolymerisation (ROCOP) of cyclic anhydrides and epoxides.[20-22] The first of these is a step-growth method and results in broad polymer dispersities, often requiring precise reagent stoichiometry, and the need to remove by-products to drive the polymerisation through energy intensive methods. The latter two routes are chain-growth methods that give no small molecule by-products and have the potential to be controlled.

ROP involves the polymerisation of cyclic forms of ester monomers to afford the resultant linear polyester and has been extensively investigated and so is effective at giving controlled polymerisations.[23] However, it is limited by the availability of commercially-viable cyclic ester monomers.[18, 20] For a ROP of a cyclic ester to be successful, the cyclic ester must possess the required ring-strain to thermodynamically drive the polymerisation.[24] The introduction of reactive functionalities or aromatic substituents onto the rings is generally found to decrease this. This limits the properties of the afforded polyesters and hence their applications are generally limited to low glass transition temperature elastomers or brittle plastics.[25, 26]

1.3 Ring-opening copolymerisation

1.3.1 Definition

The ROCOP of cyclic anhydrides and epoxides involves the alternating copolymerisation of monomers to form polyesters.[18, 27] An advantage that ROCOP has over ROP is its ease in accommodating a wide-range of functionalised monomers to afford functionalised polyesters. This is because ROCOP is not thermodynamically

constrained in the same manner as ROP, having two distinct monomer sets that allow for easy manipulation of the resultant polymer's properties by substitution of just one of the monomers. While functionalised lactones and cyclic carbonates used in ROP need to be synthesised, which can require multiple, challenging steps that decrease overall yield, epoxides and cyclic anhydrides are often commercially-available without further modification needed. Additionally, in the pursuit of synthesising polyesters from biomass feedstock, it has been found that diverse structures and functionalities (such as aromatic and unsaturated groups) are readily-available in epoxide and anhydride monomers sourced from biomass, which would have to be accessed through laborious multi-step process from petrochemical sources.[18, 27] Thus, a wide range of polymer backbone structures and side-chain functionalities can be accessed allowing for widely tuneable polymer properties that can compete with conventional fossil-fuel derived plastics.

1.3.2 General mechanism

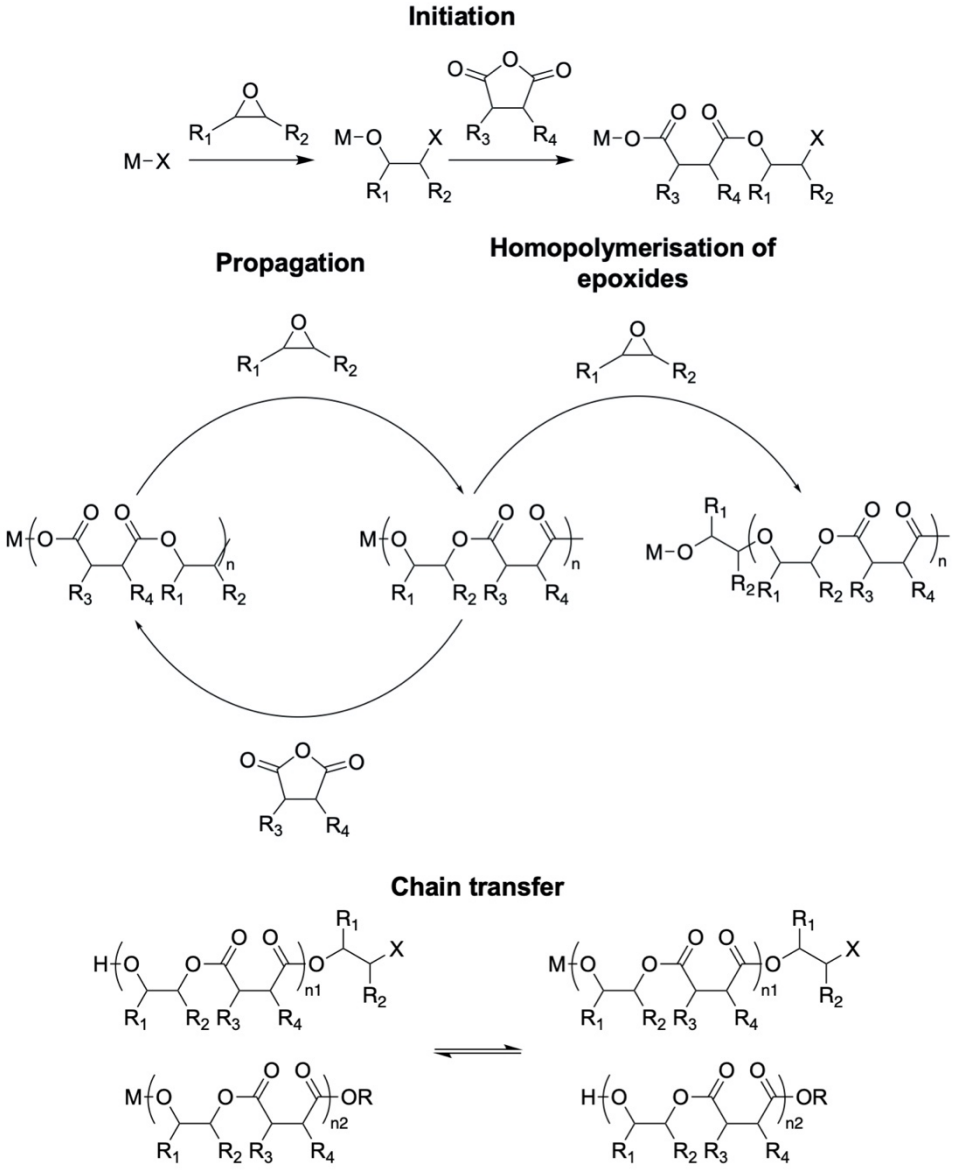

Scheme 1. The general mechanism for ring-opening copolymerisation of cyclic anhydrides and epoxides. M represents the metal site where catalysis occurs, and X represents the nucleophilic initiator.

The exact mechanism for each anhydride and epoxide ROCOP varies based on the catalyst system employed. However, a general mechanism has been established for ROCOP (**Scheme 1**).[22, 27] A catalyst, or more accurately an initiator, is required for ROCOP. ROCOP sees an initiation phase and a propagation phase but due to its living nature is only terminated through external action.

In the initiation step, an epoxide is ring-opened by attack by a nucleophile forming an alkoxide that then undergoes rapid anhydride insertion to generate a carboxylate species (the first repeating unit). Interestingly, in the first ROCOP of anhydrides and epoxides reported, Fisher proposed a mechanism in which the organocatalyst activated the anhydride forming a zwitterionic species that then enchained an epoxide in the first step of propagation. However, mechanisms since then have proposed the ring-opening of an epoxide as the first step of initiation. Propagation then occurs through sequential addition of anhydrides and epoxides with the enchainment of epoxide generally found to be the rate determining step. Therefore, polymerisation rates are found to only be dependent on epoxide concentration allowing for polymerisation to take place in neat epoxide which negates need for an alternative solvent. Termination occurs either through manipulating the conditions (reducing the temperature or monomer removal) or the addition of water, alcohols or acids.

Common deviations from this mechanistic pathway are caused by unwanted side reactions and either wanted or unwanted chain transfer. Homopolymerisation of epoxides can occur through unwanted ROP as the Lewis basic endocyclic oxygen in highly ring-strained epoxide lends itself to monomer activation by coordination to a Lewis acid or protonation. To avoid this the active alkoxide initiating/propagating species must selectively attack anhydrides and not epoxides. Another big consideration for ROCOP is chain transfer reactions in which the growing polymer chain equilibrates with protic compounds present, known as chain transfer agents (CTAs). As the anhydrides and epoxides contain protic impurities even after stringent purification and removing trace amounts of water is not cost-effective, inevitably chain transfer plagues ROCOP reactions and is one of their potential significant limitations.

Some co-catalytic bases are also known to act as chain transfer agents in reactions. Chain transfer typically occurs more rapidly than propagation reactions and so the polymerisations can remain “pseudo-controlled” maintaining narrow dispersity polymers that have lower chain lengths than theoretically expected. The resultant species can subsequently initiate further polymerisation. This is often taken advantage of by the deliberate addition of chain transfer agents to control the molecular weight of afforded polymers.

Bimodal distributions of polymer chains can occur when bifunctional species such as diols or diacids (such as the monomer impurities) are present. Due to propagation being possible in both directions, they grow at twice the speed of chains from the monofunctional species. Therefore, bimodal polymer molar mass distributions are often seen in anhydride and epoxide ROCOP without intention to produce them. The higher molar mass distribution features different (telechelic α,ω-hydroxy) end capped species to the lower molar mass distribution (α-X-ω-hydroxy, where X = initiator) and causes a problem when a specific end-chain functionality is desired. Multiple equivalents of a desired CTA can be added to overcome this but will never fully suppress other distributions and, in many cases, will lead to lowering the molecular weight of the polymer chains in proportion with initial CTA concentration.

1.4 ROCOP catalyst development

1.4.1 Catalytic performance

ROCOP polymerisation requires the application of a catalyst to activate polymerisation. For industrially relevant catalysts, a high catalytic activity is required so that polymerisations can occur as efficiently as possible. Typically, catalytic activity is

measured by three parameters: the turnover number (TON), which is the number of monomer units converted into polymer by one mole of catalyst; the turnover frequency (TOF), which is the TON achieved in a definite time; and the observed rate constant.[27] Overall, a catalysts' performance is evaluated based on its ability to deliver a controlled polymerisation (achieve an expected number average molecular weight, lack of side reactions, low dispersity), its activity and in some cases its control of regio- and stereochemistry during monomer enchainment.

Even with these parameters in mind, comparisons between ROCOP catalysts are difficult as methods for analysis of catalytic performance have developed over the time that reports of catalysts have been published and such a wide range of monomers and reaction conditions that can be accommodated mean that often reported copolymerisations cannot be directly compared with each other. Typically, the copolymerisation of propylene oxide (PO), or the less volatile cyclohexene oxide (CHO), with phthalic anhydride (PA) are used as standard comonomers to compare catalysts.

1.4.2 Early catalysts

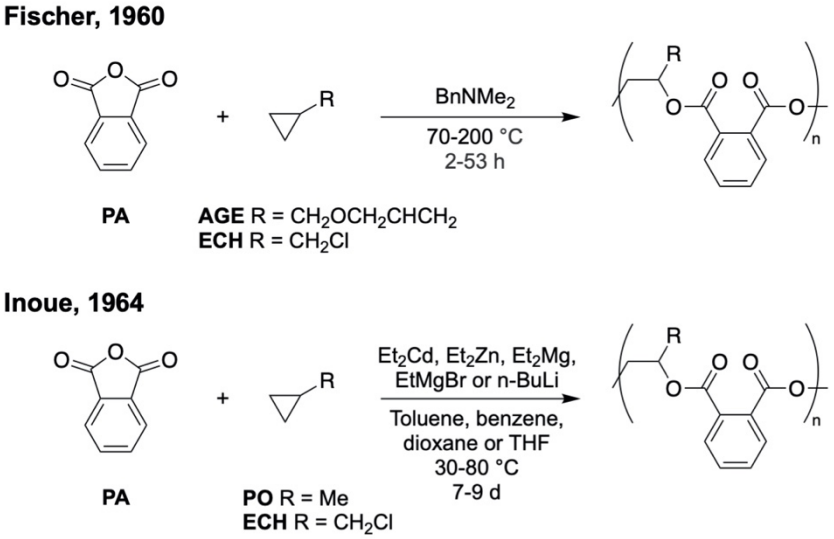

Scheme 2. Reaction schemes of the first successful ROCOP of anhydrides and epoxides by Fischer in 1960 and the first metal-initiated ROCOP of anhydrides and epoxides by Inoue in 1964.

The first successful ROCOP of anhydrides and epoxides was reported by Fischer in 1960 who used the tertiary amine, dimethylbenzylamine ($BnNMe_2$), to mediate the ROCOP of PA or allyl glycidyl ether (AGE) in a range of conditions (T = 70–200 °C, 2–53 h) affording perfectly alternating polyesters (>99% ester linkages, M_n ≤ 18,400 $g \cdot mol^{-1}$).[28] However, when the range of epoxides was expanded, homopolymerisation increased up to 40%. The first metal-initiated copolymerisation of anhydrides and epoxides was reported in 1964 by Inoue for the ROCOP of PA with epichlorohydrin (ECH) and PO using metal-alkyl catalysts $ZnEt_2$, $MgEt_2$, EtMgBr, $CdEt_2$ and *n*-BuLi.[29] Mild reaction temperatures and long reaction times (T = 30–80 °C, 7–9 days) afforded corresponding polyesters (28–88% yield).

These initial findings were followed by reports of inorganic salts, tertiary amines, main group Lewis acids and metal-alkyl initiators as successful ROCOP catalysts.[30-35] This first generation of catalysts established the field of ROCOP catalysis but they suffered poor catalytic activity, afforded low molecular weight polymers and were accompanied

by a lack of fundamental understanding of the mechanism impeding further catalyst development.

1.4.3 Well-defined metal catalysts

The need for highly controlled ROCOP led to the exploration of well-defined metal catalysts supported by ancilliary ligands (to suppress side reactions), often employed alongside a co-catalyst with the role of labilising the initiating group or propagating polymer chain.[27]

1.4.3.1 Metalloporphyrins

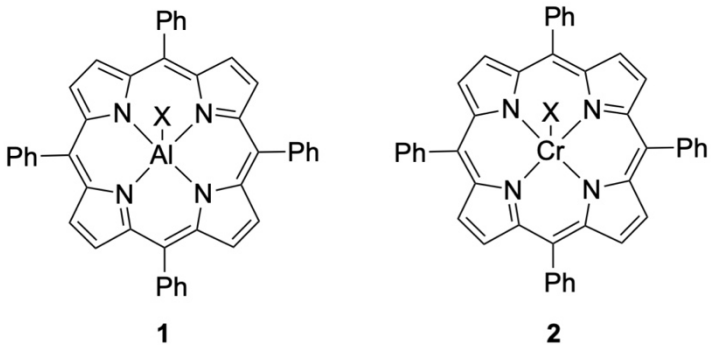

Figure 1. Key metalloporphyrin complexes used in catalysts for the ROCOP of anhydrides and epoxides.

In 1985, the first use of a well-defined metal complex in the ROCOP of anhydrides and epoxides was reported by Inoue and co-workers using an aluminium porphyrin complex (**1**).[36] Alongside a quaternary organic salt co-catalyst, it mediated copolymerisations in mild conditions (T = 25 °C, 4–7 days to reach 100% conversion) and afforded low molecular weight polymers with no polyether (M_n ≤ 3,000 g·mol^{-1}, $Đ_M$ = 1.1). However, very low activities were achieved (TOF = 3.6–6.3 d^{-1}, 4 mol% catalyst loading *vs*. anhydride). The work established a better fundamental understanding of ROCOP, key to the development of further catalysts. Using NMR spectra analysis of

small molecule references and reaction products it was found that the coligand of **1** and the anion of the quarternary salt acted as initiators and that epoxide insertion was likely the rate determining step as there was a lack of signals attributable to an aluminium-alkoxide bound species.

Since Inoue's discovery, the porphyrin complexes have been optimised through the metal centre and ligand tuning.[37-39] Most significantly, chromium was employed as a more active metal centre due to its relative affinity to achieve six-coordination. Duchateau and co-workers employed an analogous chromium porphyrin complex (**2**) alongside co-catalyst 4-dimethylaminopyridine (DMAP) for anhydride-epoxide ROCOP, which gave higher activity compared to Inoue's aluminium catalyst when applied to the ROCOP of CHO with anhydrides (TOF ≤ 107 h^{-1}, 4% *vs.* anhydride).[37] A follow-up study showed a chromium porphyrin complex's superior activity (TOF = 150 h^{-1}) over cobalt and manganese analogues (TOF ≤ 43 h^{-1}) for the mediation of the ROCOP of styrene oxide (SO) and PA.[38]

Porphyrin complexes catalysed controlled copolymerisation of anhydrides and epoxides with good activities reached especially when chromium metal centres and a co-catalytic base at employing high temperatures. However, their ligand structure gave limited tunability to optimise the catalysts further.

1.4.3.2 β-diiminate (BDI) complexes

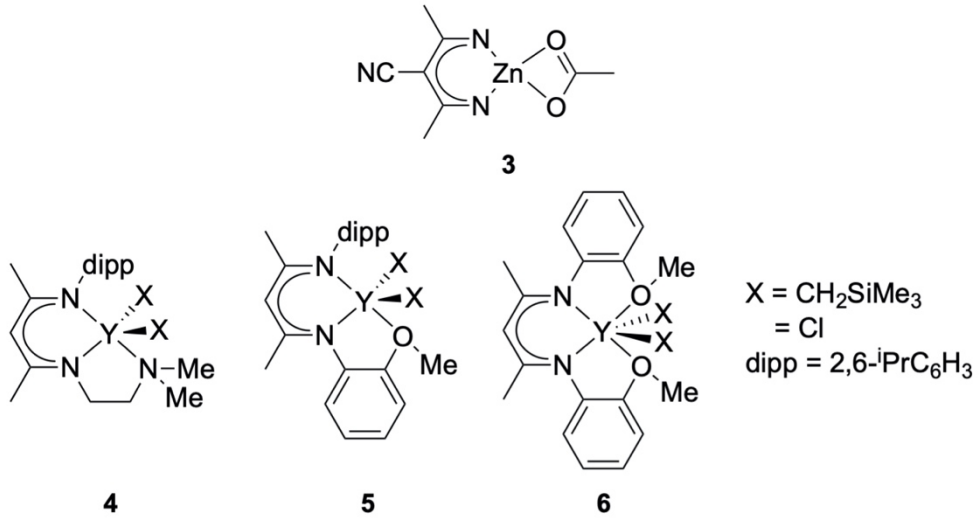

Figure 2. Key BDI complexes used in catalysts for the ROCOP of anhydrides and epoxides.

Coates and co-workers achieved a breakthrough in 2007 with the zinc β-diketiminate complex (**3**) achieving the first high molecular weight (M_n ≤ 55,000 g·mol^{-1}) copolymers from the ROCOP of anhydrides and epoxides, which reignited exploration of the field.[40] A wide range of epoxides and anhydrides were copolymerised in mild conditions (T = 30–70 °C, 0.5% *vs.* anhydride) to afford polyesters with high ester linkage (> 95%) and low dispersities ($Đ_M$ = 1.1–1.5). A good catalytic activity of TOF = 31 h^{-1} was achieved for ROCOP of CHO and diglycolic anhydride (DGA) at 50 °C. A study of the mechanism revealed a dimer of the complex as the active species. The ligand system was also employed more recently with yttrium to exploit the advantages of rare-Earth metals (high abundance and ability to support a wide range of ligand environments). The catalysts (**4-6**) were versatile, being able to effectively copolymerise mono- and disubstituted epoxides and bicyclic anhydrides (TOF ≤ 11 h^{-1}) but struggled with the more challenging tricyclic anhydride carbic anhydride (CA) giving significant amounts of polyether from slower polymerisations (34% conversion after 8 h).[41]

1.4.3.3 Metal salen-based complexes

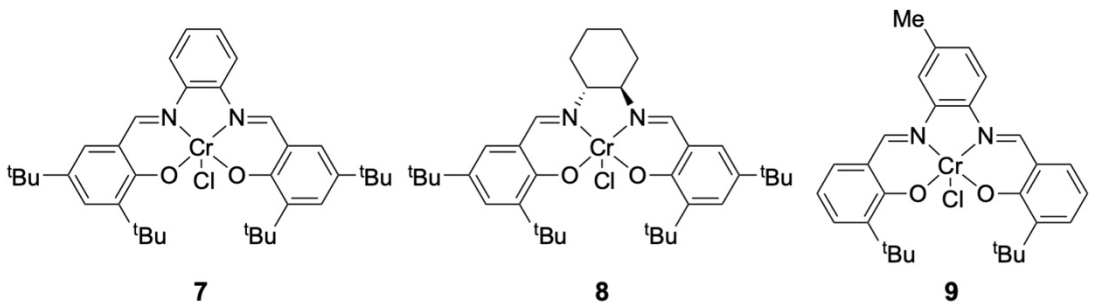

Figure 3. Key metal-salen complexes used in catalysts for the ROCOP of anhydrides and epoxides.

Metal salen complexes are some of the most ubiquitous anhydride and epoxide ROCOP catalysts in literature thanks to their high activities, control, and wide ligand tunability. Duchateau and co-workers first reported a chromium salen complex (**7**) used alongside co-catalytic DMAP for the ROCOP of anhydrides and epoxides in 2011.[37] As seen with the metalloporphyrins, a co-catalyst was needed to be effective. CHO was copolymerised with anhydrides (T = 100 °C, 140–300 min) to give copolymers with high ester linkage (67–100%) and narrow to moderate dispersities (M_n ≤ 16,060 g·mol^{-1}, $Đ_M$ ≤ 1.6). Catalytic activity (TOF = 71 h^{-1}) exceeded that of the metalloporphyrin (TPP)CrCl in the ROCOP of CHO and PA in bulk but was slower for the copolymerisation of CHO with other anhydrides. As with porphyrin complexes, chromium was found to give a higher metal reactivity than aluminium and cobalt metal centres for salen complexes in a follow-up study that screened different ligand backbones, metal centres and co-catalysts.[42] The study saw the highest catalytic activity with catalyst **8** (TOF ≤ 245 h^{-1}, 0.4% *vs*. anhydride, T = 110 °C) when used alongside bis(triphenylphosphine)iminium chloride (PPNCl).[43] An extremely high catalytic activity was later reported using catalyst **8** (TOF = 1200 h^{-1}, 100 °C) by Williams and co-workers when being used as a comparison to other catalysts. Further optimisation of the ligand structure in chromium salen complexes saw very high

catalytic activities (TOF ≤ 640 h^{-1}, T = 110 °C) for anhydride and epoxide ROCOP using catalyst **9** and DMAP.[44]

The extensive options for modifying ligand structure in salen-complexes allowed for further investigations to fine-tune the catalyst to master a wide-range of difficult copolymerisations including the facilitating the previously challenging ROCOP of maleic acid (MA) or tricyclic anhydrides with epoxides and the ROCOP of bulky, terpene-derived renewable monomer limonene oxide (LO) with anhydrides.[45-47]

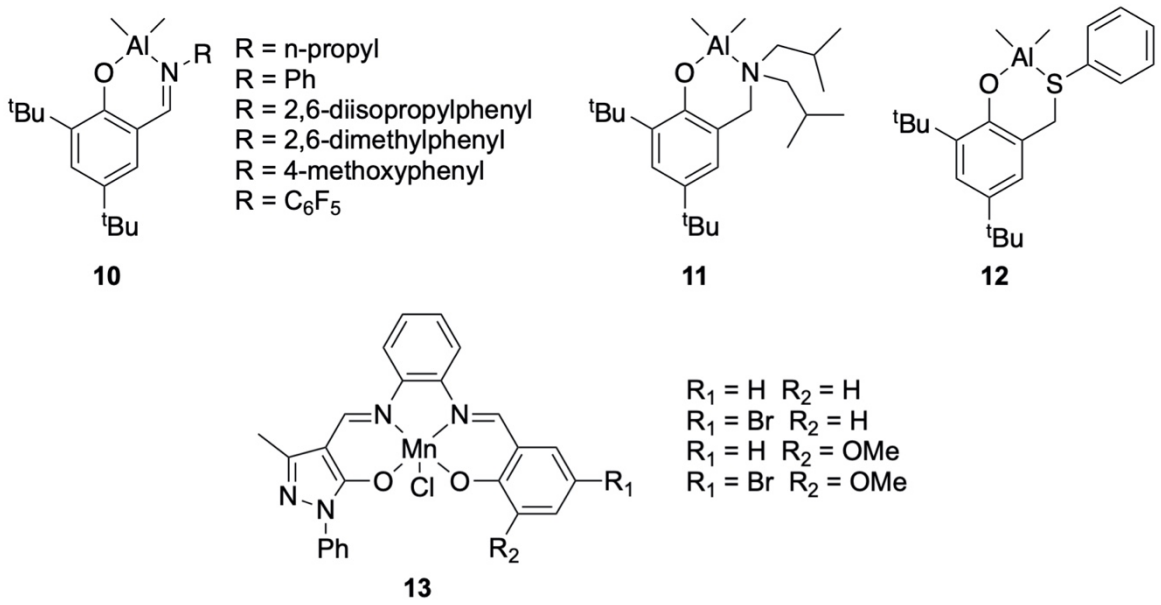

Figure 4. Key half-salen and asymmetric salen complexes used in catalysts for the ROCOP of anhydrides and epoxides.

Ligand flexibility was also exploited to increase the catalytic activity of metal-salen complexes that employed less expensive, more environmentally benign but less active metal centres to compete with those of chromium. A series of half-salen aluminium complexes (**10-12**) all showed higher activities (TOF ≤ 105 h^{-1}) than those of pentacoordinate salen aluminium complexes giving a basis for competitivity with chromium-based catalysts and a series of asymmetric manganese salen complexes

(**13**) were found to be more effective than symmetrical catalysts described in literature especially in the case of CHO and MA copolymerisation (TOF = 104 h^{-1}).[48-50] Another route to improved catalytic activity for manganese and aluminium salen catalysts was found by mixing the catalyst, co-catalyst and reaction solvent in a pre-contact step for up to 24 h before ROCOP of CHO and PA with catalysts performing comparatively with chromium salen catalysts for polymerisation rates, molecular weight and glass transition temperature of the resultant copolymers.[51] This was proposed to be due to both time facilitating the solubility of phosphonium salt co-catalysts in toluene and so that the active species could form in advance of monomer addition.

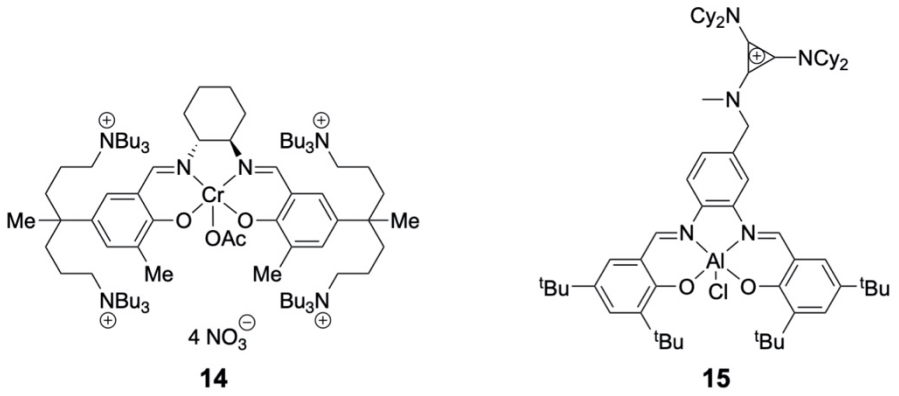

Figure 5. Key bifunctional salen complexes used in catalysts for the ROCOP of anhydrides and epoxides.

A significant step-forward in the development of more highly active salen-based catalysts was the employment of a bifunctional complex in which the salen catalyst and co-catalytic base are tethered within the same molecule. It was proposed that this would overcome poor catalytic activity suffered at low catalytic loadings where dilution of catalyst and co-catalyst hampers the suppression of side reactions. Lee and co-workers employed a cobalt salen complex (**14**) which tethered four quarternary ammonium salts in the ROCOP of PO and PA (TOF ≤ 33 h^{-1}, T = 80 °C, 0.027% *vs*.

anhydride) affording unprecedented molecular weights of resultant copolymers (M_n ≤ 170,000 g·mol^{-1}, $Đ_M$ ≤ 1.5) at a catalyst loading of 1% *vs*. anhydride.[52] This was followed by Coates and co-workers' use of aminocyclopropenium-tethered metal salen catalysts (**15**) which demonstrated excellent catalytic activity (TOF ≤ 93 h^{-1}) for the ROCOP of anhydrides and epoxides at low catalyst loadings (≥ 0.025 mol %) and mild conditions (60 °C) in comparison with suppressed polymerisation rates in comparable binary systems (TOF ≤ 22 h^{-1}).[53] At slightly higher catalyst loading (0.25 mol%), a cobalt catalyst gave very high catalytic activity (TOF = 376 h^{-1}) but was deactivated when applied at lower loadings.

1.4.3.4 Multinuclear metal complexes

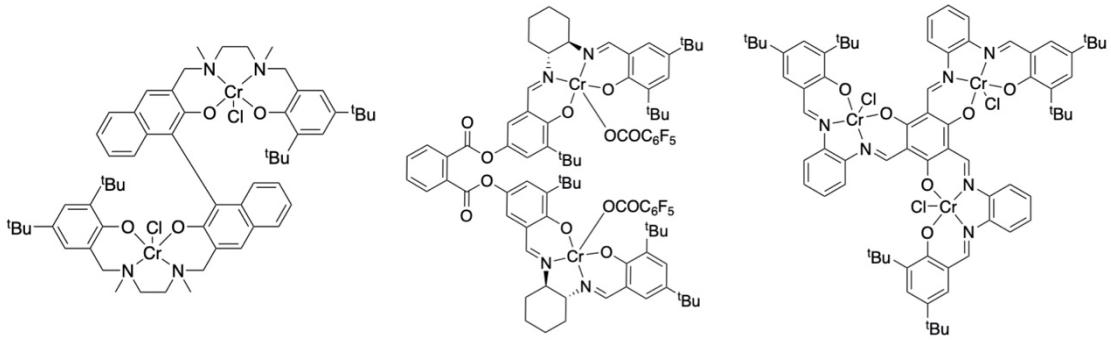

Figure 6. Key multidinuclear metal complexes used in catalysts for the ROCOP of anhydrides and epoxides.

Multinuclear catalysts were investigated to explore the effects of a synergic effect between multiple metal centres on catalytic activity.[54-62] At first, salen complexes were tethered together to achieve this such as in the example employed for anhydride and epoxide copolymerisation in 2013 by Lu and co-workers who used a dinuclear chromium-salan complex (**16**) to give higher activity than mononuclear chromium-salen complexes (e.g. the ROCOP of MA and ECH: $TOF_{dinuclear}$ = 3.7 h^{-1} vs

$TOF_{mononuclear} \leq 1.4\ h^{-1}$ at 45 °C).[60] A chiral dicobalt salen catalyst with a benzene linker (**17**) demonstrated higher activities than analogous mononuclear cobalt salen catalysts. For example, for PO and PA copolymerisation in mild conditions (T = 30 °C, 0.25% *vs*. anhydride) using co-catalyst [PPN][$OCOC_6F_5$], the complex was found to be extremely active (TOF = 908 h^{-1}), producing narrowly disperse polyester ($M_n \leq 12{,}000$ $g \cdot mol^{-1}$, $Đ_M \leq 1.14$).[61] A trinuclear chromium salen catalyst (**18**) used alongside PPNCl showed unprecedentedly high activities at low catalyst loadings (TOF = 10,620 h^{-1}, T = 100 °C, 0.01% *vs*. anhydride) for the copolymerisation of PA and CHO.[62]

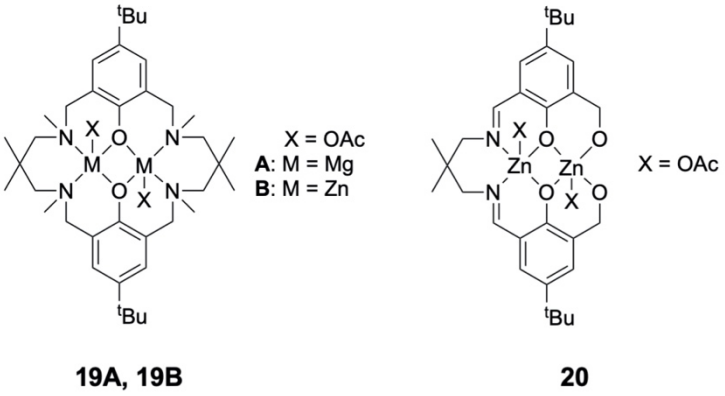

Figure 7. Key homodinuclear metal complexes used in catalysts for the ROCOP of anhydrides and epoxides.

Despite the superior catalytic activities achieved, tethered multinuclear salen complexes were laborious to synthesise rendering them difficult to implement in a commercial setting. To overcome this, Williams and co-workers applied dinuclear magnesium and zinc complexes with macrocyclic ligands (**19A, 19B**), which respectively mediated the ROCOP of CHO and PA with good catalytic activities reached (TOF = 97 h^{-1}, 100 °C, 1% *vs*. anhydride) affording perfectly alternating, narrowly disperse polymer ($M_n \leq 12{,}300$ $g \cdot mol^{-1}$, $Đ_M \leq 1.20$).[63] Unlike with tethered multinuclear salen complexes, these catalysts did not require co-catalysts to prevent

polyether formation. The group then explored a series of dinuclear salen zinc catalysts deriven from *o*-vanillin for the same copolymerisation, with one species (**20**) showing higher activities than the previous study (TOF = 198 h^{-1}, 100 °C).[64]

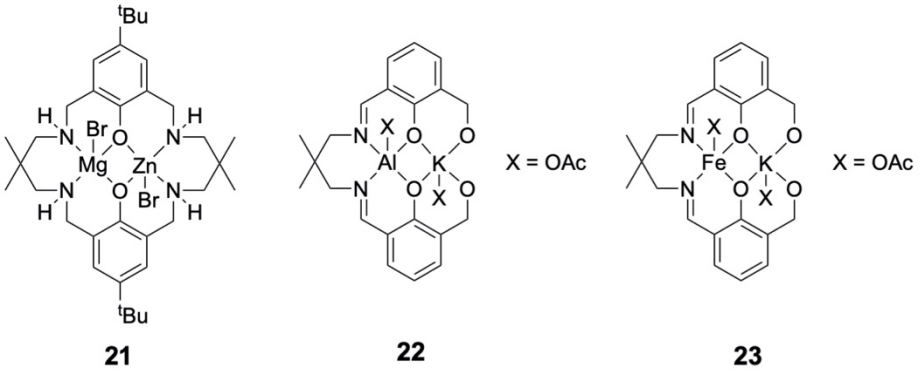

Figure 8. Key heterodinuclear metal complexes used in catalysts for the ROCOP of anhydrides and epoxides.

To improve catalytic activities further, Williams and co-workers developed and applied heterometallic dinuclear complexes to anhydride-epoxide ROCOP exploiting the mixing of two different catalytic sites together, which results in a synergic effect on catalytic activity that is greater than the sum of its parts. In their first use, the Mg/Zn dinuclear catalyst (**21**), which was complexed to a similar macrocycle to those reported by the group for homodinuclear catalysts, displayed a 40 times greater activity for the copolymerisation of CHO and PA than an equimolar mixture of the analogous homodinuclear Mg and Zn complexes (TOF = 188 h^{-1} vs 5 h^{-1}, T = 100 °C).[65] Afforded perfectly alternating copolymer saw moderate molecular weights and narrow dispersities (M_n ≤ 10,900 g·mol^{-1}, $Đ_M$ ≤ 1.09). Catalytic activity was improved further by using analogous heterodinuclear complexes containing Al(III) and an alkali metal (Na, K, Rb or Cs).[66] Aluminium mononuclear catalysts had been shown to be highly active when tethered with co-catalysts, whereas group 1 metal carboxylates had been

shown to be easy to use but suffered from slow polymerisation rates. The synergy of aluminium and potassium gave very high catalytic activity for CHO and PA copolymerisation using catalyst **22** (TOF = 1072 h^{-1}, 100 °C, 0.25 mol% catalyst loading vs anhydride), even at low loadings (TOF = 1010 h^{-1}, 100 °C, 0.025 mol% catalyst loading vs anhydride). In addition to this both types of metal were earth-abundant, inexpensive and expected to be low/nontoxic. A good scope of other epoxides and anhydrides were copolymerised in the same conditions while maintaining good activities (TOF = 20–592 h^{-1}). Most recently, the group used a Fe(III)/K(I) dinuclear catalyst (**23**) for ROCOP displaying competitive activities (TOF = 1152 h^{-1}, 100 °C) for the copolymerisation of CHO and PA and exceptional activity at high temperature (TOF = 4,800 h^{-1}, 140 °C).[67]

1.4.3.5 Other discrete metal complexes

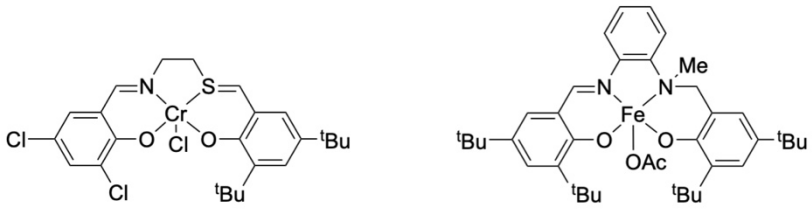

Figure 9. Key [ONNO] and [ONSO] salen metal complexes used catalysts for the ROCOP of anhydrides and epoxides.

Ligands containing soft sulfur donors that were analogous to [ONNO]-salen ligands were employed in ROCOP to access more catalytic activities.[68-70] Notably, a *cis*/*trans* stereoselective [ONSO]-salen chromium complex (**24**) was found to be extremely active (TOF ≤ 970 h^{-1}, 110 °C) when used alongside a co-catalytic base for the ROCOP of *exo*-NA and CHO and an air-stable iron complex based on a [ONSO] ligand (**25**)

successfully afforded highly alternating (97% ester linkage), narrowly disperse copolymers ($Đ_M$ = 1.19) from the ROCOP of CHO and PA performed at 100 °C for 3 days.[70]

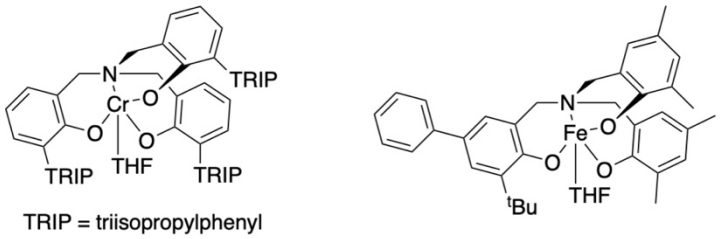

Figure 10. Key triphenolate metal complexes used in catalysts for the ROCOP of anhydrides and epoxides.

Amino- and imino-triphenolate complexes have been explored as ROCOP catalyst alternatives to salen-based catalysts as they are geometrically more flexible than the latter and therefore can allow for coordination of sterically demanding substrates. [55, 71-73] A chromium-aminotriphenolate complex (**26**) and co-catalytic PPNCl were employed to afford perfectly alternating polyesters with high molecular weights (M_n ≤ 43,800 g·mol^{-1}) from the ROCOP of anhydrides and epoxides.[73] The catalyst was highly active at small catalytic loading (TOF = 380 h^{-1}, 100 °C, 0.125 mol% catalyst loading vs anhydride). An iron-aminotriphenolate complex (**27**) was shown to display extremely high activity for the ROCOP of CHO and PA (TOF = 1160 h^{-1}, 100 °C, 0.2 mol% catalyst loading vs anhydride).[55]

1.4.4 Simple catalysts

Though well-defined organometallic catalysts have demonstrated highly controlled and efficient ROCOP of anhydrides and epoxides, they have significant drawbacks including laborious ligand syntheses and the use of highly toxic, expensive, rare

metals.[74] This has prompted interest over the recent few years in the development of alternate simple catalysts. Compared to well-defined metal catalysts, research into these catalysts is still in its infancy.

1.4.4.1 Organobases

Small organic molecule catalysts have the advantages of being more widely available, possessing lower sensitivity to moisture and oxygen, potentially less toxic and more eco-friendly than specific well-defined organometallic complexes.[22] It was already known that organic compounds used as co-catalysts in ROCOP catalysis could perform ROCOP on their own. Indeed, some of the early catalysts used for the ROCOP of anhydride and epoxide were organobases.[28, 75-77] In early investigations, phosphonium and ammonium quarternary onium salts were shown to be viable, if slow (TOF < 1 h^{-1}, 130 °C) copolymerisation catalysts for giving polyester with reasonable molecular weights (M_n ≤ 11,100 g·mol^{-1}, $Đ_M$ ≤ 1.43).[78]

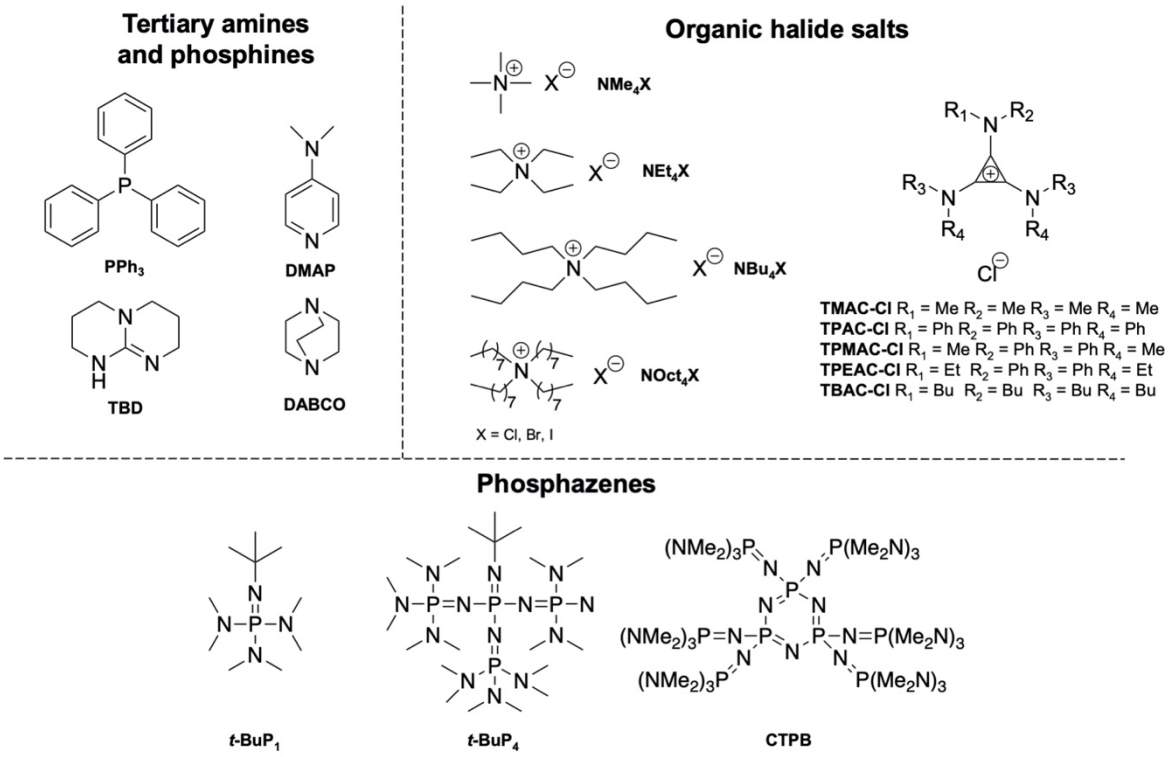

Figure 11. Key organocatalysts used as catalysts for the ROCOP of anhydrides and epoxides.

More recently, in deliberate pursuit of simple catalysts, systematic investigations were conducted into organocatalysts. In 2017, Merna and co-workers studied the ROCOP of PA and CHO using PPNCl (**Figure 11**) as a catalyst.[79] The catalyst was effective (T = 110 °C, 5 h, 57% conversion) giving highly alternating copolymer with low dispersity (98% ester linkage, M_n = 11,700 g·mol^{-1}, $Đ_M$ ≤ 1.30) and accommodated a wide range of other monomers. DMAP, Bu_4NCl, Bu_4NBr, and PPh_3 (**Figure 11**) were also found to be effective but TBD and DABCO were found to be ineffective. Monomer conversion and molecular weight of the resultant polymer were found to be dependent on the purity of monomers as impurities contained protic agents which could promote chain transfer reactions. Halide salts were seen as preferable to neutral organocatalysts due to their high thermal stability. An optimisation screen of catalytic organic halide salts (PPNCl, TMA-X, TEA-X, TBA-X, TOA-Cl, TMAC-Cl, TPMAC-Cl, TPEAC-Cl and TBAC-Cl where

X = Cl, Br or I) (**Figure 11**) was tested for the ROCOP of CHO and PA. PPNCl performed best of all the quarternary ammonium chloride salts (TOF = 25.8 h^{-1}, T = 100 °C), but bromide and iodide variants had the capacity to give higher activities (TOF ≤ 60 h^{-1}).[80] A chloride-based salt was able to give higher activity than PPNCl when aminocyclopropenium chlorides were applied (TOF ≤ 46.8 h^{-1}). Expected theoretical molecular weights of afforded copolymers could be superseded by continuing the reaction beyond completion where post-polymerisation transesterification led to longer chain lengths (M_n ≤ 44,300 g·mol^{-1}).

Phosphazenes are organobases which have drawn interest due to their use as catalysts/initiators in anionic polymerisations of various monomers. *t*-BuP_1 (**Figure 11**) was used to mediate the ROCOP of PA and EO by Zhao and co-workers to give perfectly alternating polyesters with expected molecular weights and narrow dispersities in mild conditions and long reaction times (TOF = 2 h^{-1}, 60 °C, 1% *vs*. anhydride).[81] The authors proposed a self-buffering mechanism in which the catalyst acts alternatively as an activator for carboxyls and deactivator for hydroxyls. *t*-BuP_1's mild basicity and non-nucleophilic nature was crucial for selectivity of the catalyst as it allowed for chain growth but avoided side reactions such as epoxide self-propagation or transesterification. On the other hand, the stronger base *t*-BuP_4 (**Figure 11**) mediated the formation of lower molecular weight, broader dispersity copolymers as the higher basicity catalysed transesterification side reactions. The group conducted a follow-up study with the catalyst producing copolyesters from a wide scope of monomers with some exceptional molecular weights achieved (M_n ≤ 124,000 g·mol^{-1}).[82] A cyclic trimer phosphazene base catalyst (CTPB) (**Figure 11**) and carboxylic acid initiator were employed as ROCOP catalysts achieving complete conversion in 12 h at

80 °C to afford narrow dispersity copolymer (M_n = 7,300 g·mol^{-1}, $Đ_M$ = 1.17) from PA and CHO.[83] Running the polymerisation in neat epoxide led to considerably shorter reaction times at the expense of broader polymer dispersities. This was because after PA was consumed, CHO was homopolymerized due to the high catalytic activity of CTPB.

1.4.4.2 Organic Lewis pair catalysts

Single-functionality organocatalysts have suffered from limited monomer scope compatibility, side reactions and low catalytic activities hindering their suitability to be a sustainable alternative to discrete metal catalysts.[84] To overcome these difficulties, cooperative organic Lewis pair catalyst systems were developed, often by pairing the organobases with a simple Lewis acid. The synergic effect of the two was hypothesised to give higher catalytic activities, greater tunability and suppress side reactions.

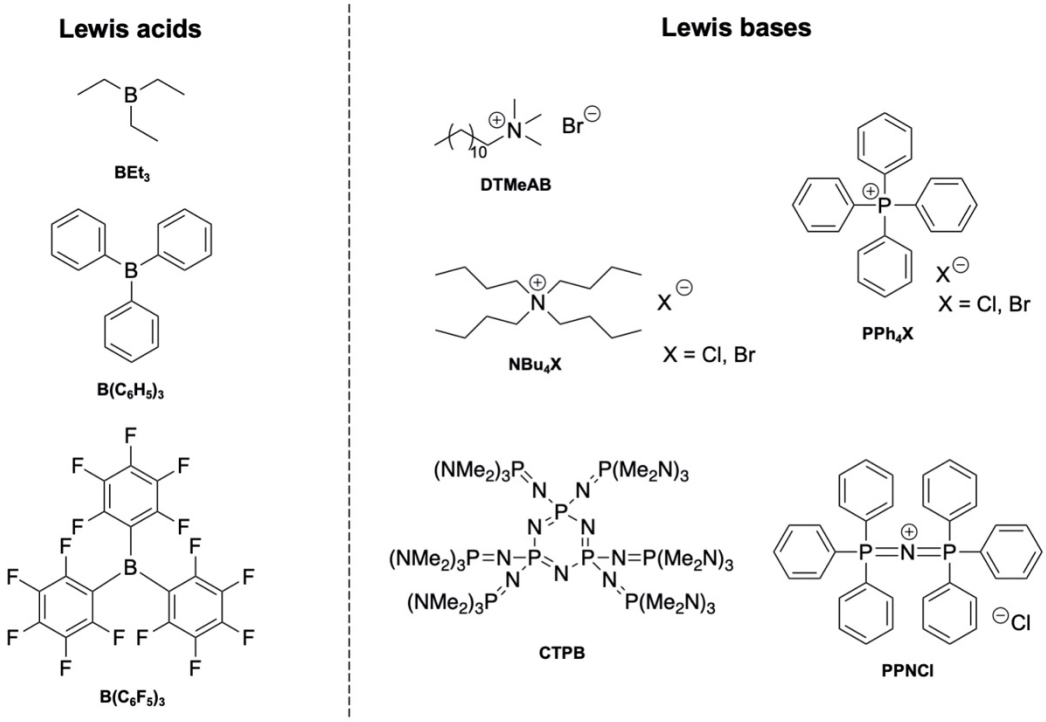

Figure 12. Organoboron lewis acids and lewis bases used in Lewis pair catalysts for the ROCOP of anhydrides and epoxides.

In 2016, Lewis pair catalysts based on organoborane were demonstrated as successful catalysts for the ROCOP of epoxides and carbon dioxide promoting an explosion of interest in their catalysis of various polymerisations.[85] Boron was selected as it is in the same group as aluminium, a common metal used in discrete complex catalysts for ROCOP, and so can be used to coordinate with the oxygen in the epoxide and nitrogen through its empty *p* orbital. Zhang and co-workers employed the first example in anhydride and epoxide copolymerisation using a series of organoborons alongside quarternary onium salts (**Figure 12**).[84] They established that catalytic activity was dramatically increased when a Lewis acid was used alongside the organobase dodecyltrimethylammonium bromide (DTMeAB) (up to > 99% conversion, 12 h, 45 °C) as opposed to when DTMeAB was used on its own (17% conversion) for the copolymerisation of MA and PO and that bulkier and stronger Lewis acids suppressed

polymerisation rates. All cooperative pair combinations gave perfectly alternating copolymers of longer chain lengths ($M_n \leq 8{,}000$ g·mol^{-1}, $Đ_M \geq 1.15$) than those initiated by organobases only. The most effective pair of BEt_3 and PPNBr achieved a high catalytic activity (TOF = 303 h^{-1}, T = 80 °C) when applied to the ROCOP of PO and PA to afford narrowly disperse, high molecular weight polyester (M_n = 20,000 g·mol^{-1}, $Đ_M$ = 1.12). Investigations into the mechanism showed that when maleic acid impurities were present, the polymer chain grew in both directions. This could be changed to one-directional growth by addition of an alcohol initiator. It was also found that generated HX (X = Br, Cl) species could react with an epoxide to give an X-substituted alcohol, which could act as a protic initiator or chain-transfer agent during polymerisation. In a following study, when strong Lewis acids, $B(C_6H_5)_3$ and $B(C_6F_5)_3$ (**Figure 12**), were applied alongside Lewis bases for the copolymerisation of challenging tricyclic anhydrides with mono-substituted epoxides, the former preferred a complex with the Lewis base and the latter initiated homopolymerisation of the epoxide only.[86] The relatively weaker Lewis acid BEt_3, however, displayed a versatile ability to copolymerise a range of monomers effectively alongside PPNCl with good catalytic activity (TOF ≤ 330 h^{-1}, 110 °C). Further work found that when two equivalents of Lewis acid to Lewis base were employed, higher monomer conversions and molecular weights could be achieved ($M_n \leq 57{,}500$ g·mol^{-1}, $Đ_M \geq 1.07$) as one equivalent of BEt_3 forms a borate species with the Lewis base for initiation of the polymerisation while the excess BEt_3 activates the epoxide.[87] BEt_3/phosphazene base combinations have been demonstrated to mediate block copolymerisation of anhydrides and epoxides in two studies.[88, 89] The relatively-strong CTPB was used in as little as a 5% ratio alongside organoboron Lewis acids to mediate ROCOP proving to be highly active for PO and

PA at low catalytic loading (TOF ≤ 500 h^{-1}, T = 100 °C, 0.06% CTPB *vs*. anhydride) and affording an extremely high molecular weight copolymer (M_n = 118,500 g·mol^{-1}, $Đ_M$ = 1.91).[90]

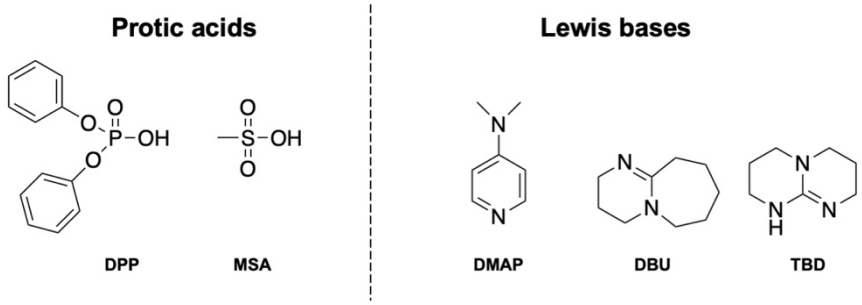

Figure 13. Protic acids and Lewis bases used in Lewis pair catalysts for the ROCOP of anhydrides and epoxides.

Kou and co-workers studied the use of protic acids MSA and DPP paired with organobases DMAP, DBU and TBD (**Figure 13**) as ROCOP catalysts with impressive catalytic activity as seen with DPP/DMAP for the ROCOP of CHO and PA (TOF = 574 h^{-1}, T = 140 °C), which produced a more monomodal mass distribution of copolymer than the DMAP and MSA Lewis pair system though the latter gave even higher activity for the same conditions (TOF = 624 h^{-1}).[91] Perfectly alternating polyesters were produced with all catalyst pairs suggesting different catalyst combinations only affected catalytic activity but not selectivity. Molecular weights achieved were below theoretical expected but high molecular weights were afforded through chain extension by addition of anhydride once the consumption of original monomers had reached

completion.

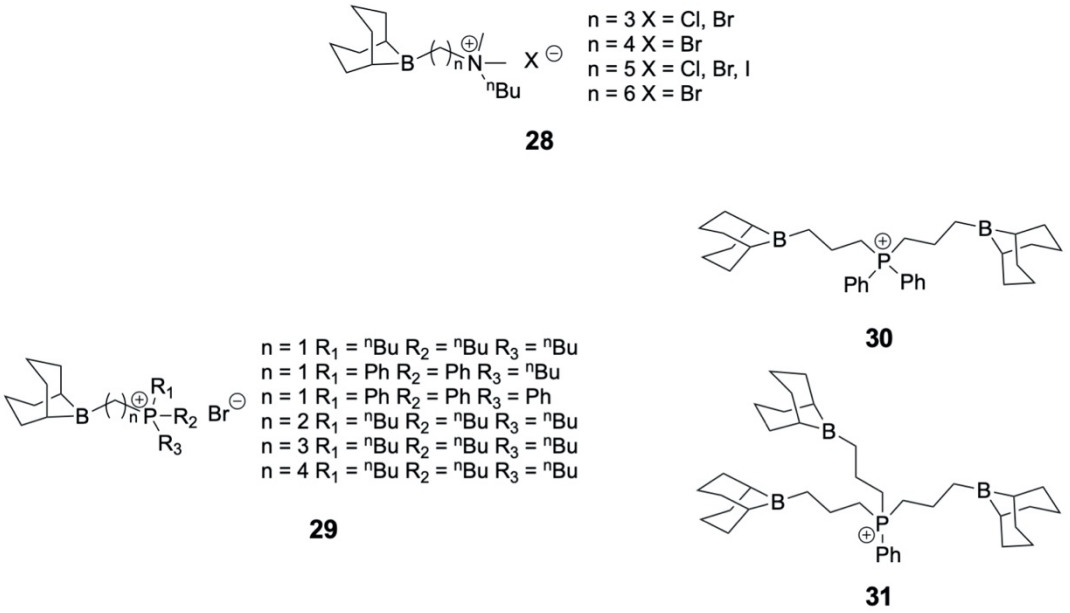

Figure 14. Key tethered organoboron bifunctional catalysts used as catalysts for the ROCOP of anhydrides and epoxides.

Wu and co-workers used a series of one-component, bifunctional organoboron catalysts (**28**) for the ROCOP of anhydrides and epoxides to achieve extraordinary catalytic activity (TOF = 9,900 h^{-1}, 150 °C) for the ROCOP of CHO and PA.[92] Highly alternating (90% ester linkage), high molecular weight copolymers were achieved (M_n ≤ 96,800 $g \cdot mol^{-1}$, $Đ_M$ = 1.34) and effective polymerisation was achieved at low catalytic loading (0.01% *vs*. anhydride). The catalysts were also very thermally robust, enduring a reaction temperature as high as 180 °C. The catalysts used incorporated a Lewis acidic boron centre, an electropositive ammonium cation, and nucleophilic anion in a modular manner into the same compound allowing for high tunability to accommodate a variety of electronic properties and steric profiles. By tethering the Lewis base and acid into the same molecular, higher catalytic activities were thus achieved. Further work replaced the nitrogen with phosphorus in the catalyst systems (**29-31**) for the

more flexible molecular structures and higher ion conductivities achievable, better thermal stability and greater steric tolerance allowing for a greater variety of substituents on the cation.[93] High catalytic activities were obtained (TOF = 1,989 h^{-1}, 150 °C and TOF = 2,856 h^{-1}, T = 200 °C). A 5.3 times faster catalytic activity was observed for one phosphonium catalyst when compared to its ammonium counterpart from the previous study in the same conditions. Effective copolymerisation was demonstrated with catalytic loading as low as 0.007% *vs*. anhydride giving highly alternating copolymer (94% ester linkage).

1.4.4.3 (Thio)urea H-bonding cooperative catalysts

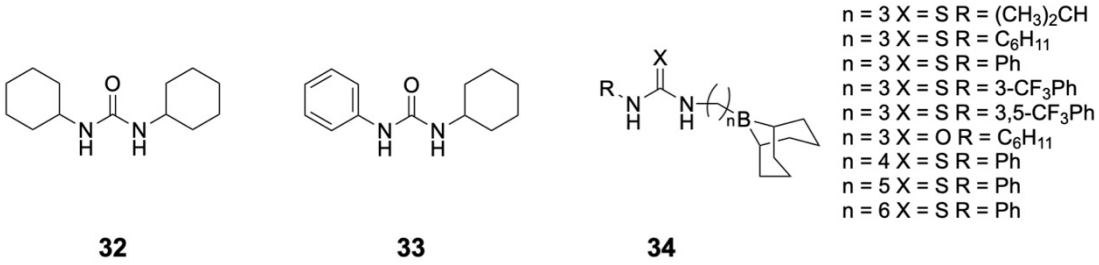

32 **33** **34**

Figure 15. Key (thio)ureas used in catalysts in the ROCOP of anhydrides and epoxides.

Inspired by their previous use as epoxide and carbonyl sulfide copolymerisation catalysts, Meng and co-workers applied (thio)urea and organobase cooperative catalysts to the ROCOP of anhydrides and epoxides.[94] The urea (**32**) that was found to be most effective and active in the ROCOP of PA and CHO was comparable to that of metal catalysts (TOF = 456 h^{-1}, 110 °C, 1 mol% catalyst loading vs anhydride). (Thio)ureas with a lower acidity were found to be preferable as those with a higher acidity led to a reduction in nucleophilic activity for monomer ring-opening by the organobase. Organobases with a lower basicity were more active (PPNCl > DMAP > DBU) as they formed weaker interactions with (thio)urea allowing for a faster rate of

dissociation and attack of the monomer. Highly alternating (≥ 94%), high molecular weight copolymers with narrow dispersities (M_n ≤ 34,600 g·mol^{-1}, $Đ_M$ ≥ 1.07) were formed. A CTPB had shown high activity when used alone but also catalysed undesirable side reactions. It was paired with a urea co-catalyst (**33**) which due to the latter's weaker basicity, reduced the nucleophilicity of the alkoxide propagating chain and therefore suppress undesirable transesterification, and thanks to their hydrogen bonding, activated the propagating chain and monomers leading to a faster polymerisation rate.[95] This hypothesis was shown correct and perfectly alternating copolymers were prepared with well-defined chain-ends and narrow dispersities (M_n ≤ 6,400 g·mol^{-1}, $Đ_M$ ≥ 1.16). A (thio)urea was tethered to an organoboron electrophile-activating group with an alkyl linker to create a series of one-component, bifunctional catalysts (**34**), which were employed alongside PPNCl to give high activities, such as a turnover frequency of 408 h^{-1} for the ROCOP of PO and PA (T = 90 °C), and afforded perfectly alternating copolymers for a variety of epoxides with PA.[96] At low catalyst loading (0.02% *vs*. anhydride), high molecular weight copolymers were afforded (M_n = 78,800 g·mol^{-1}, $Đ_M$ = 1.15). The catalyst showed twenty times the catalytic activity of the tethered boron-ammonium organocatalyst, and three times the activity of Williams' heterodinuclear Al(III)/K(I) catalyst under the same conditions. The authors described the mechanism as a "tug-of-war" process where the polymer chain chooses between two inequivalent catalytic sites, preferring the thiourea for epoxide insertion and the boron for anhydride insertion. *N*-(*p*-tolyl)thiourea and diphenyl thiourea was employed alongside a base as cooperative pair catalysts for the solvent-free, open-air ROCOP of CHA and AGE to create polyesters for 3D-printing applications.[97] Resultant

polyesters (M_n ≤ 25,500 g·mol^{-1}, $Đ_M$ ≥ 1.24) possessed moieties suitable for thiol-ene cross-linking.

1.4.4.4 Simple metal-based Lewis pairs

Simple metal salts were used to mediate the ROCOP of anhydrides and epoxides in early investigations, such as halides and alkoxides of zinc, magnesium and aluminium, but were deemed to be sluggish and uncontrolled thanks to broad dispersities and polyether formation.[29] These results have since been improved by the discovery of new, more versatile metal salts and their pairing with co-catalytic bases in Lewis pair systems.

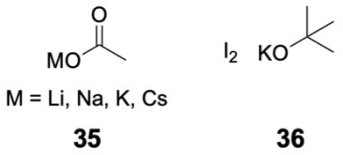

Figure 16. Alkali metal carboxylates and alkoxides used as catalysts for the ROCOP of anhydrides and epoxides.

Alkali metal carboxylates (AMCs) have attracted a lot of attention as simple, inexpensive, low-toxic and environmentally-benign catalysts which have mediated effective ROCOP of anhydrides and epoxides. A handful of studies in the 1980s and 90s employed them on modified carbon blocks but they had failed to give extensive insights into the mechanism of the polymerisation and resulting copolymer structures.[98-100] The last two years have seen a revival of interest with extensive studies accomplished. Luo and co-workers investigated a range of AMCs: NaOAc, KOAc, CsOAc, LiOAc (**35**) and two other metal carboxylayes: $Mg(OAc)_2$, $Zn(OAc)_2$ as anhydride and epoxide ROCOP catalysts.[101] $Mg(OAc)_2$ and $Zn(OAc)_2$ only produced polyether likely due to their high Lewis acidities preferring to initiate the cationic

polymerisation of the epoxide. For the AMCs, the metal cation and carboxylate anion dissociate and act as a Lewis pair for catalysis. Catalytic activity order for the ROCOP of PA and CHO at 110 °C (1% *vs*. anhydride) was CsOAc (TOF = 66.0 h^{-1}) > KOAc (TOF = 22.0 h^{-1}) > NaOAc (TOF = 1.95 h^{-1}) ≈ LiOAc (TOF = 1.03 h^{-1}). Smaller cations had stronger cation-anion interaction within the acetate and thus lowered initiation efficiency. Solvation effects were key with a polar, coordinating solvent weakening the cation-anion interaction and thus increasing initiation efficiency. Perfectly alternating, narrowly disperse copolymers were afforded (M_n ≤ 11,700 g·mol^{-1}, $Đ_M$ ≥ 1.17). Higher temperature polymerisation (150 °C) saw an increase in catalytic activity (LiOAc: TOF = 9.9 h^{-1}) at the expense of lower selectivity (86% ester linkage). Using KOAc, a large monomer scope was efficiently copolymerised showing great versatility. The KOAc was a more inexpensive catalyst to use than CsOAc but suffered lower catalytic activity due to its strong interaction between the potassium cation and carboxylate anion. KOAc was improved by use in combination with 18-crown-6.[102] Complexation with the crown ether weakened potassium's affinity with the carboxylate anion leading to an increase in the basicity of the carboxylate chain end and allowing for chain transfer to occur faster. High catalytic activities (TOF ≤ 313 h^{-1}, T = 110 °C) were therefore seen for the ROCOP of PA and *n*-butyl glycidyl ether (NBGE). With the use of an alcohol CTA, the system afforded diverse polydiols from a range of epoxides and anhydrides with tunable molecular weight, narrow distribution (M_n ≤ 21,000 g·mol^{-1}, $Đ_M$ ≥ 1.08). The catalyst even remained effective at low catalytic loadings (0.002% *vs*. anhydride) as it did not require the expected purification of anhydride thanks to its high tolerance to protic agents. A further study showed that introducing different alcohol CTAs alongside AMC catalysts allowed different functionalised polyesters to be afforded.[103]

The most active copolymerisations were seen for Cs_2CO_3 (TOF ≤ 156.6 h^{-1}) which gave highly alternating (≤ 98% ester linkage), high molecular weight copolymers (M_n ≤ 24,500 g·mol^{-1}, $Đ_M$ ≥ 1.30). Copolymerisations with PA saw similar polymerisation activity but the system was inactive to succinic anhydride (SA) or camphoric anhydride.

The addition of molecular iodine to simple alkali metal alkoxides (MeOLi/Na/K, *i*PrOLi/Na/K and *t*BuOLi/Na/K) was demonstrated by Chakraborty and co-workers to efficiently catalyse the copolymerisation of PA with a range of epoxides.[104] Halogen-based salts were successful simple, less expensive agents used in catalyst development for the copolymerisation of epoxides with CO_2, so it was thought that by mixing I_2 with the simple and inexpensive yet limited metal alkoxides, loose ionic pairs containing more labile iodide anions could form promoting anionic ROCOP. The remaining more positively charged iodonium could also act as a Lewis acid for activating the epoxides. Sodium and potassium alkoxides combined with iodine showed the higher activities. Notably, I_2/*t*BuOK (**36**) showed activities comparable with metal-based complex catalysts for a range of ROCOP reactions (TOF = 16-50 h^{-1}, T= 90 °C). Perfectly alternating copolymers were demonstrated in all monomer combinations with a range of molecular weights and dispersities (M_n ≤ 37,140 g·mol^{-1}, 1.93 ≥ $Đ_M$ ≥ 1.02).

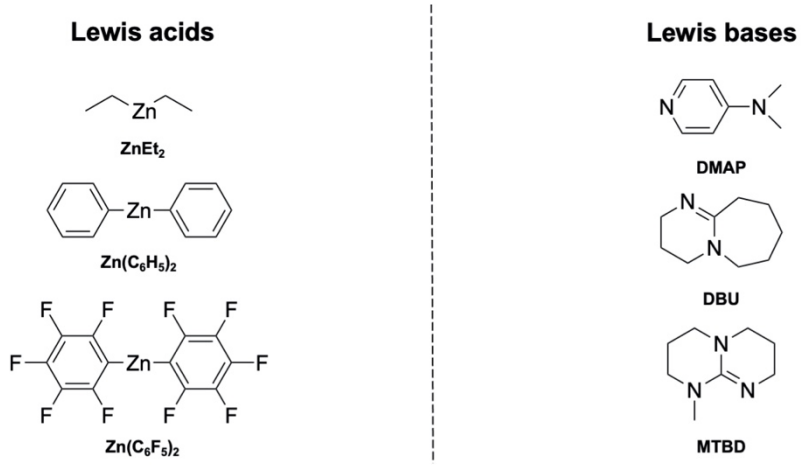

Figure 17. Zinc alkyl Lewis acids and organobases used as Lewis pair catalysts for the ROCOP of anhydrides and epoxides.

Simple zinc alkyl metals were paired with organobases (**Figure** 17) by Li and co-workers to produce Lewis pair catalysts for controlled anhydride and epoxide copolymerisation.[105] Catalysts showed good catalytic activities (TOF ≤ 210 h^{-1}, T = 110 °C) affording perfectly alternating, low dispersity polyesters (M_n ≤ 17,900 $g \cdot mol^{-1}$). Changing the Lewis acid had little effect on polymerisation rate. Whereas changing the Lewis base from DMAP to DBU and MTBD saw a significant decrease in catalytic activity. This suggested that Lewis bases have a stronger influence over copolymerisation rates. Indeed lowering the concentration of DMAP relative to the Lewis acid to a ratio of a half afforded copolymer with significant ether linkage (73%).

Within the last year, a new field of research into YCl_3-based Lewis pair catalyst systems for epoxide and anhydride ROCOP has been investigated as an improved alternative to AMC systems which suffered poor rates and low polymer dispersities compared to organometallic catalysts. Fieser and co-workers reported the use of simple yttrium chloride salts $YCl_3THF_{3.5}$ and $YCl_3 \cdot 6H_2O$ used in combination with PPNCl.[106] Yttrium had shown good control of ROCOP in a previous catalyst species, so the simple YCl_3

salt was used as a base to develop a simple catalyst. The tetrahydrofuran (THF) salt $YCl_3THF_{3.5}$ was applied for practical considerations as YCl_3's small molecular weight made it difficult to weigh out in a static-prone glovebox and the THF salt decreased the solubilisation timeframes in CHO during the polymerisation. The catalyst showed a competitive catalytic activity with organometallic catalysts (TOF = 402 h^{-1}, T = 110 °C, 1 mol% catalyst loading vs anhydride) in mediating the ROCOP of BO and CA to afford perfectly alternating, low molecular weight polyester (M_n = 4,800 g·mol^{-1}, $Đ_M$ = 1.08). Upon mechanistic investigation, the $YCl_3THF_{3.5}$ mediated copolymerisation of BO and CA saw polymer chains couple with each other beyond full conversion of the monomer leading to molecular weights double that expected. They exploited this to give incredibly high molecular weight polyester at 0.04% *vs*. anhydride (M_n = 302,200 g·mol^{-1}, $Đ_M$ = 1.62), which was not usually achievable in ROCOP systems without using excessive initial monomer concentrations and thus slower polymerisation rates due to catalyst dilution. The hydrated salt $YCl_3·6H_2O$ was then investigated as a cheaper alternative that can be used in open-air reactions. Surprisingly, it was highly active for a range of copolymerisations (TOF ≤ 648 h^{-1}) affording perfectly alternating polyesters and showing good dispersity control ($Đ_M$ ≥ 1.03). However the presence of moisture did lower afforded polymer molecular weights below that expected. The catalyst system was further adapted by introducing an ionic liquid into the system with the aim of minimising the presence of water through saturation of the coordination sphere of the rare-Earth metal with the counter anions of the ionic liquid.[107] Different phosphonium-based ionic liquids at different ratios to the salt were screened to find the promising $YCl_3·6H_2O$/([H3DP]Cl (1:1 ratio) homogeneous ionic liquid active at 95 °C. This was then screened alongside other $LnCl_3·6H_2O$/([H3DP]Cl (where Ln = Gd, Ho,

Nd) catalysts for various anhydride and epoxide copolymerisations. The yttrium catalyst had a similar catalytic activity to those of the other lanthanoid catalysts but due to its lower cost and diamagnetic properties (allowing for post-polymerisation catalyst extraction), it was continued for the rest of the study. The rest of the study focused on the best manner to prepare the catalyst for polymerisation that was controlled, fast and gave high molecular weight polymers. Four types of the catalyst were prepared and screened: the metal ionic liquid formed neat, the metal ionic liquid formed in DCM (to help ensure a homogeneous mixture) and the dried versions of both catalysts. A labour intensive process was required to dry the catalyst: heating at 50 °C for 36 hours under a dynamic vacuum (10^{-3} Torr). Even then, 2.5 equivalents of water were still detected. The wet catalysts showed higher turnover frequencies than the dry catalysts likely due to residual water increasing polymerisation rates but molecular weights proved hard to control through initial conditions. Another metal ionic liquid BMI·Fe_2Cl_7 was employed to mediate the copolymerisation of anhydrides and LO.[108] The catalyst had been used as an effective initiator for homopolymerisations of styrene and ε-caprolactone with good versatility and robustness in presence of water. For the ROCOP of MA and LO at 110 °C, a turnover frequency of 16.6 h^{-1} was achieved to afford low molecular weight polyester with moderate dispersity (M_n = 1,559 g·mol^{-1}, $Đ_M$ = 1.34).

1.5 Project aims and objectives

This thesis explored the use of Lewis pair catalysts composed of metal halide salts and organic Lewis bases in the ring-opening copolymerisation of anhydrides and epoxides as a potentially low-cost and low labour-intensive route to polyesters. It aimed to expand the field of simple metal catalysts to help discover catalysts which display a competitive catalytic activity and polymerisation control with organometallic catalysts

for anhydride and epoxide ROCOP but that avoided the limitations of these catalysts (expensive, toxic and requiring complex synthesis procedures).

Recent research into simpler anhydride and epoxide ROCOP catalysts has demonstrated many effective options. However, the leading catalysts in the field, tethered organoboron catalysts and AMCs suffer from limitations related to laborious synthesis procedures and limited catalytic activities respectively.[92, 93, 101-103] Beyond AMCs, there is limited research into the use of simple metal catalysts. Metal halides offer greater ability to be tuned through selection of the metal centre or halide ligand, are readily available and have shown promise in Lewis pair systems for the lactide ROP.[109] Furthermore, during the course of this thesis' research another group has reported simple yttrium chloride based Lewis pair catalysts which demonstrated excellent catalytic activities, air-stability and unprecedently high molecular weight polyester production for the ROCOP of anhydrides and epoxides.[106]

Chapter 2 investigated a model copolymerisation using a $ZnCl_2$/DMAP Lewis pair to determine its ability to control the resultant molecular weight of a model PA and CHO copolymerisation, its relative catalytic activity compared to controls and its selectivity to produce highly alternating polyester. Chapter 3 optimised the catalyst system *via* screening of alternative organobases and metal halides to establish a competitive catalytic activity for the PA-CHO copolymerisation. Chapter 4 applied the improved copolymerisation system to the copolymerisation of a range of anhydride and epoxide monomers to demonstrate the catalyst system's capacity to synthesise functionally diverse polyesters. Chapter 5 summarised the key findings from chapters 2 to 4 and elaborates on their contribution to the field, suggesting further work to establish the

system as a viable simple catalyst alternative for the synthesis of polyesters from anhydrides and epoxides.

1.6 References

1. "Global Plastics Outlook: Economic Drivers, Environmental Impacts and Policy Options", *OECD Publishing*, Paris, https://doi.org/10.1787/de747aef-en.
2. R. Geyer, J. R. Jambeck and K. L. Law, *Sci. Adv.*, **3**, e1700782.
3. C. G. Alimba and C. Faggio, *Environ. Toxicol. Pharmacol.*, 2019, **68**, 61-74.
4. L. Cabernard, S. Pfister, C. Oberschelp and S. Hellweg, *Nat. Sustain.*, 2022, **5**, 139-148.
5. S. Shafiee and E. Topal, *Energy Policy*, 2009, **37**, 181-189.
6. Y. Zhu, C. Romain and C. K. Williams, *Nature*, 2016, **540**, 354-362.
7. M. Hong and E. Y. X. Chen, *Trends Chem.*, 2019, **1**, 148-151.
8. "Gaining momentum – Bio-based polymers grow at a CAGR of 14% between 2022 and 2027", *Nova Institute*, 2023, https://nova-institute.eu/press/?id=398.
9. J.-G. Rosenboom, R. Langer and G. Traverso, *Nat. Rev. Mater.*, 2022, **7**, 117-137.
10. M. Vert, *Biomacromolecules*, 2005, **6**, 538-546.
11. D. A. Olson, S. E. A. Gratton, J. M. DeSimone and V. V. Sheares, *J. Am. Chem. Soc.*, 2006, **128**, 13625-13633.
12. M. A. Hillmyer and W. B. Tolman, *Acc. Chem. Res.*, 2014, **47**, 2390-2396.
13. A. J. Ragauskas, C. K. Williams, B. H. Davison, G. Britovsek, J. Cairney, C. A. Eckert, W. J. Frederick, J. P. Hallett, D. J. Leak, C. L. Liotta, J. R. Mielenz, R. Murphy, R. Templer and T. Tschaplinski, *Science*, 2006, **311**, 484-489.

14. J. Yu, S. Xu, B. Liu, H. Wang, F. Qiao, X. Ren and Q. Wei, *Eur. Polym. J.*, 2023, **193**, 112076.

15. A. Di Bartolo, G. Infurna and N. T. Dintcheva, *Polymers*, 2021, **13**, 1229.

16. S. Inkinen, M. Hakkarainen, A.-C. Albertsson and A. Södergård, *Biomacromolecules*, 2011, **12**, 523-532.

17. M. J. L. Tschan, E. Brulé, P. Haquette and C. M. Thomas, *Polym. Chem.*, 2012, **3**, 836-851.

18. S. Paul, Y. Zhu, C. Romain, R. Brooks, P. K. Saini and C. K. Williams, *Chem. Commun.*, 2015, **51**, 6459-6479.

19. M. Hirschmann, F. Andriani and T. Fuoco, *Eur. Polym. J.*, 2023, **183**, 111766.

20. G. Odian, *Principles of polymerization*, John Wiley & Sons, 2004.

21. A. S. Narmon, L. M. Jenisch, L. M. Pitet and M. Dusselier, *Biodegradable Polymers in the Circular Plastics Economy*, 2022, DOI: https://doi.org/10.1002/9783527827589.ch7, pp. 205-271.

22. D. Ryzhakov, G. Printz, B. Jacques, S. Messaoudi, F. Dumas, S. Dagorne and F. Le Bideau, *Polym. Chem.*, 2021, **12**, 2932-2946.

23. O. Nuyken and S. D. Pask, *Polymers*, 2013, **5**, 361-403.

24. P. Olsén, K. Odelius and A.-C. Albertsson, *Biomacromolecules*, 2016, **17**, 699-709.

25. S. Farah, D. G. Anderson and R. Langer, *Adv. Drug Deliv. Rev.*, 2016, **107**, 367-392.

26. H. T. H. Nguyen, P. Qi, M. Rostagno, A. Feteha and S. A. Miller, *J. Mater. Chem. A*, 2018, **6**, 9298-9331.

27. J. M. Longo, M. J. Sanford and G. W. Coates, *Chem. Rev.*, 2016, **116**, 15167-15197.

28. R. F. Fischer, *J. Polym. Sci.*, 1960, **44**, 155-172.

29. T. Tsuruta, K. Matsuura and S. Inoue, *Makromol. Chem.*, 1964, **75**, 211-214.

30. V. E. Schwenk, K. Gulbins, M. Roth, G. Benzing, R. Maysenhölder and K. Hamann, *Makromol. Chem.*, 1962, **51**, 53-69.

31. K. Matsuura, T. Tsuruta, Y. Terada and S. Inoue, *Makromol. Chem.*, 1965, **81**, 258-260.

32. V. A. Hilt, K. H. Reichert and K. Hamann, *Makromol. Chem.*, 1967, **101**, 246-270.

33. J. Schaefer, R. J. Katnik and R. J. Kern, *J. Am. Chem. Soc.*, 1968, **90**, 2476-2480.

34. H. L. Hsieh, *J. Macromol. Sci. A - Chem.*, 1973, **7**, 1525-1535.

35. W. Kuran and A. Niestochowski, *Polym. Bull.*, 1980, **2**, 411-416.

36. T. Aida and S. Inoue, *J. Am. Chem. Soc.*, 1985, **107**, 1358-1364.

37. S. Huijser, E. HosseiniNejad, R. Sablong, C. de Jong, C. E. Koning and R. Duchateau, *Macromolecules*, 2011, **44**, 1132-1139.

38. E. Hosseini Nejad, A. Paoniasari, C. E. Koning and R. Duchateau, *Polym. Chem.*, 2012, **3**, 1308-1313.

39. A. Bernard, C. Chatterjee and M. H. Chisholm, *Polymer*, 2013, **54**, 2639-2646.

40. R. C. Jeske, A. M. DiCiccio and G. W. Coates, *J. Am. Chem. Soc.*, 2007, **129**, 11330-11331.

41. Y. Manjarrez, M. D. C. L. Cheng-Tan and M. E. Fieser, *Inorg. Chem.*, 2022, **61**, 7088-7094.

42. E. Hosseini Nejad, C. G. W. van Melis, T. J. Vermeer, C. E. Koning and R. Duchateau, *Macromolecules*, 2012, **45**, 1770-1776.

43. W. T. Diment, T. Stößer, R. W. F. Kerr, A. Phanopoulos, C. B. Durr and C. K. Williams, *Catal. Sci.*, 2021, **11**, 1737-1745.

44. K. Bester, A. Bukowska, B. Myśliwiec, K. Hus, D. Tomczyk, P. Urbaniak and W. Bukowski, *Polym. Chem.*, 2018, **9**, 2147-2156.

45. I. Grimaldi, F. Santulli, M. Lamberti and M. Mazzeo, *Int. J. Mol. Sci.*, 2023, **24**, 7642.

46. M. J. Sanford, L. Peña Carrodeguas, N. J. Van Zee, A. W. Kleij and G. W. Coates, *Macromolecules*, 2016, **49**, 6394-6400.

47. A. M. DiCiccio and G. W. Coates, *J. Am. Chem. Soc.*, 2011, **133**, 10724-10727.

48. F. Isnard, F. Santulli, M. Cozzolino, M. Lamberti, C. Pellecchia and M. Mazzeo, *Catal. Sci.*, 2019, **9**, 3090-3098.

49. F. Isnard, M. Lamberti, C. Pellecchia and M. Mazzeo, *ChemCatChem*, 2017, **9**, 2972-2979.

50. D.-F. Liu, L.-Q. Zhu, J. Wu, L.-Y. Wu and X.-Q. Lü, *RSC Adv.*, 2015, **5**, 3854-3859.

51. M. Proverbio, N. Galotto Galotto, S. Losio, I. Tritto and L. Boggioni, *Polymers*, 2019, **11**, 1222.

52. J. Y. Jeon, S. C. Eo, J. K. Varghese and B. Y. Lee, *Beilstein J. Org. Chem.*, 2014, **10**, 1787-1795.

53. B. A. Abel, C. A. L. Lidston and G. W. Coates, *J. Am. Chem. Soc.*, 2019, **141**, 12760-12769.

54. L.-y. Wu, D.-d. Fan, X.-q. Lü and R. Lu, *Chin. J. Polym. Sci.*, 2014, **32**, 768-777.

55. Z. Shi, Q. Jiang, Z. Song, Z. Wang and C. Gao, *Polym. Chem.*, 2018, **9**, 4733-4743.

56. S. J. Gray, K. Brown, F. Y. T. Lam, J. A. Garden and P. L. Arnold, *Organometallics*, 2021, **40**, 948-958.

57. J. Li, Y. Liu, W.-M. Ren and X.-B. Lu, *J. Am. Chem. Soc.*, 2016, **138**, 11493-11496.

58. J. Li, B.-H. Ren, S.-Y. Chen, G.-H. He, Y. Liu, W.-M. Ren, H. Zhou and X.-B. Lu, *ACS Catal.*, 2019, **9**, 1915-1922.

59. J. Li, B.-H. Ren, Z.-Q. Wan, S.-Y. Chen, Y. Liu, W.-M. Ren and X.-B. Lu, *J. Am. Chem. Soc.*, 2019, **141**, 8937-8942.

60. J. Liu, Y.-Y. Bao, Y. Liu, W.-M. Ren and X.-B. Lu, *Polym. Chem.*, 2013, **4**, 1439-1444.

61. Y. Hiranoi and K. Nakano, *Beilstein J. Org. Chem.*, 2018, **14**, 2779-2788.

62. L. Cui, B.-H. Ren and X.-B. Lu, *J. Polym. Sci.*, 2021, **59**, 1821-1828.

63. P. K. Saini, C. Romain, Y. Zhu and C. K. Williams, *Polym. Chem.*, 2014, **5**, 6068-6075.

64. A. Thevenon, J. A. Garden, A. J. P. White and C. K. Williams, *Inorg. Chem.*, 2015, **54**, 11906-11915.

65. J. A. Garden, P. K. Saini and C. K. Williams, *J. Am. Chem. Soc.*, 2015, **137**, 15078-15081.

66. W. T. Diment, G. L. Gregory, R. W. F. Kerr, A. Phanopoulos, A. Buchard and C. K. Williams, *ACS Catal.*, 2021, **11**, 12532-12542.

67. W. T. Diment, G. Rosetto, N. Ezaz-Nikpay, R. W. F. Kerr and C. K. Williams, *Green Chem.*, 2023, **25**, 2262-2267.

68. G. Si, L. Zhang, B. Han, Z. Duan, B. Li, J. Dong, X. Li and B. Liu, *Polym. Chem.*, 2015, **6**, 6372-6377.

69. B. Han, L. Zhang, M. Yang, B. Liu, X. Dong and P. Theato, *Macromolecules*, 2016, **49**, 6232-6239.

70. O. J. Driscoll, J. A. Stewart, P. McKeown and M. D. Jones, *Macromolecules*, 2021, **54**, 8443-8452.

71. C. Martín, A. Pizzolante, E. C. Escudero-Adán and A. W. Kleij, *Eur. J. Inorg. Chem.*, 2018, **2018**, 1921-1927.

72. Y. Jeong, M. K. Cho, S. Seo, H. Cho, K.-s. Son and H. Kim, *ChemCatChem*, 2023, **15**, e202201086.

73. H. K. Ryu, D. Y. Bae, H. Lim, E. Lee and K.-s. Son, *Polym. Chem.*, 2020, **11**, 3756-3761.

74. X. Liang, F. Tan and Y. Zhu, *Front Chem*, 2021, **9**, 647245.

75. J. Lustoň and Z. Maňásek, *Makromol. Chem.*, 1980, **181**, 545-555.

76. J. Lustoň and Z. Maňásek, *J. Macromol. Sci. A Chem.*, 1978, **12**, 983-994.

77. H. Yamaguchi, M. Nagasawa and Y. Minoura, *J. Polym. Sci. A Polym. Chem.*, 1972, **10**, 1207-1216.

78. A. Kameyama, K. Ueda, H. Kudo and T. Nishikubo, *Macromolecules*, 2002, **35**, 3792-3794.

79. Z. Hošťálek, O. Trhlíková, Z. Walterová, T. Martinez, F. Peruch, H. Cramail and J. Merna, *Eur. Polym. J.*, 2017, **88**, 433-447.

80. J. Xu, P. Zhang, Y. Yuan and N. Hadjichristidis, *Angew. Chem. Int. Ed.*, 2023, **62**, e202218891.

81. H. Li, J. Zhao and G. Zhang, *ACS Macro Lett.*, 2017, **6**, 1094-1098.

82. H. Li, H. Luo, J. Zhao and G. Zhang, *Macromolecules*, 2018, **51**, 2247-2257.

83. X. Kou, Y. Li, Y. Shen and Z. Li, *Macromol. Chem. Phys.*, 2019, **220**, 1900416.

84. L.-F. Hu, C.-J. Zhang, H.-L. Wu, J.-L. Yang, B. Liu, H.-Y. Duan and X.-H. Zhang, *Macromolecules*, 2018, **51**, 3126-3134.

85. D. Zhang, S. K. Boopathi, N. Hadjichristidis, Y. Gnanou and X. Feng, *J. Am. Chem. Soc.*, 2016, **138**, 11117-11120.

86. H.-Y. Ji, X.-L. Chen, B. Wang, L. Pan and Y.-S. Li, *Green Chem.*, 2018, **20**, 3963-3973.

87. A. Kummari, S. Pappuru and D. Chakraborty, *Polym. Chem.*, 2018, **9**, 4052-4062.

88. H. Li, G. He, Y. Chen, J. Zhao and G. Zhang, *ACS Macro Lett.*, 2019, **8**, 973-978.

89. H.-Y. Ji, D.-P. Song, B. Wang, L. Pan and Y.-S. Li, *Green Chem.*, 2019, **21**, 6123-6132.

90. J. Zhang, L. Wang, S. Liu and Z. Li, *J. Polym. Sci.*, 2020, **58**, 803-810.

91. X. Zhu and X. Kou, *Chem. Pap.*, 2022, **76**, 2145-2152.

92. R. Xie, Y.-Y. Zhang, G.-W. Yang, X.-F. Zhu, B. Li and G.-P. Wu, *Angew. Chem. Int. Ed.*, 2021, **60**, 19253-19261.

93. Y.-Y. Zhang, C. Lu, G.-W. Yang, R. Xie, Y.-B. Fang, Y. Wang and G.-P. Wu, *Macromolecules*, 2022, **55**, 6443-6452.

94. L. Lin, J. Liang, Y. Xu, S. Wang, M. Xiao, L. Sun and Y. Meng, *Green Chem.*, 2019, **21**, 2469-2477.

95. X. Zhu, R. Wang, X. Kou, F. Liu and Y. Shen, *Macromol. Chem. Phys.*, 2021, **222**, 2100104.

96. J. Wang, Y. Zhu, M. Li, Y. Wang, X. Wang and Y. Tao, *Angew. Chem. Int. Ed.*, 2022, **61**, e202208525.

97. D. Merckle, O. King and A. C. Weems, *ACS Sustain. Chem. Eng.*, 2023, **11**, 2219-2228.

98. N. Tsubokawa, A. Yamada and Y. Sone, *Polym. J.*, 1984, **16**, 333-340.

99. N. Tsubokawa, A. Kogure and Y. Sone, *J. Polym. Sci., Part A: Polym. Chem.*, 1990, **28**, 1923-1933.

100. N. Tsubokawa and T. Yoshihara, *J. Polym. Sci., Part A: Polym. Chem.*, 1993, **31**, 2459-2464.

101. C.-M. Chen, X. Xu, H.-Y. Ji, B. Wang, L. Pan, Y. Luo and Y.-S. Li, *Macromolecules*, 2021, **54**, 713-724.

102. X. Dou, X.-H. Liu, B. Wang and Y.-S. Li, *Chin. J. Chem .* 2023, **41**, 83-92.

103. H. Xie, L. Zheng, J. Feng, X. Wang, S. Kuang, L. Zhou, J. Jiang, Y. Xu, Y. Zhao and Z. Xu, *Polym. Chem.*, 2023, **14**, 1630-1638.

104. A. Kummari, S. Pappuru, S. Singha Roy and D. Chakraborty, *Polym. Chem.*, 2022, **13**, 4684-4691.

105. H.-Y. Ji, B. Wang, L. Pan and Y.-S. Li, *Green Chem.*, 2018, **20**, 641-648.

106. Z. A. Wood, M. K. Assefa and M. E. Fieser, *Chem. Sci.*, 2022, **13**, 10437-10447.

107. Y. Manjarrez, A. M. Clark and M. E. Fieser, *ChemCatChem*, 2023, **n/a**, e202300319.

108. M. S. Melchiors, T. Y. Vieira, L. P. S. Pereira, P. E. Feuser, V. Ferrão, F. Machado, B. A. M. Carciofi, P. H. H. de Araújo, D. de Oliveira and C. Sayer, *J. Polym. Res.*, 2022, **29**, 336.

109. S. Naumann, P. B. V. Scholten, J. A. Wilson and A. P. Dove, *J. Am. Chem. Soc.*, 2015, **137**, 14439-14445.

Chapter 2 – Kinetic study of the copolymerisation of anhydrides and epoxides mediated by a metal halide-organobase catalyst

2.1 Introduction

The ring-opening copolymerisation (ROCOP) of cyclic anhydrides and epoxides can be effectively mediated by well-defined organometallic catalyst systems with a high degree of polymerisation control and catalytic activity.[1-4] However, laborious synthetic procedures and the use of rare, expensive, and toxic metals limit their commercial application.

This has led to the research of alternative, simple anhydride-epoxide ROCOP catalysts which have aspired to compete with the well-established organometallic catalyst systems with the most promising including alkylborane-based Lewis pairs and alkali metal carboxylates (AMC)s. Alkyl (or aryl) borane-based Lewis pair systems provide metal-free ROCOP catalyst alternatives with competitive catalytic activities to organometallic catalysts (TOF ≤ 9,900 h^{-1}) but are pyrophoric and acutely toxic, which complicates their handling and storage.[5-7] In addition to this, to reach the higher catalytic activities demonstrated, the alkyl ligands have to be modified by tethering them with a quarternary salt, which requires extra synthetic steps and therefore limits their commercial viability. AMCs, on the other hand, employ commercially available, benchtop metal salts which contain inexpensive, non-toxic metals. These exceptionally simple catalysts have shown good control of copolymerisations but suffer from uncompetitive catalytic activities (TOF = 22.0 h^{-1}) without the use of further additives, such as complexation agents, or limiting the alkali metal to caesium, which is less abundant and more expensive than other alkali metals used.[8-11] These two promising catalyst systems have demonstrated that simple catalysts can deliver competitive catalytic activities and control but also remain effective while using cheap and

abundant components. However, research in the field of these simple catalysts is still in an early stage and there is scope for further investigation.

Underpinning further investigation into simple ROCOP catalysts is their need to mediate controlled polymerisations. Controlled polymerisations are desirable when studying the correlation between a polymer's structure and properties as these can be predictably manipulated by the initial conditions of the polymerisation. A controlled polymerisation is defined as one which follows first order kinetics, has a predictable degree of polymerisation and produces polymers with a narrow molecular weight distribution.[12] A polymerisation displays first order kinetics when there is a linear relationship between the logarithm of the monomer concentration and time.[13] This is shown in the equation below where [M] is the concentration of the monomer, t is time and k is the rate constant.

$$\ln[\mathrm{M}] = \ln[\mathrm{M}]_0 - kt$$

This equation can be plotted (**Figure 18**). Deviations away from a linear relationship imply either the undesired early deactivation and termination of polymerisation (downward curve) or a slow initiation therefore increasing concentration of propagating species during the polymerisation (upward curve).

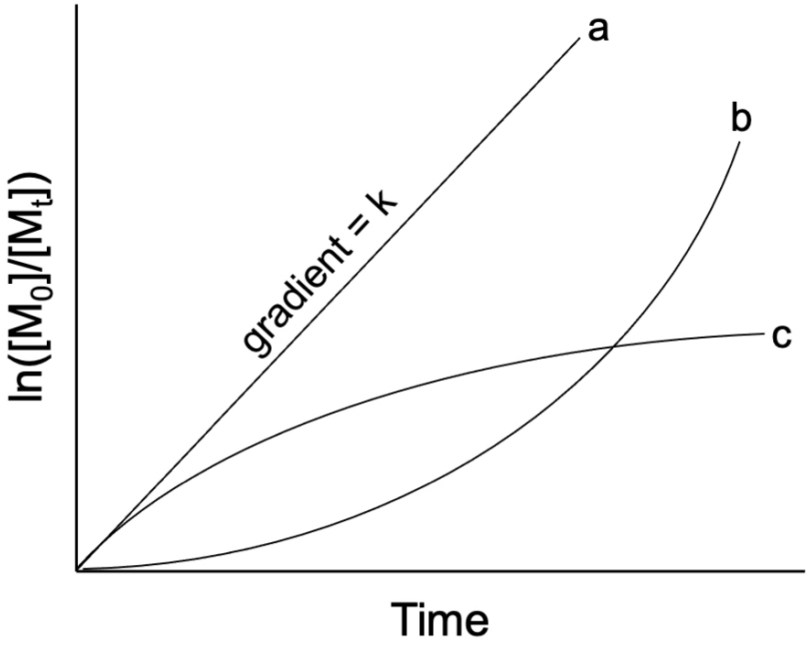

Figure 18. A kinetic plot for monomer concentration over time. a. First order polymerisation kinetics. b. Upward deviation caused by an increase in active species (slow initiation). c. Downward deviation caused by a decrease in active species (termination). Adapted from Matyajaszewski and co-workers.[12]

A predictable degree of polymerisation can be attained by the specific ratio of initial monomer concentration and initiator concentration. This means that the number-average molecular weight is a linear function of conversion throughout the polymerisation and so the initiation step must be so fast relative to propagation step that all chains start to grow simultaneously, and the number of propagating chains remains constant throughout. A narrow molecular weight distribution is achieved if polymer chains to grow simultaneously meaning that the rate of initiation is at least comparable to the rate of propagation, termination and side reactions must be negligible and the rate of propagation is faster than the rate of depolymerisation. Well-controlled polymerisation will give uniform polymer chains with similar number-average molecular weights and narrow dispersities. These values can be measured by size

exclusion chromatography, a technique that separates polymer chains by their hydrodynamic volume (size).

An early report in the development of simple anhydride and epoxide ROCOP catalysts employed simple alkyl (or aryl) zinc Lewis acids paired with common tertiary amine bases to create an effective Lewis pair catalyst system (TOF ≤ 210 h^{-1}).[14] As with alkyl (or aryl) boron reagents, the zinc salts were pyrophoric rendering them difficult to handle and store. However, a competitive catalytic activity was shown in a system that did not have to be limited to boron or alkali metal salts. The mechanistic behaviour of the copolymerisation followed a zwitterionic route (**Scheme 2**).[14] This involved the dissociation of the Lewis pair triggered by reaction conditions such as an increase in temperature. The Lewis acid then activated the epoxide monomer by increasing the electrophilicity of the epoxide moiety allowing for the Lewis base to ring-open the monomer through nucleophilic attack. The alkoxide in the zwitterion generated from this then selectively reacted with anhydride to form an ester moiety and a carboxylate nucleophile. Propagation saw the alternate regeneration of alkoxide and carboxylate intermediates in a growing chain end. This report inspired us to investigate a simple metal-based Lewis acid series, which didn't have pyrophoric characteristics.

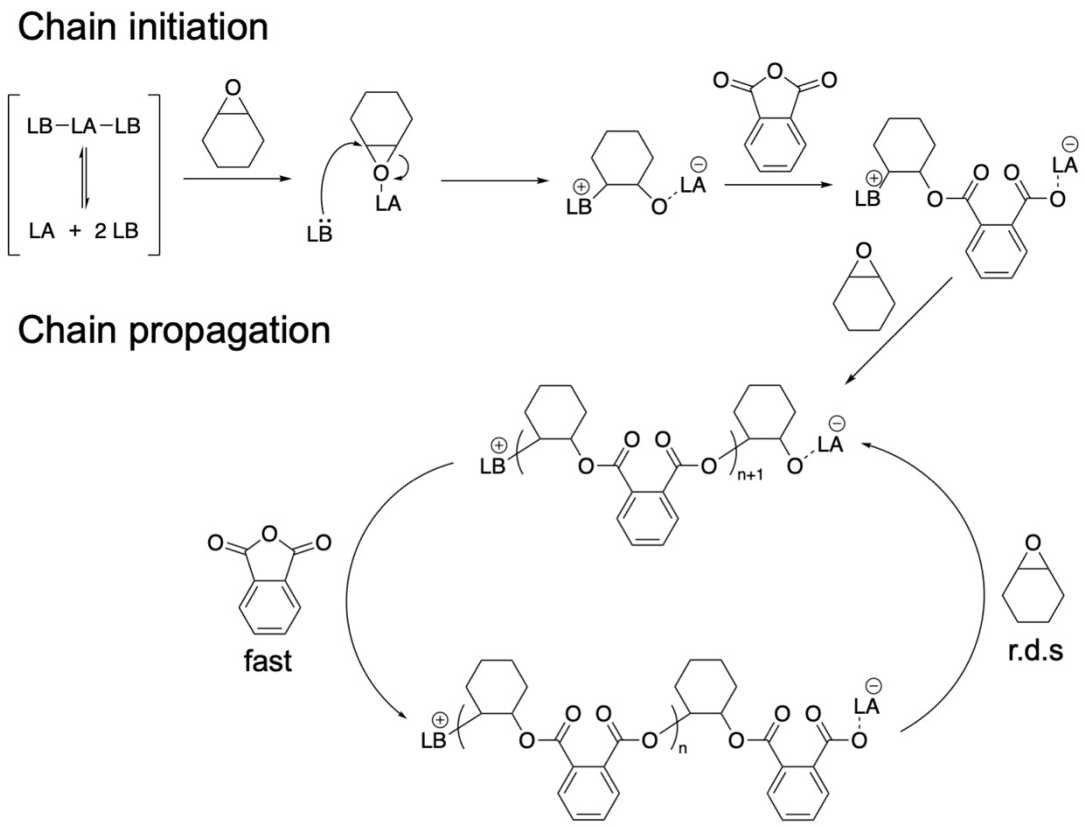

Scheme 3. A general mechanism for Lewis pair catalysed ROCOP of CHO and PA. Adapted from Li and co-workers.[14]

Metal halide salts fit the requirement for simple, commercially available reagents. In addition, they have a wide scope of tunability with both metal centre and ligand. This showed potential for their employment as a Lewis acid in a simple Lewis pair ROCOP catalyst. Indeed, during the course of our research, the Fieser group reported the successful use of metal halide-based $YCl_3THF_{3.5}$ (THF = tetrahydrofuran) and $YCl_3 \cdot 6H_2O$ salts alongside PPNCl as Lewis pairs for catalysing the ROCOP of anhydrides and epoxides.[15] The catalysts gave competitive catalytic activities (TOF ≤ 648 h^{-1}) and afforded polymers with unprecedentedly high molecular weights (M_n = 302,200 $g \cdot mol^{-1}$), although limited to a specific combination of comonomers. Furthermore, the hydrated solvent gave excellent control by preventing side reactions when used in air (which was unusual for ROCOP catalysts).

For a systematic investigation into the use of cheaper and more available metal halide salts as anhydride-epoxide ROCOP catalysts, a general understanding of the nature of the copolymerisation needed to be established. In this chapter, a model copolymeristion was established to systematically investigate the behaviour of anhydride and epoxide copolymerisation using the previously unreported metal halide zinc chloride ($ZnCl_2$) and organobase 4-dimethylaminopyridine (DMAP) Lewis pair catalyst system. Initially, a kinetic investigation aimed to determine if the copolymerisation was controlled, compare its catalytic activity with other reported catalyst systems and evaluate its ability to afford high molecular weight polyester. However, the study revealed that the copolymerisation lacked control and so the focus of the chapter shifted to understanding the behaviour of the copolymerisation.

2.2 Results and discussion

2.2.1 Establishing a model copolymerisation

To compare the nature and effectiveness of metal halide-based Lewis pair catalysts in the ROCOP of anhydrides and epoxides with previously reported catalyst systems, a model copolymerisation was established (**Scheme 3**). Zinc chloride Lewis acid and DMAP Lewis base were explored as a catalytic Lewis pair. The use of toluene (110 °C reaction temperature) and comonomers CHO and PA were standard reaction conditions used in literature which allowed for ease of comparison.[16] 4-methoxybenzyl alcohol (4-MBA) was added as a chain-transfer agent (CTA) with the intention of manipulating the end-group selectivity of the resultant polyester towards easily-reactable alcohol groups.[17] Special care was taken to avoid the problems of unwanted initiation and chain-transfer from monomer impurities and adventitious moisture which have been reported in literature.[16] Rigorous measures were taken to purify both monomers (see section 2.5.4 in the experimental details) and the reaction was conducted in an inert atmosphere with all reagents stored in an inert atmosphere glove box after drying.

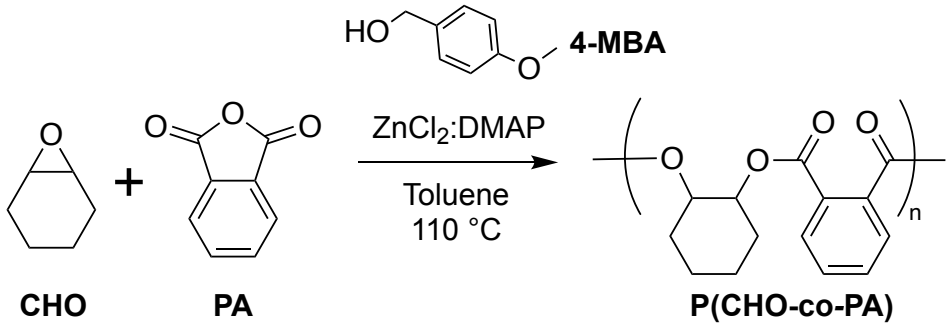

Scheme 4. The model copolymerisation. Components' initial concentrations were $[PA]_0/[CHO]_0/[ZnCl_2]_0/[DMAP]_0/[4\text{-}MBA]_0$ = 50:50:1:1:1 and a 2 mol·dm^{-3} concentration was used for each respective monomer in toluene.

Due to the low solubility of zinc chloride in toluene at room temperature, a stock solution of the salt could not be employed and so copolymerisations had to be conducted at a scale that a minimum amount of catalyst could be measured out in a static-prone glove box (≥ 2 mg). Furthermore, when aliquots were retrieved from the reaction mixture during copolymerisation moisture contamination was found to be unavoidable, which prompted unwanted side reactions and afforded polymers with high ether content. Therefore, the copolymerisation was conducted in a sealed teflon vial which once loaded inside the glove box was transferred to an oil bath and then upon completion of the desired reaction time was quenched in an ice bath.

The $ZnCl_2$/DMAP system was found to successfully catalyse the copolymerisation with a moderate catalytic activity (93% conversion in 5 h). ^{1}H NMR spectroscopy analysis of the precipitated polymer confirmed that it was poly(CHO-*co*-PA) in accordance with literature reports (**Figure 19**).[15, 18] As expected for successful copolymerisation, the epoxide moiety in the CHO monomer at δ = 2.92 ppm was absent and instead an ester (C) (δ = 5.14 ppm) indicating successful alternating copolymerisation of the epoxide and anhydride comonomers was formed. A small ether peak (F) (δ = 3.47-3.63 ppm) was seen indicating that the side-reaction of homopolymerisation of CHO had occurred to a small degree (4% ether linkages). The incorporation of 4-MBA in the polyester was evidenced by two peaks: the prominent methoxy environment (H) at δ = 3.77 ppm and an aryl ring environment (G) at δ = 6.86 ppm. Neither of these environments had shifted significantly from their position in free 4-MBA as when incorporated as a chain-end group, both environments were furthest away from the rest of the polymer. The other two 4-MBA environments nearer the rest of the polymer were hypothesised to have shifted from their position in free 4-MBA and were hidden behind the ester peak and

incorporated-PA peaks in the ^{1}H NMR spectrum respectively. DMAP was also present in the copolymer with its methyl environment (K) at δ = 2.84 and two aryl environments (I and J) at δ = 8.31 and δ = 6.40 respectively. A comparison of the integral of the methyl peaks of each DMAP and 4-MBA respectively showed a 1.6:1 ratio of 4-MBA to DMAP present.

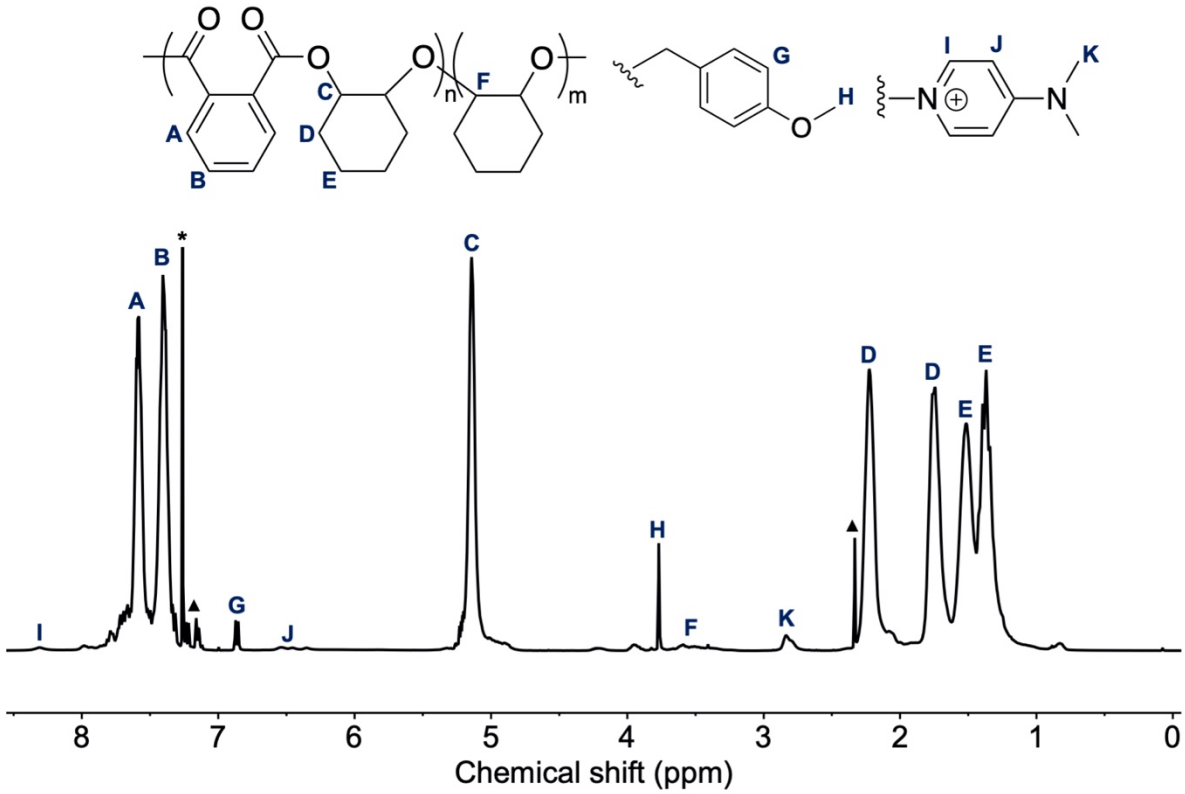

Figure 19. The ^{1}H NMR spectrum of precipitated (from $CHCl_3$ into methanol/HCl) P(PA-co-CHO) copolymer derived from the model copolymerisation after 5 h ($CDCl_3$, 400 MHz, 298 K). * = $CHCl_3$, ▲ = toluene.

^{13}C–{^{1}H} NMR spectroscopy analysis (**Figure 20**) backed up the findings of ^{1}H NMR spectroscopy for a successful copolymerisation in accordance with literature reports.[18] The epoxide environment for CHO at δ = 51.8 ppm was absent and instead the ester environment (E, E') at δ = 74.7 ppm was present. It gave clearer evidence of 4-MBA present as a chain end-group with environments H-L representing present. Only the

methyl environment M from DMAP could be seen due to its low concentration in the copolymer.

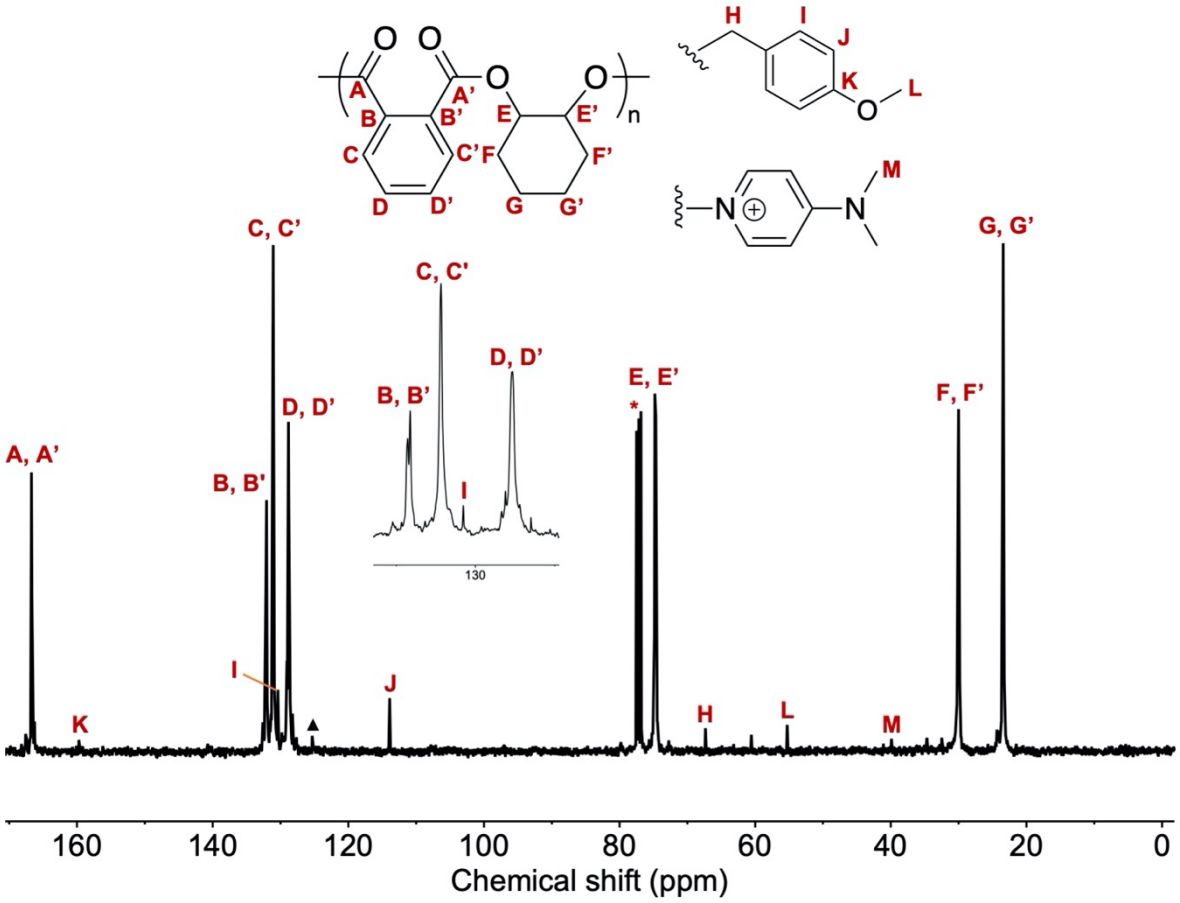

Figure 20. The $^{13}C–\{^{1}H\}$ NMR spectrum of precipitated (from $CHCl_3$ into methanol/HCl) P(PA-co-CHO) copolymer derived from the model copolymerisation after 5 h ($CDCl_3$, 101 MHz, 298 K). * = $CHCl_3$, ▲ = toluene.

Size exclusion chromatography (SEC) analysis of the precipitated polymer confirmed the synthesis of a polymer (M_n = 2,718 g·mol^{-1}, $Đ_M$ = 1.20) (**Figure 21**). As expected, employment of 4-MBA as a CTA led to a monomodal molecular weight distribution. This contrasted with the bimodal distribution often seen in ROCOP due to the presence of phthalic acid impurities which can initiate copolymerisation on both ends of the molecule to give polymer chains with double the length of those initiated by monofunctional initiators. It was hypothesised based on previous literature reports of

the use of CTAs that chain transfer reactions had transferred the polymer chains from the phthalic acid to the monofunctional alcohol resulting in a monomodal distribution.[19, 20]

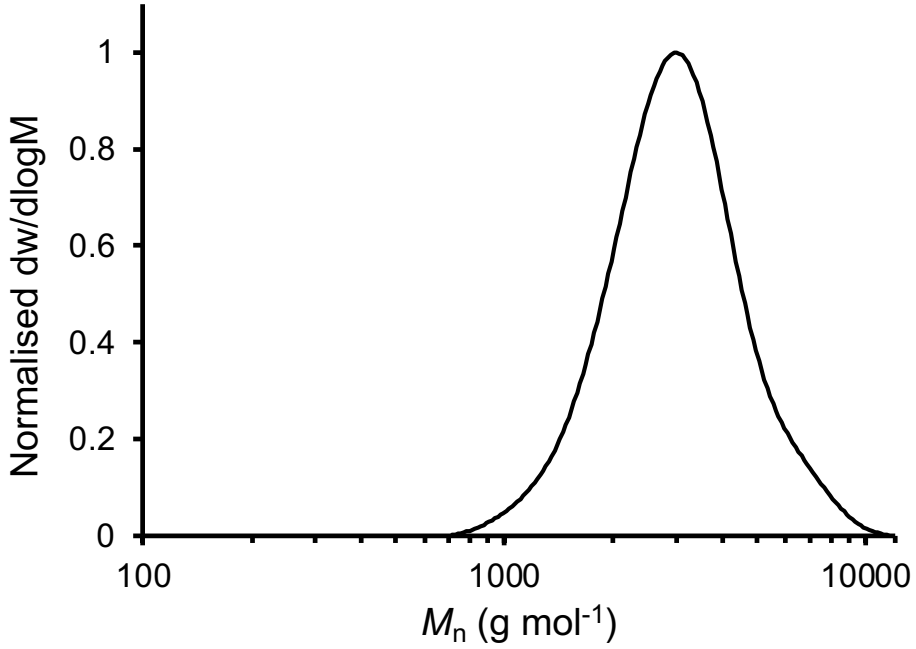

Figure 21. The size exclusion chromatogram of the molecular weight distribution of the P(PA-co-CHO) copolymer derived from the model copolymerisation after 5 h. Molecular weight was determined against poly(styrene) standards using tetrahydrofuran (THF) (0.5% NEt_3) as an eluent.

Based on these results, it was confirmed that $ZnCl_2$/DMAP effectively mediated the ROCOP of PA and CHO with minimal homopolymerisation and suggested that both 4-MBA and DMAP were present as an end-group in the resultant copolymer.

2.2.2 Kinetic study

To determine if the copolymerisation was controlled, a kinetic study was conducted for the model copolymerisation established previously which measured monomer conversion, afforded polymer molecular weight and molecular weight distribution over a series of six timepoints (**Table 1**).

Table 1. Kinetic study of the model copolymerisation. All copolymerisations were conducted with $[PA]_0/[CHO]_0/[ZnCl_2]_0/[DMAP]_0/[4\text{-}MBA]_0$ at 50:50:1:1:1, in toluene (2 mol dm^{-3} monomer concentration in toluene) at 110 °C.

Entry	Time (h)	Monomer conversion[a] (%)	M_n (SEC)[b] ($g \cdot mol^{-1}$)	$Đ_M$
1	0.5	10	414	1.19
2	1	21	566	1.26
3	2	34	874	1.31
4	3	53	1348	1.24
5	4	77	-	-
6	5	93	2718	1.20

[a]Conversion of CHO calculated from the ^1H NMR spectrum ($CDCl_3$, 400 MHz) of the reaction mixture at the given timepoint. [b]Molecular weight as calculated by SEC analysis using THF (0.5% NEt_3) as an eluent with PS standards.

The kinetic study of the copolymerisation found that polymerisation rate did not follow a first-order relationship with time (**Figure 22**). Instead, the rate of polymerisation increased over time, indicating an increase in the number of propagating chains during the copolymerisation. These unexpected results were not observed for similar copolymerisations in literature. The main difference between the catalyst system and literature systems was the specific use of a metal halide as the Lewis acid. It was speculated that either the poor solubility of the metal halide salt was causing the effect of the Lewis acid on initiation to increase over the time taken for all of the salt to dissolve once heated or that there was a difference in the mechanism of copolymerisation compared with Lewis pair systems used previously in literature. Fieser and co-workers had noted that solubility issues had been a problem when they

employed YCl_3/PPNCl Lewis pair catalysts for anhydride/epoxide ROCOP.[15] On the other hand Dove and co-workers had noted that poor solubility of metal halides in toluene used in Lewis pair systems to catalyse lactide ROP had not been a factor in polymerisation performance.[21]

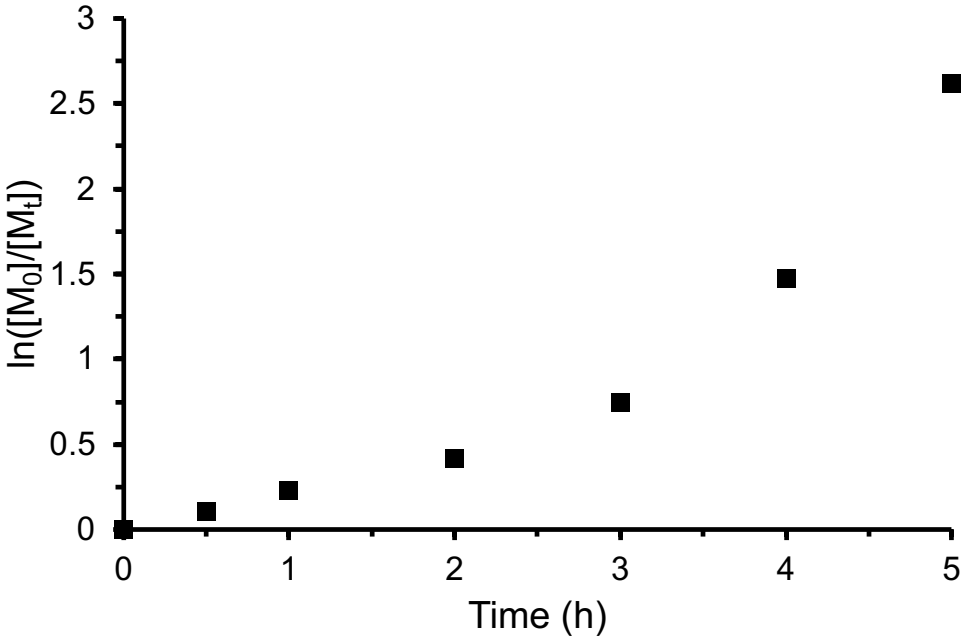

Figure 22. The kinetic plot for the model copolymerisation of PA and CHO at 110 °C using $ZnCl_2$, DMAP and 4-MBA ($[PA]_0/[CHO]_0/[ZnCl_2]_0/[DMAP]_0/[4\text{-}MBA]_0$ = 50:50:1:1:1) in toluene (2 mol dm^{-3} PA concentration).

The chain length of the afforded polyester did not show a linear relationship with monomer conversion as expected from a controlled polymerisation (**Figure 23**). Before 20% conversion was reached, chain length remained short (M_n < 600 $g \cdot mol^{-1}$), suggesting that initiation was occurring instead of propagation. This correlated with the understanding that the number of propagating chains had increased over time. The induction time was further elaborated on by the size exclusion chromatograms taken at each timepoint which revealed multimodal molecular weight distributions at early timepoints with little increase in number average molecular weight (M_n) over time,

which later converged into monomodal distributions at higher molecular weights over time (**Figure 24**). This data suggested that multiple components were acting as initiators in the system causing a variety of molecular weight distributions to form that were then transferred to one (or fewer) chain-end acting as a CTA during propagation once the initiators were consumed. The lack of control in the polymerisation was not due to unwanted side reactions as the ^{1}H NMR spectrum of the resultant polyester did not show significant ether linkages (5%) (**Figure 19**) and the polymer dispersities were narrow once monomodal ($Đ_M$ = 1.20) (**Table 1**). This indicated that the copolymerisation had the potential to be controlled.

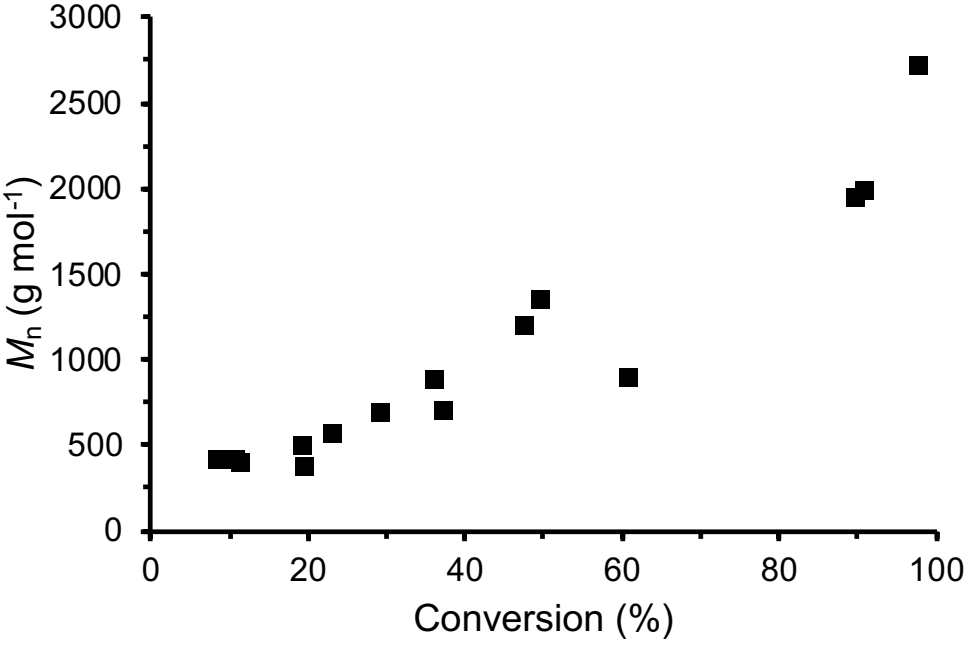

Figure 23. Number average molecular weight (M_n) plotted against monomer conversion for the model copolymerisation of PA and CHO at 110 °C using $ZnCl_2$, DMAP and 4-MBA ($[PA]_0/[CHO]_0/[ZnCl_2]_0/[DMAP]_0/[4\text{-}MBA]_0$ = 50:50:1:1:1) in toluene (2 mol dm^{-3} PA concentration).

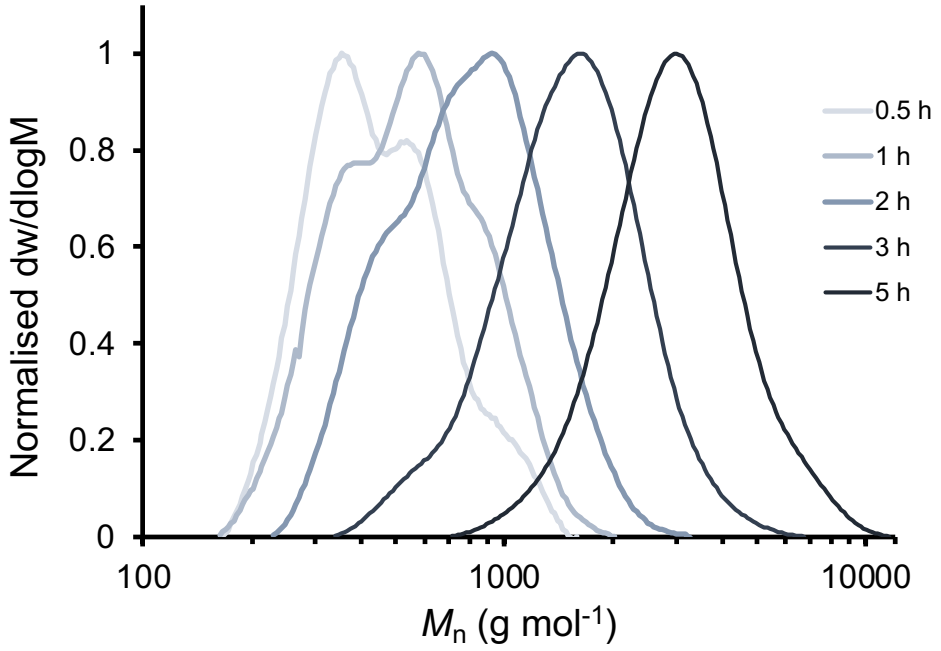

Figure 24. The size exclusion chromatograms of the molecular weight distribution of the P(PA-co-CHO) copolymer derived from the model copolymerisation at each timepoint during the kinetic study. Molecular weight was determined against poly(styrene) standards using tetrahydrofuran (THF) (0.5% NEt_3) as an eluent.

2.2.3 Control polymerisations

A series of control copolymerisations were run with the aim of identifying each catalytic component's role on the control and activity of the copolymerisation (**Table 2**).

Table 2. A comparison of the model copolymerisation and control copolymerisations with one or more components omitted. All copolymerisations were conducted in toluene (2 mol dm^{-3} monomer concentration in toluene) at 110 °C for 5 h.

Entry	$[PA]_0/[CHO]_0/[ZnCl_2]_0/[DMAP]_0/[4\text{-}MBA]_0$	Monomer conversion[a] (%)	M_n (SEC)[b] ($g \cdot mol^{-1}$)	$Đ_M$	Ester linkage[c] (%)
6 ($ZnCl_2$ + DMAP + 4-MBA)	50:50:1:1:1	93	2216	1.19	95
7 ($ZnCl_2$ + DMAP)	50:50:1:1:0	59	911	1.26	98
8 (DMAP + 4-MBA)	50:50:0:1:1	97	3761	1.31	99
9 ($ZnCl_2$ + 4-MBA)	50:50:1:0:1	99	-	-	42
10 (DMAP)	50:50:0:1:0	52	9831	1.18	90

[a]Conversion of CHO calculated from the ^{1}H NMR spectrum ($CDCl_3$, 400 MHz) of the reaction mixture at the given timepoint. [b]Molecular weight as calculated by SEC analysis using THF (0.5% NEt_3) as an eluent with PS standards. [c]Percentage of ester linkages determined by the ratio of the integrated height of the ester peak and ether peak in the ^{1}H NMR spectrum of the precipitated polyester product.

DMAP was shown to be crucial for the catalyst system's selectivity. In its absence, the homopolymerisation of CHO was catalysed (**Entry 9**) as was shown by the big polyether peaks in the ^{1}H NMR spectrum of the resultant copolymer (**Figure 25**). This was expected as in early ROCOP catalyst systems which employed simple metal salts and an alcohol, the cationic homopolymerisation of CHO was promoted in numerous cases.[22, 23] DMAP was also capable of catalysing the copolymerisation without a Lewis acid as reported in literature (**Entry 8** and **Entry 10**).[24] A comparison of the ^{1}H NMR spectra between the model copolymerisation (**Entry 6**) and an analogous

copolymerisation without 4-MBA (**Entry 7**) showed that the selectivity does not suffer in the absence of 4-MBA (**Figure 26**).

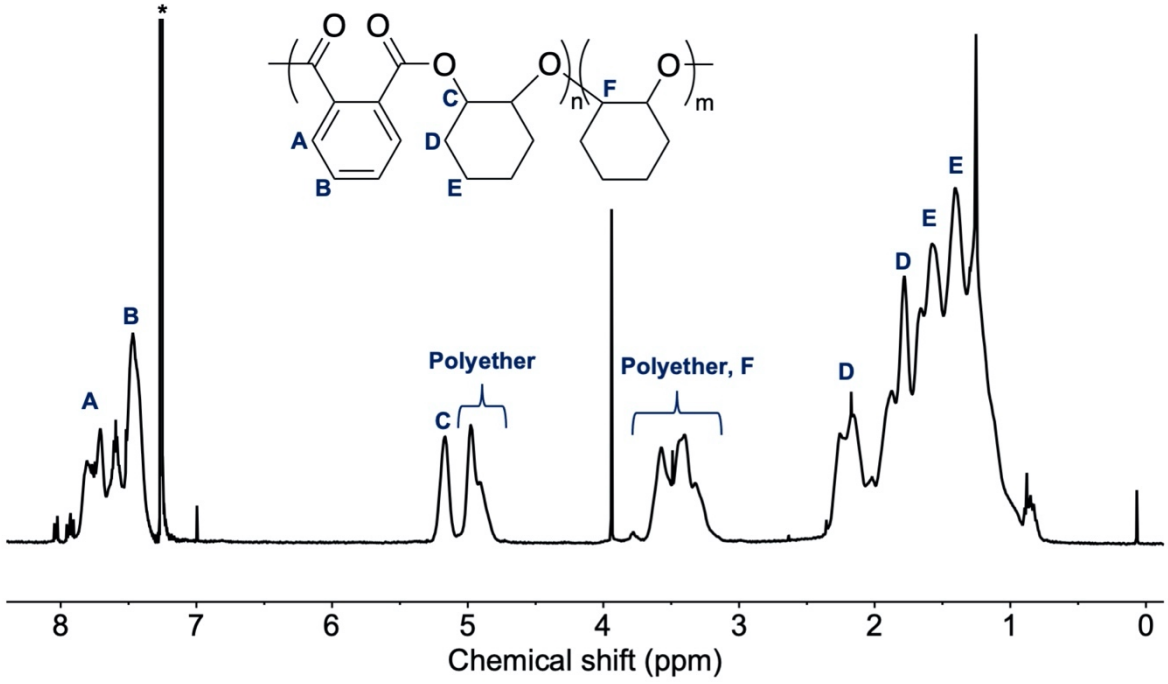

Figure 25. The ^{1}H NMR spectrum of precipitated (from $CHCl_3$ into methanol/HCl) P(PA-co-CHO) copolymer derived from a copolymerization of PA and CHO using $ZnCl_2$/4-MBA as a catalyst system after 5 h ($CDCl_3$, 400 MHz, 298 K). * = $CHCl_3$.

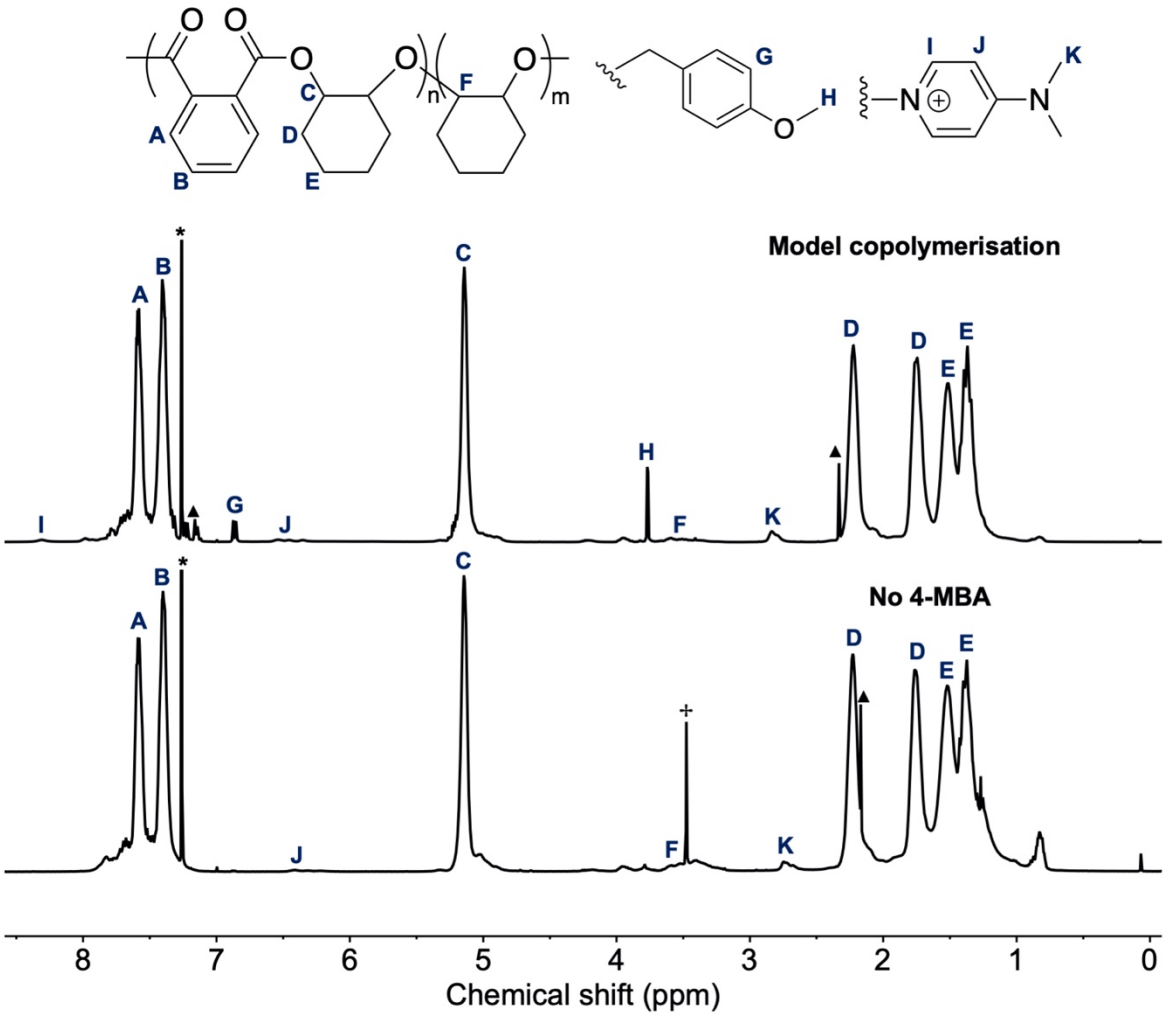

Figure 26. A comparison of the ^{1}H NMR spectra of precipitated (from $CHCl_3$ into methanol/HCl) P(PA-co-CHO) copolymer derived from copolymerizations of PA and CHO using $ZnCl_2$/DMAP as a catalyst with (**Entry 6**, top) or without (**Entry 7**, bottom) 4-MBA after 5 h ($CDCl_3$, 400 MHz, 298 K). * = $CHCl_3$, ▲ = toluene, $^{+}$ = methanol.

A comparison of the kinetic studies of each of the control conditions and the model copolymerisation (**Figure 27**) revealed that zinc chloride had a regressive effect on the polymerisation rate (**Entry 6**) with a higher polymerisation rate achieved in its absence (**Entry 8**). This suggested that the Lewis acid was playing a role in the mechanism of copolymerisation as anticipated, albeit not a positive one with zinc chloride. It was also shown that the addition of zinc chloride led to a loss in control of the copolymerisation

and instead produced an accelerating copolymerisation rate over time. This backed up the hypothesis drawn from previous data that its solubility or unknown effect on the copolymerisation's mechanism was responsible for the lack of first-order copolymerisation rate. The addition of 4-MBA served to increase the rate of copolymerisation (**Entry 8** *vs.* **Entry 10** or **Entry 6** *vs.* **Entry 7**). This was unexpected as literature reports suggested that chain transfer agents have no effect on copolymerisation rate. For example, Duchateau and co-workers carried out a systematic investigation of the effect of alcohol, water, acids and amines CTAs on the ROCOP of limonene oxide and PA using a chromium salen and PPNCl catalyst system.[25] They found that when CTAs were added, they had a negligible effect on monomer conversion compared to when they were absent as chain transfer reactions occurred at a faster rate than chain growth.

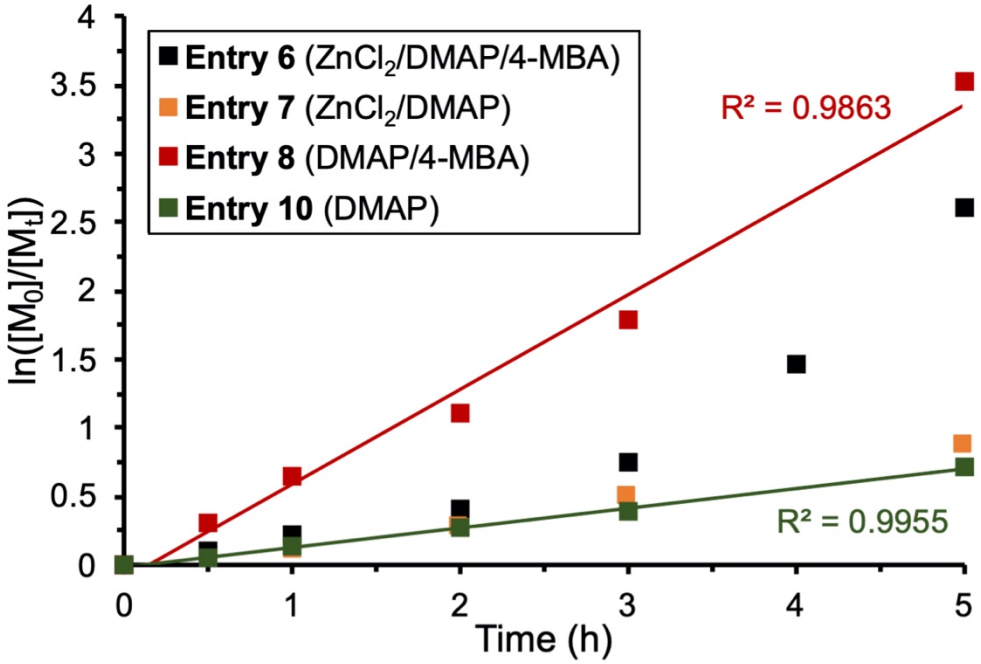

Figure 27. A comparison of the kinetic plots for the copolymerisation of PA and CHO at 110 °C using the model copolymerisation conditions (**Entry 6**) and control conditions (**Entries 7**, **8** and **10**) in toluene (2 mol dm^{-3} PA concentration).

A comparison of monomer conversion and afforded polyester chain length (**Figure 28**) showed that 4-MBA acted to shorten the chain length as expected. Interestingly, zinc chloride also acted to shorten the chain length suggesting that it may play a role in chain transfer. If zinc chloride did play this role and could only dissolve over the course of the experiment, this may have explained why chain propagation accelerated over time in its presence.

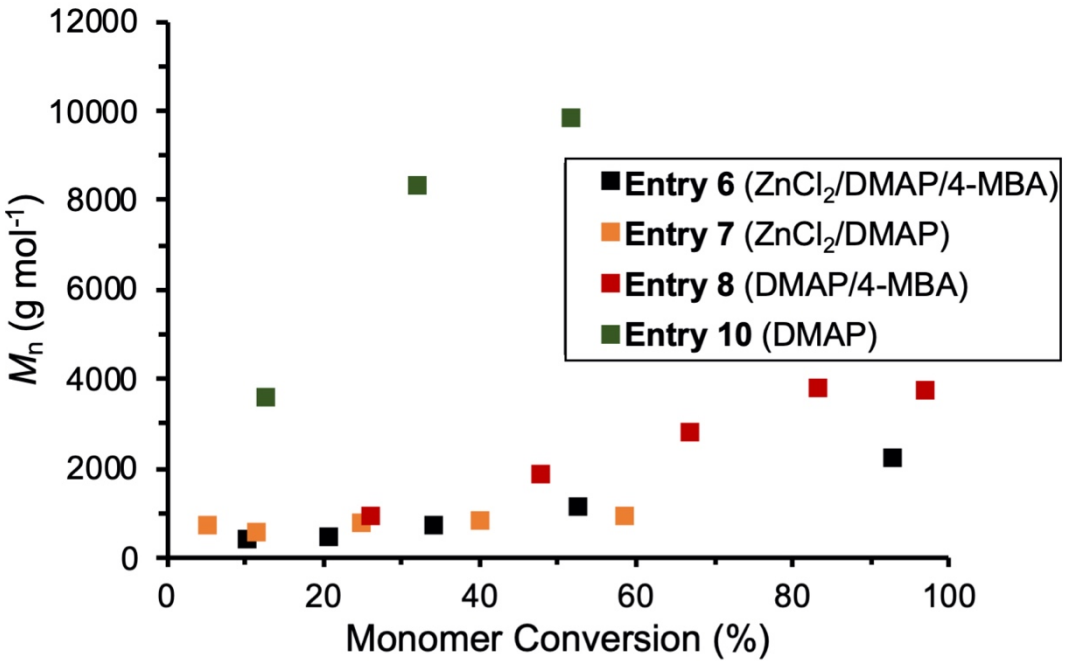

Figure 28. A comparison of the number average molecular weight (M_n) plotted against monomer conversion for the model copolymerisation (**Entry 6**) and control copolymerisations (**Entries 7**, **8** and **10**) at each timepoint during the kinetic study.

2.2.4 Molecular weight control

Molecular weights of the synthesised polyesters had been lower than theoretically expected when a single initiator was assumed. This was common for ROCOP because of adventitious water and monomer impurities present acting as CTAs. To gain a better understanding of which components were playing a role as an initiator or CTA and

whether the resultant polymer chain length could be controlled by the ratio of initial catalyst to monomer concentrations, a series of experiments were conducted (**Table 3**).

Table 3. A series of copolymerisations with different concentrations of 4-MBA. All copolymerisations were conducted in toluene (2 mol dm^{-3} monomer concentration in toluene) at 110 °C for 5 h.

Entry	$[PA]_0/[CHO]_0/[ZnCl_2]_0/[DMAP]_0/[4\text{-}MBA]_0$	Monomer conversion[a] (%)	M_n (SEC)[b] ($g \cdot mol^{-1}$)	$Đ_M$
11	50:50:1:1:0.2	90	2673	1.19
12	50:50:1:1:0.5	93	2611	1.20
13	50:50:1:1:1	96	2279	1.18
14	50:50:1:1:2	95	1493	1.18
15	50:50:1:1:5	100	993	1.18

[a]Conversion of CHO calculated from the ^1H NMR spectrum ($CDCl_3$, 400 MHz) of the reaction mixture at the given timepoint. [b]Molecular weight as calculated by SEC analysis using THF (0.5% NEt_3) as an eluent with PS standards.

Firstly, the effect of varying the concentration of 4-MBA on the M_n of the resultant polymer was studied (**Table 3, Figure 29**). It was expected that decreasing the amount of 4-MBA would lead to an increase in the polymer's M_n as a lower concentration of CTA present would lead to fewer propagating chains. Decreasing the concentration of 4-MBA did see an increase in afforded polymer molecular weight, but the effect plateaued off at a molecular weight lower than theoretically expected with no CTA present. This indicated that other components were also acting as CTAs and so when the concentration of 4-MBA became insignificant, chain transfer was still present.

When 4-MBA concentration was increased, this increased the concentration of CTAs and so lowered the chain lengths further.

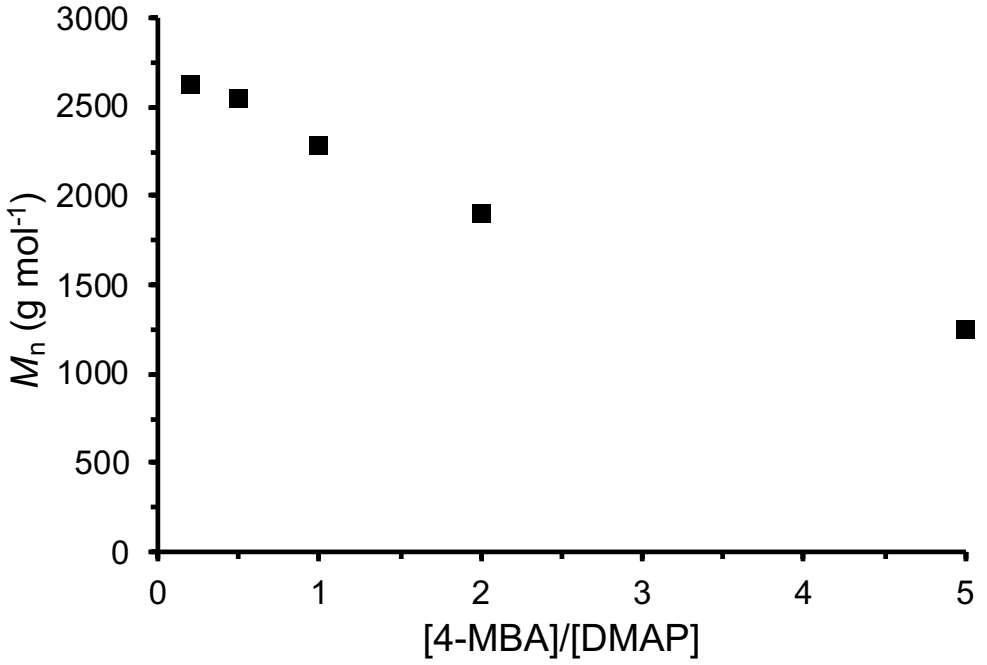

Figure 29. The number average molecular weight (M_n) plotted against against the ratio of 4-MBA against DMAP used in the catalyst system (**Entries 11-15**).

Secondly, when the concentration of DMAP was varied relative to other components a significant change was observed. Halving the concentration of DMAP ($[PA]_0/[CHO]_0/[ZnCl_2]_0/[DMAP]_0/4\text{-}MBA]_0$ = 50:50:1:0.5:1) afforded a polyester with 45% ether linkages afforded indicating significant CHO hompolymerisation. This supported how important the Lewis base was in the mechanism at preventing homopolymerisation side reaction which can be catalysed by the metal salt and alcohol. Manipulating its initial concentration to tune molecular weight is therefore not possible.

Thirdly, the concentration of the comonomers together were varied relative to the catalyst system components seeing an increase of number average molecular weight

afforded with increase in initial monomer concentration (**Table 4**, **Figure 30**). Tentatively, a linear relationship was seen to occur below and including a $[PA]_0/[4\text{-}MBA]_0$ ratio of 50:1. However, at a ratio of 100:1, the molecular weight achieved was lower than expected from the linear trend. At an even higher ratio of 250:1, the polymerisation would not achieve more than a 40% conversion of monomer within 24 h. This was unlikely to be the result of catalyst dilution deactivating the catalyst as the increase in monomer concentration was negligible against the unvarying amount of toluene that the catalyst dissolves in. Instead, an explanation for the observation has been reported by Merna and co-workers in literature who noticed the same trend. They attributed it to the fact that when there was an increase in PA concentration, the diacid impurity in the PA had become relatively more concentrated compared to the catalyst and so became the dominant growing centre. This meant that molecular weight of the afforded polyester became dependent not on catalyst concentration but on PA purity after this point. The catalyst still retained a determining effect on the rate of the polymerisation as it was required to activate the phthalic anhydride. According to rough ^1H NMR spectroscopy analysis, the purity of the PA used in this work was found to be 99.47% (see section 2.5.4 of the experimental details). This meant that at a $[PA]_0/[4\text{-}MBA]_0$ ratio of 100:1, the ratio of $[4\text{-}MBA]_0$ to $[\text{phthalic acid}]_0$ was 1:0.53 confirming that the monomer impurity's concentration would have been great enough to act as a competitive initiator or CTA.

Table 4. A series of copolymerisations with different concentrations of comonomers. All copolymerisations were conducted in toluene (2 mol dm^{-3} monomer concentration in toluene) at 110 °C.

Entry	$[PA]_0/[CHO]_0/[ZnCl_2]_0/[DMAP]_0/[4\text{-}MBA]_0$	Time (h)	Monomer conversion[a] (%)	M_n (SEC)[b] ($g \cdot mol^{-1}$)	$Đ_M$
16	10:10:1:1:1	3	95	604	1.20
17	25:25:1:1:1	6	98	1233	1.26
18	50:50:1:1:1	6	96	2279	1.18
19	100:100:1:1:1	6	95	3463	1.27
20	250:250:1:1:1	9	40	3256	1.26

[a]Conversion of CHO calculated from the ^1H NMR spectrum ($CDCl_3$, 400 MHz) of the reaction mixture at the given timepoint. [b]Molecular weight as calculated by SEC analysis using THF (0.5% NEt_3) as an eluent with PS standards.

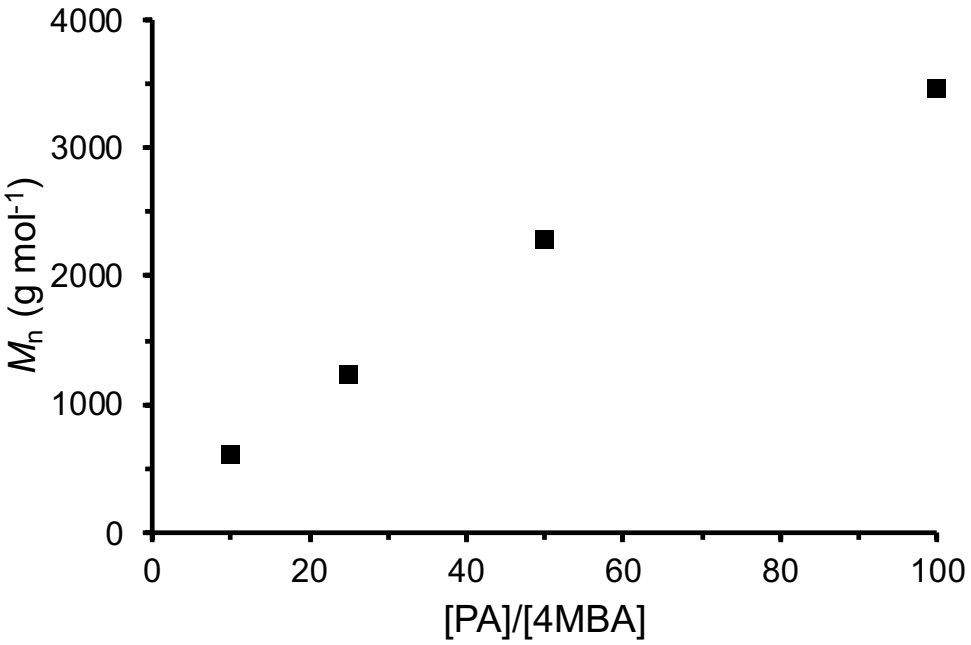

Figure 30. A plot of afforded polyester's number average molecular weight against the ratio of monomer (e.g. PA) against catalyst component (e.g. 4-MBA) used in the catalyst system (**Entries 16-20**).

2.2.5 Chain-end analysis

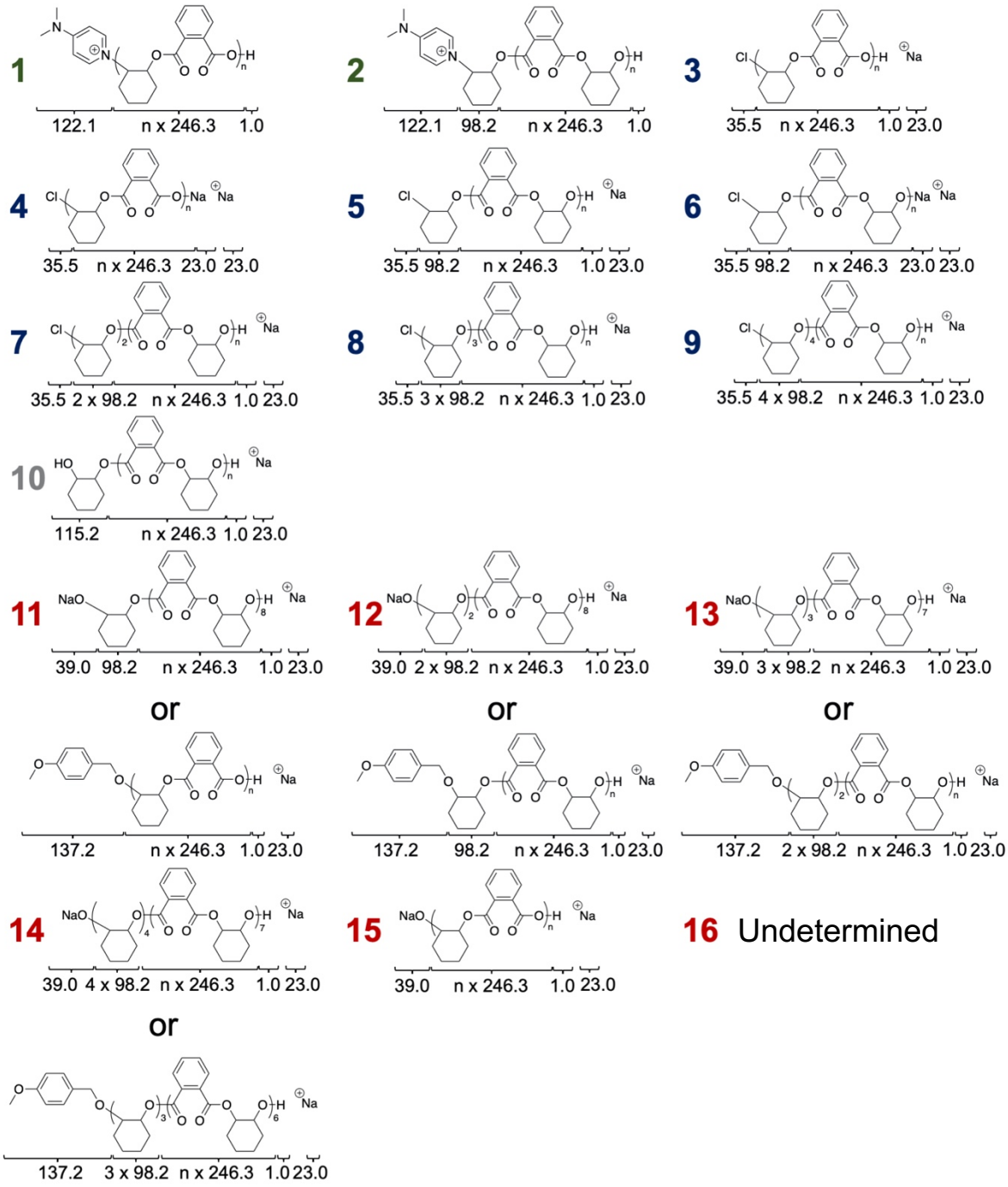

Figure 31. Polymer structures with chloride, sodium, hydroxide, and 4-MBA end-capped chains relating to peaks seen in MALDI-ToF MS analysis. Peak 16 was not able to be matched to an expected structure.

It was clear that the mechanism of the catalyst system was more complex than initially expected. For this reason, matrix-assisted laser desorption/ionisation time of flight

mass spectroscopy (MALDI-ToF MS) analysis was conducted with the aim of determining what chain-ends existed in the afforded polyester and which were dominant (see section 2.5.2.4 in the experimental details for the method). This information could then be used to help determine which components played the roles of initiators and chain-transfer agents.

Table 5. Copolymerisations planned for analysis with MALDI-ToF MS. All copolymerisations were conducted at 110 °C. Copolymerisations conducted in toluene used a 2 mol dm^{-3} monomer concentration in the solvent.

Entry	LA	LB	$[PA]_0/[CHO]_0/[LA]_0/[LB]_0/[4\text{-MBA}]_0$	Solvent	Time (min)
18	$ZnCl_2$	DMAP	50:50:1:1:1	Toluene	300
21	$ZnCl_2$	PPNCl	50:50:1:1:1	Toluene	300
22*	-	PPNCl	50:100:1:1:0	-	8
23*	-	PPNCl	50:100:1:1:1	-	8
24	$MgCl_2$	PPNCl	50:100:1:1:1	-	8
25	$MgBr_2$	PPNCl	50:100:1:1:1	-	8
26	MgI_2	PPNCl	50:100:1:1:1	-	8

The MALDI-ToF MS spectrum for the model copolymerisation (**Entry 18, Figure 32**) showed the expected bell-shaped molecular weight distribution of polymer chains interspersed with an m/z interval of 246.3 $g \cdot mol^{-1}$ between consecutive peaks corresponding to the addition of a [CHO + PA] repeating unit to the growing chain, which indicated a successfully alternating microstructure. The two most prominent peaks (1, 2) corresponded with polymer structures containing DMAP end-groups.

These two distributions had been observed in literature when DMAP was employed in catalyst systems for anhydride and epoxide ROCOP and confirmed that DMAP directly initiated polymer chains as expected.[14, 18, 26, 27] A multitude of lower intensity peaks could also been seen in the spectrum. These were suspected to be polyester without DMAP end-groups. Due to the DMAP end-group's cationic nature, it was known to disproportionately dominate MALDI-ToF MS spectra as seen by Duchateau and co-workers in literature due to the DMAP end-groups cationic charge.[25] While a cationic agent had initially been employed to observe expected structures that were not DMAP end-capped, to confirm which peaks corresponded to DMAP, the MALDI-ToF MS analysis was re-run without the cationic agent required to ionise polymer chains (**Figure 32**). Indeed, the multitude of smaller peaks disappeared, while the peaks attributed to DMAP end-capped structures (1, 2) remained. This both confirmed that DMAP end-capped the polymer chains dominated the MALDI-ToF MS spectrum and that polymer chains end-capped by other species existed.

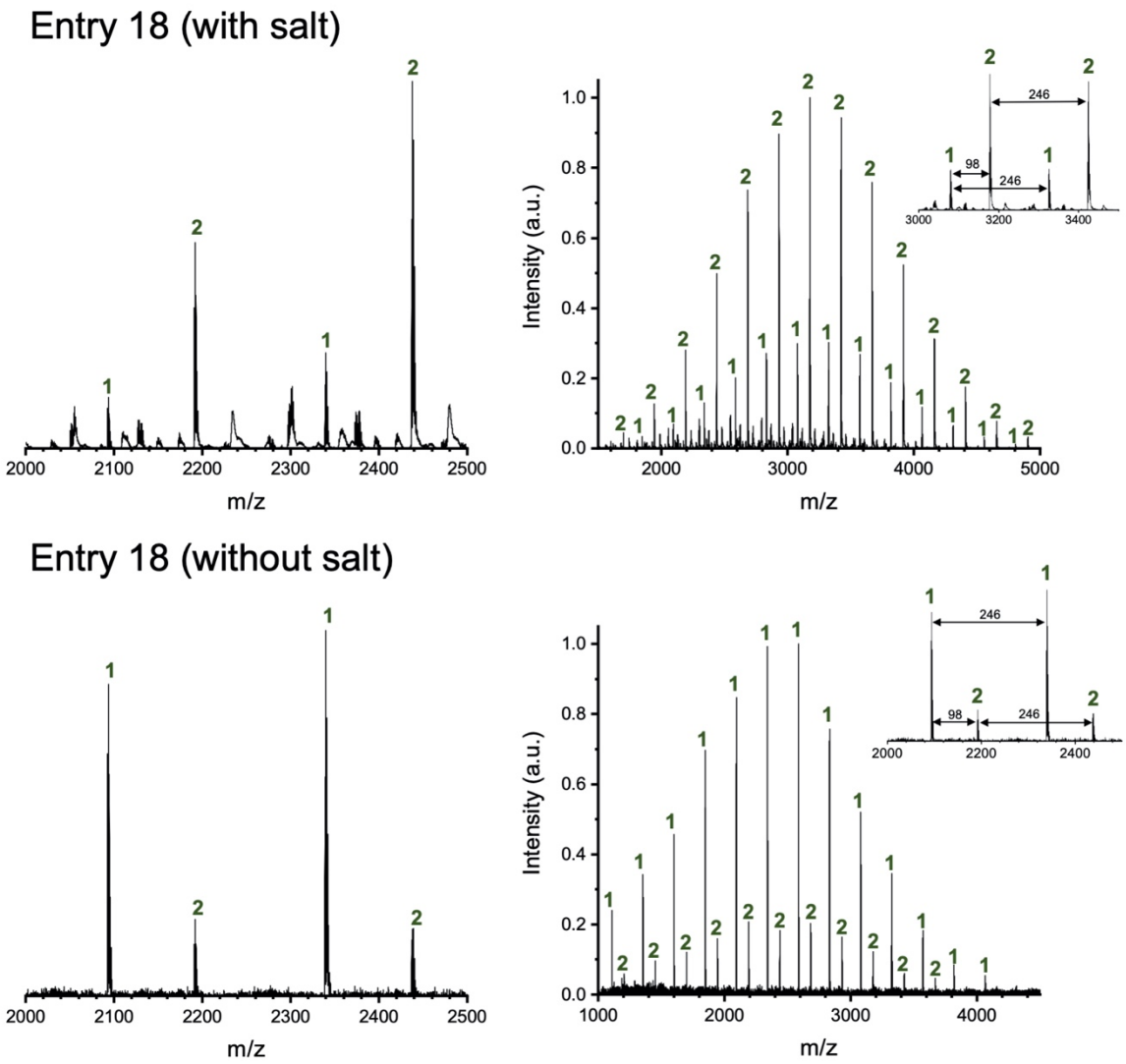

Figure 32. A comparison of the MALDI-ToF MS spectra of PA-CHO copolymer afforded from the model copolymerisation (**Entry 18**) with (top) and without (bottom) the NaI cationic agent.

Following in the steps of Duchateau and co-workers who reported this phenomenon, DMAP was swapped for PPNCl which had not obscured their spectra (**Entry 21, Figure 33**). This allowed for clearer end-chain analysis. Peaks corresponding to DMAP end-capped chains (1, 2) were absent as expected. The peaks in the PPNCl spectrum (3-9, 10, 11-13, 15, 16) matched the m/z values of the minor peaks seen in the DMAP spectrum. As expected, peaks matching the m/z values of 4-MBA end-capped polyester chains were seen (11-13). Similar structures had been reported in literature

when alcohol and carboxylic acid species were present in the ROCOP of anhydrides and epoxides.[8, 28] However, the same m/z values were given for sodium end-capped polyesters formed when the sodium ion from the cationic agent introduced in MALDI-ToF MS preparation displaces the end-group of the polymer chain. As 4-MBA had been observed as an end-group in ^{1}H NMR and ^{13}C–{^{1}H} NMR spectra, it was tentatively assumed that at least a portion of the intensity of these peaks came from 4-MBA end-capped chains. The other peaks present corresponded with chloride end-capped chains (3-9). This was expected for the PPNCl-catalysed copolymerisation as literature studies have shown that chloride dissociates to initiate the copolymerisation through epoxide ring-opening.[18, 24] However, these peaks were also present in the DMAP-catalysed copolymerisation. The only source of chloride present in the DMAP-catalysed copolymerisation was the zinc chloride. This discovery reinforced the conclusion that zinc chloride was playing a role in the copolymerisation beyond simply coordinating monomers as a Lewis acid. Interestingly, these peaks were of a similar intensity to peaks end-capped by 4-MBA, suggesting that the role of chlorides from the Lewis acid as initiators or CTAs was substantial.

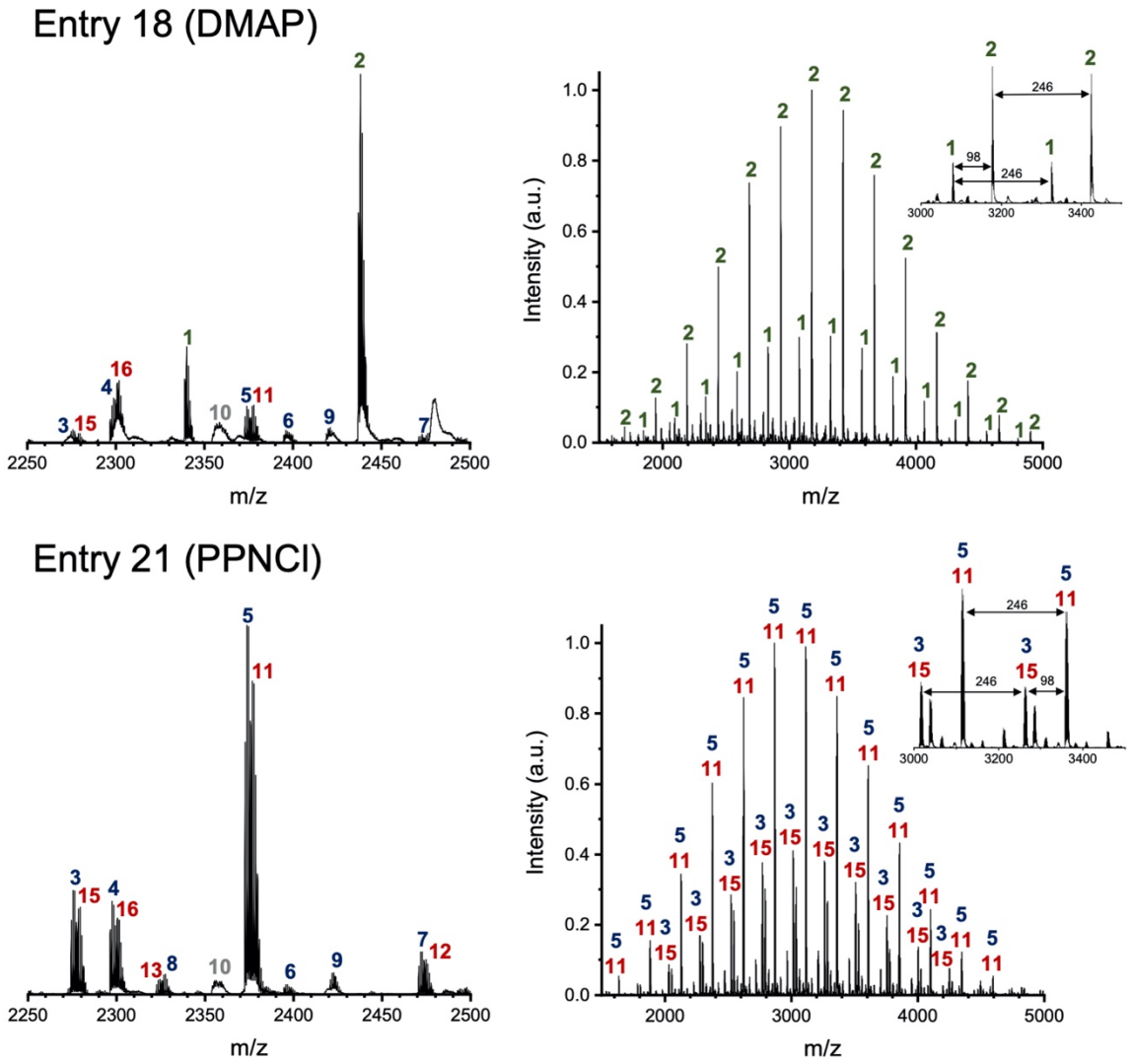

Figure 33. A comparison of the MALDI-ToF MS spectra of PA-CHO copolymer afforded from the model copolymerisation (**Entry 18**) and an analogous copolymerisation using PPNCl instead of DMAP as the Lewis base (**Entry 21**).

Though some peaks represented polymer chains containing ether linkages from the homopolymerisation of CHO, these were of a significantly lower intensity than the peaks corresponding to perfectly alternating polyester chains. This corresponded with the ^{1}H NMR spectrum of the polyester which had indicated a small amount of polyether was present.

To clarify further that 4-MBA end-groups were present in the afforded polyester, MALDI-ToF MS analysis was used to compare a polyester afforded from a copolymerisation with just PPNCl as a catalyst (**Entry 22**) to one afforded from PPNCl and 4-MBA as a catalyst and a CTA respectively (**Entry 23**), which were copolymerisations studied in Chapter 3 (**Figure 34**). The spectra showed that 4-MBA end-capped polyester chains 11, 12, sodium end-capped polyester chain 15 (likely formed when the cationic agent displaces 4-MBA) and unidentified peak 16 were only present when 4-MBA is employed. Peaks 13 and 14 which could be identified as 4-MBA end-capped polyester chains or sodium end-capped polyester chains were present in both spectra. Therefore, it was concluded that they were sodium end-capped polyester chains formed when PPN^+ was displaced by Na^+ in MALDI-ToF MS preparation.

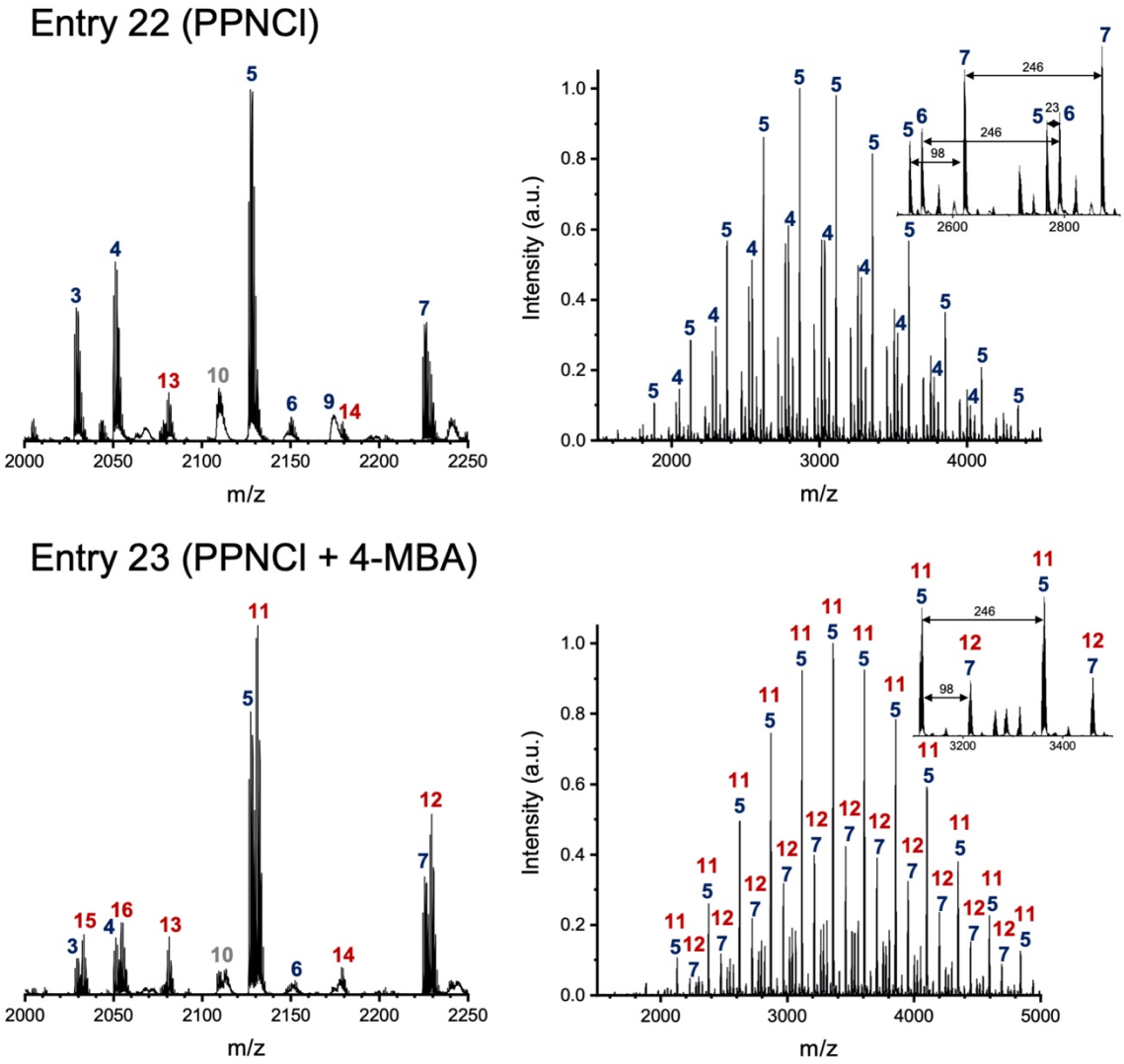

Figure 34. A comparison of the MALDI-ToF MS spectra of PA-CHO copolymer afforded from a PPNCl-catalysed copolymerisation (**Entry 22**) and an analogous copolymerisation also employing 4-MBA (**Entry 21**).

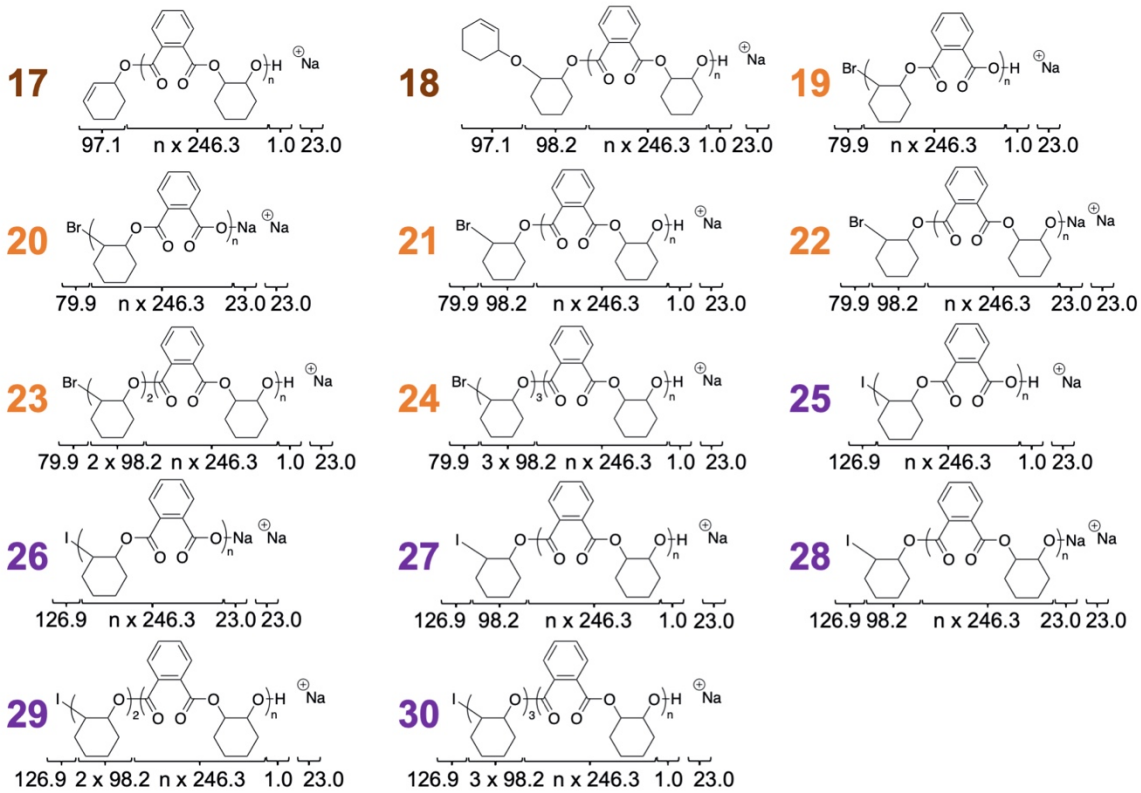

Figure 35. Polymer structures with bromide, iodide and cyclohexenol end-capped chains relating to peaks seen in MALDI-ToF MS analysis.

To clarify further that the halide ligand on the Lewis acid existed as an end-group on polyester chains, the polyester products of copolymerisations studied in Chapter 3 which were catalysed by Lewis pairs containing magnesium chloride, magnesium bromide and magnesium iodide respectively were analysed by MALDI-ToF MS (**Figure 36**). In both the magnesium bromide and magnesium iodide samples, new peaks appeared, including as major distributions, with m/z values corresponding to polyester chains end-capped by bromide and iodide (19-24 for bromide and 25-30 for iodide). Some new peaks appeared with m/z values corresponding to a cyclohexene alcohol end-group (17, 18), which was formed when a halide on the cyclohexanol ring was eliminated during the MALDI-ToF MS ionisation. As bromide and iodide are heavier atoms, they are more likely to be eliminated than chloride. This data suggests that the

halide ligands on the metal halide play a role in initiation or chain-transfer of polymer chains.

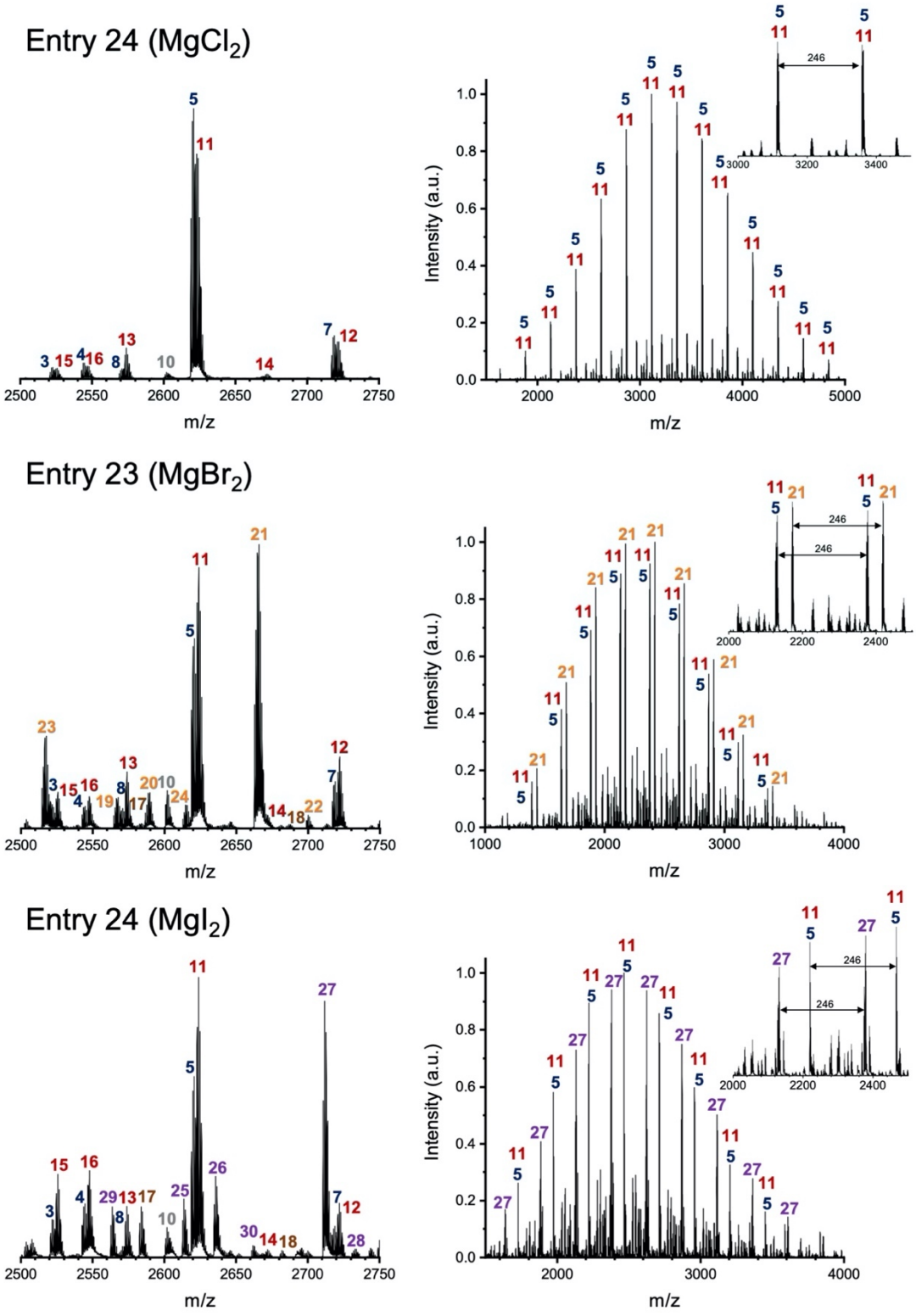

Figure 36. A comparison of the MALDI-ToF MS spectra of PA-CHO copolymer afforded from copolymerisations catalysed by Lewis pairs with different Lewis acids (**Entry 24**, **Entry 25** and **Entry 26**).

2.3 Conclusions

Using a model copolymerisation, it was demonstrated that metal-halide Lewis pair catalysis of the ROCOP of anhydrides and epoxides alongside the use of an alcohol CTA is effective at affording highly alternating polyester (95% ester linkages). The polymerisation rate (93% conversion in 5 h) of the $ZnCl_2$/DMAP system was reasonable in comparison with other simple catalysts in literature but lower than when DMAP was used alone. This showed that the introduction of metal halides influenced the polymerisation rate and therefore by applying the correct metal-halide as a Lewis acid in the Lewis pair catalyst, an improved polymerisation rate may be achieved.

Despite the production of narrowly disperse polyester, and unimodal molecular weight distributions, copolymerisations did not display a controlled behaviour in kinetic analysis. Instead, the kinetic plot showed an increasing rate of polymerisation indicating an increase in the number of propagating chains over time in the copolymerisation. By isolating each component's effect on polymerisation rate and molecular weight, and by analysing the afforded polymer microstructure, it was determined that the metal halide itself was the determining factor for an uncontrolled copolymerisation. It was hypothesised that the halide ligands can dissociate or be displaced from the metal halide and act as initiators in the copolymerisation thereby complicating copolymerisation initiation through the introduction of an extra initiator. This was further compounded by the poor solubility of the metal halide, which was not fully dissolved at the start of the copolymerisation and solubilises as the copolymerisation is heated. During this research, a report on the use of a $YCl_3 \cdot THF_{3.5}$/PPNCl Lewis pair catalysis system in the controlled ROCOP of anhydrides and epoxides gave promise that the effect of halide ligands on the copolymerisation

could be controlled.[15] The main difference between the system reported here and the $YCl_3 \cdot THF_{3.5}$/PPNCl system was the use of THF to increase the solubility of the metal halide. This suggested that the solubility of the metal halide may be the non-linear factor causing a deviation from a controlled copolymerisation. It was proposed that a controlled system could therefore be attained by investigating the use of THF or other similar salts, by manipulating the reaction conditions to allow for the metal halides to dissolve in the reaction mixture or by pre-heating the metal halide in the solvent before the other reaction components were added for the copolymerisation to begin.

2.4 Experimental details

2.4.1 General considerations

All reagents for the copolymerisations were stored in a nitrogen-filled glovebox. Dry toluene, chloroform and dichloromethane were obtained from a SPS system, degassed by three freeze-pump-thaw cycles and stored over activated 3 Å or 4 Å molecular sieves in a nitrogen-filled glovebox nitrogen. Before use in an air-free reaction, all glassware was dried in the oven at 180 °C overnight.

2.4.2 Instruments

2.5.2.1 NMR Spectrometer

^{1}H NMR and ^{13}C–{^{1}H} NMR spectra were recorded at 298 K on an Ascend Bruker 400 spectrometer equipped with a BBFO smart probe operating at 400 MHz and 101 MHz respectively. Chemical shifts on the 1H NMR spectra were referenced to the solvent residual proton resonance signals: δ 7.26 ppm for d_1–$CDCl_3$. The data obtained was processed and analysed using MestReNova 12.0.3 software.

2.5.2.2 Size exclusion chromatography

Size exclusion chromatography (SEC) in THF was performed on an Agilent 1260 Infinity II LC system equipped with a Wyatt Optilab T-rEX differential refractive index detector, an Agilent guard column (PLGel 5 μM, 50 × 7.5 mm) and two Agilent Mixed-C columns (PLGel 5 μM, 300 × 7.5 mm). The mobile phase was THF (HPLC grade) at flow rate of 1.0^{-1} mL·min. Number average molecular weights (M_n), weight average molecular weights (M_w) and dispersities ($Đ_M = M_w/M_n$) were determined using Wyatt ASTRA v7.1.3 software against poly(styrene) (PS) standards.

2.5.2.3 Centrifuge

Ohaus FC5706 Frontier Centrifuge Multi 230V.

2.5.2.4 Matrix-assisted laser desorption/ionisation time-of-flight mass spectrometry (MALDI-ToF MS)

Matrix-assisted laser desorption/ionisation time-of-flight mass spectrometry (MALDI-ToF MS) was carried out n a Bruker Ultraflex Extreme mass spectrometer using a nitrogen laser delivering 2 ns pulses at 337 nm with positive ion ToF detection performed using an accelerating voltage of 25 kV. For samples tester with a cationic agent, *trans*-2-[3-(4-*tert*-butylphenyl)-2- methyl-2-propenylidene] malononitrile (DCTB) was used as a matrix (40 g L^{-1} solution in THF), with sodium iodide (NaI) or sodium trifluoroacetate (NaTFA) used as a cationic agent (5 g L^{-1} solution in THF). Analyte (5 µL, 1 g L^{-1} solution in THF) was mixed with DCTB solution (10 µL) and sodium salt solution (1 µL) and 1 µL of the resultant mixture was applied to form a thin matrix-analyte film. For samples tested without a cationic agent, 2,5-dihydroxybenzoic acid (DHB) was used as a matrix (40 g L^{-1} solution in THF). Analyte (5 µL, 1 g L^{-1} solution in THF) was mixed with DHB solution (10 µL) and 1 µL of the resultant mixture was applied to form a thin matrix-analyte film. All samples were calibrated against a 3000 g·mol-1 poly(ethylene glycol) standard.

2.5.3 Materials

Zinc chloride anhydrous (anhydrous, 98+%) and 4-methoxybenzyl alcohol (dissolved in dry dichloromethane, dried over CaH_2, distilled under nitrogen, degassed and stored under an inert atmosphere, 98%) were purchased from Alfa Aesar. 4-

dimethylaminopyridine (dried over molecular sieves, ≥99%), toluene (99.8%), sodium iodide (≥99.5%), sodium trifluoroacetate (98%), methanol (99.8%), magnesium chloride (anhydrous, ≥98%), phthalic anhydride (≥99%), bis(triphenylphosphine)iminium chloride (97%), chloroform (≥99%), tetrahydrofuran (HPLC grade, ≥99.9%, inhibitor-free), triethylamine (≥99.5%), *trans*-2-[3-(4-*tert*-butylphenyl)-2-methyl-2-propenylidene]malononitrile (≥98%) and calcium hydride (95%) were purchased from Sigma Aldrich. Magnesium iodide (anhydrous, 99.997%) was purchased from VWR. Magnesium bromide (anhydrous, 98%), cyclohexene oxide (98%), dichloromethane (≥99.5%) and 2,5-dihydroxybenzoic acid (99%) were purchased from Acros Organics. Hydrochloric acid (37%) was purchased from Fisher Scientific. Deuterated chloroform (dried over CaH_2 and distilled under nitrogen twice, degassed and stored under an inert atmosphere, 98%) was purchased from Apollo Scientific. Unless stated otherwise, all chemicals and compounds were used as received.

2.5.4 Monomer preparation

Given the ease by which monomer impurities can disrupt anhydride and epoxide ring-opening copolymerisation, it was important to stringently purify and dry the phthalic anhydride and cyclohexene oxide comonomers.

Phthalic anhydride (20 g) was stirred in dry toluene (500 mL) and then cannula filtered under nitrogen. Toluene was then removed under reduced pressure before the solid was recrystallised in dry chloroform. The crystals were then sublimed twice in a nitrogen filled sublimation chamber under reduced pressure and heat (80 ºC). The

resultant white crystals (~ 5 g) were analysed with ^{1}H NMR and $^{13}C–\{^{1}H\}$ NMR spectroscopy to determine the purity.

Cyclohexene oxide (200 mL) was stirred over CaH_2 and distilled under nitrogen twice followed by degassing through freeze-pump thawing thrice. The resultant colourless liquid was analysed with ^{1}H NMR and $^{13}C–\{^{1}H\}$ NMR spectroscopy to determine the purity.

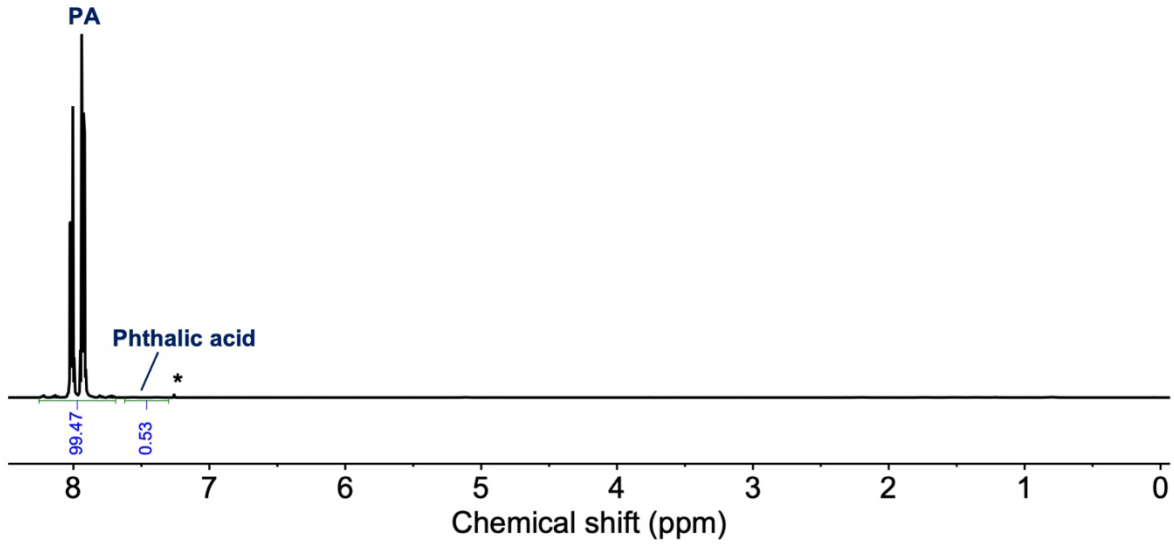

Figure 37. The ^{1}H NMR spectrum of phthalic anhydride after purification and drying ($CDCl_3$, 400 MHz, 298 K). * = $CHCl_3$.

2.5.5 General copolymerisation procedure

In a nitrogen-filled glove box, a 7 mL teflon-sealed vial with a magnetic stirrer bar was primed with zinc chloride (2.7 mg, 0.02 mmol), 4-dimethylaminopyridine (2.4 mg, 0.02 mmol), phthalic anhydride (148 mg, 1 mmol) and a stock solution of a chosen multiple amount of 4-methoxybenzyl alcohol (2.5 µL, 0.02 mmol), cyclohexene oxide (101 µL, 1 mmol) and toluene (500 µL, 4.7 mmol) respectively. For each control copolymerisation, the relevant components were omitted from the above mixture. For

copolymerisations run in neat epoxide, no toluene was added and twice the molar amount of CHO was used. The vial was stirred and heated to 110 ºC for a set time to allow the copolymerisation to occur. When the desired time was reached, the vial was quenched in an ice bath and then opened to air. $CDCl_3$ was added and a sample taken for ^1H NMR and $^{13}C–\{^1H\}$ NMR analysis. A sample was also taken and diluted in tetrahydrofuran (1 mL) for SEC analysis. The polymer was crashed out of the remaining reaction mixture by precipitation into a MeOH/HCl mixture cooled using liquid nitrogen. Polymers were dried under reduced pressure at 60 ºC.

2.5.6 Synthesis of poly(PA-*co*-CHO)

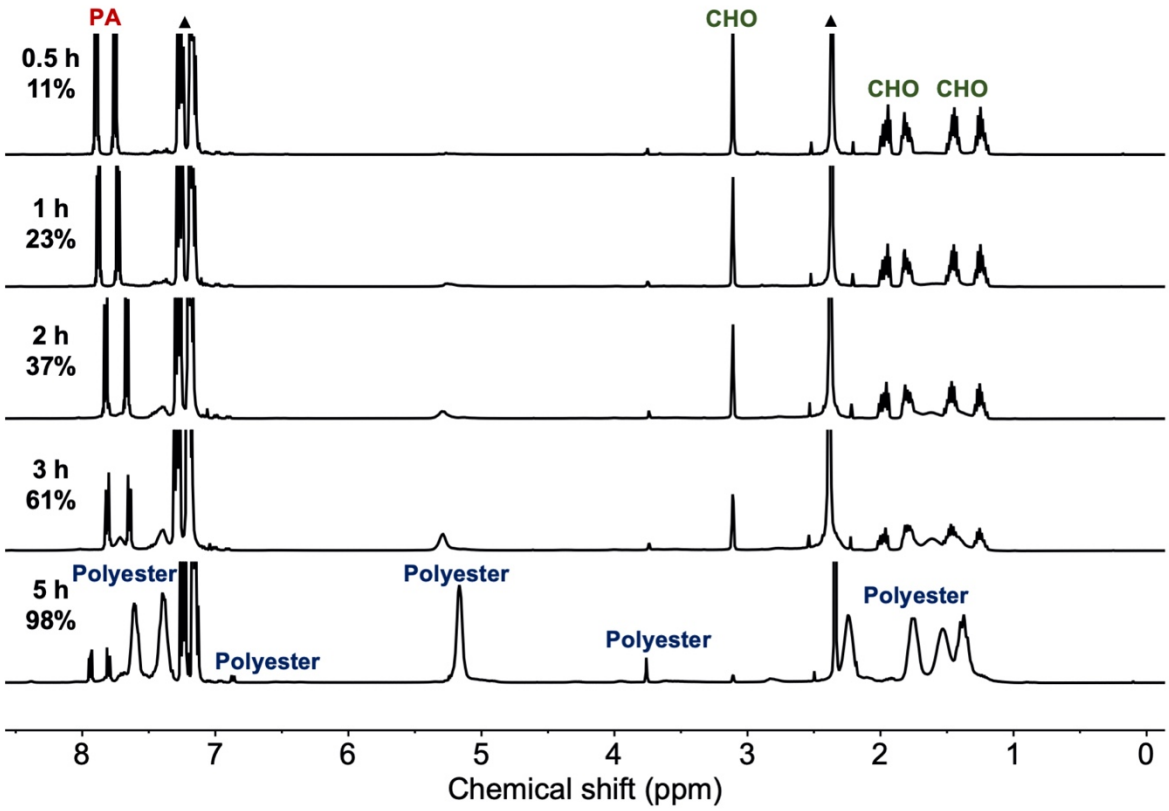

Figure 38. The ^1H NMR spectra of crude reaction mixtures of the model copolymerisation taken at different timepoints throughout its kinetic study ($CDCl_3$, 400 MHz, 298 K). The time and monomer conversion is given next to each spectrum. ▲ = toluene.

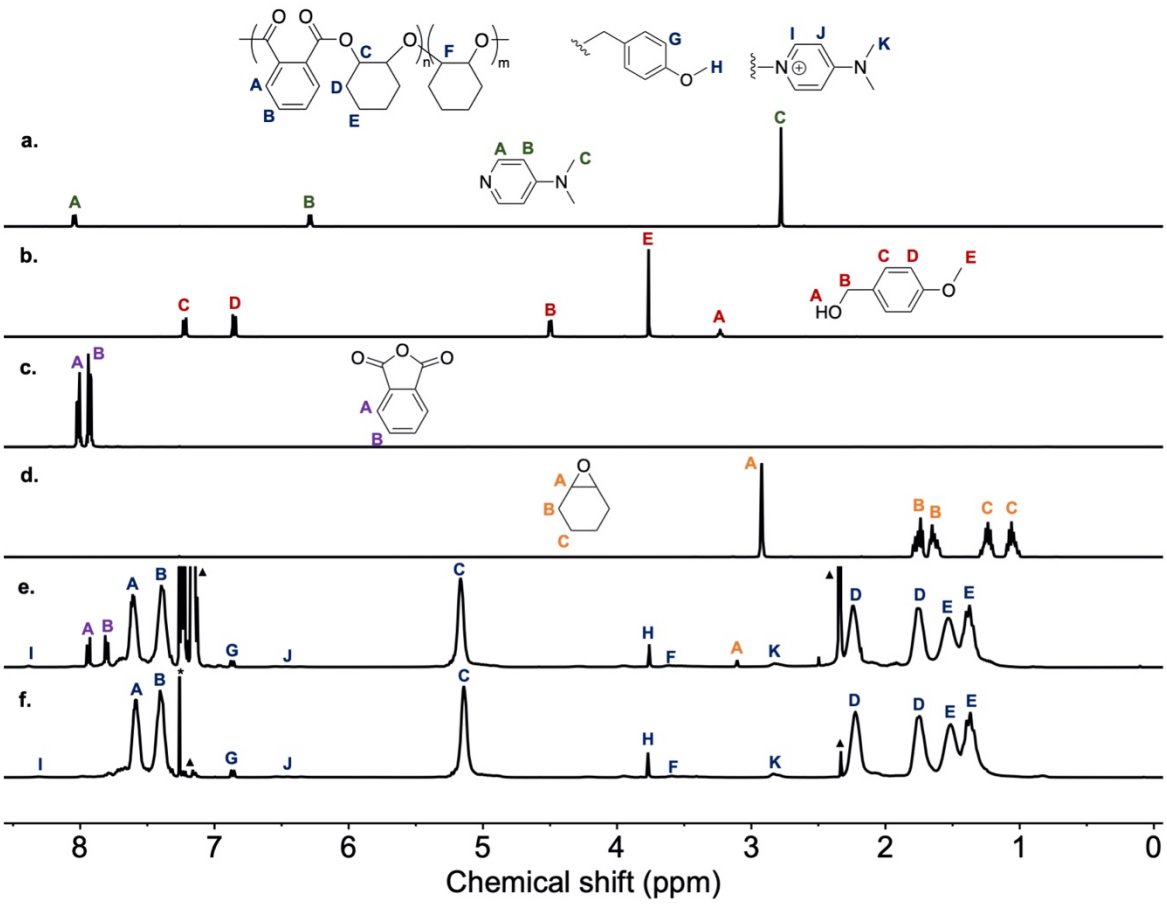

Figure 39. The ^{1}H NMR spectra of a. DMAP, b. 4-MBA, c. PA, d. CHO, e. the crude reaction mixture of the model copolymerisation at 5 h, f. the precipitated polyester product from the model copolymerisation at 5 h ($CDCl_3$, 400 MHz, 298 K). * = $CHCl_3$, ▲ = toluene.

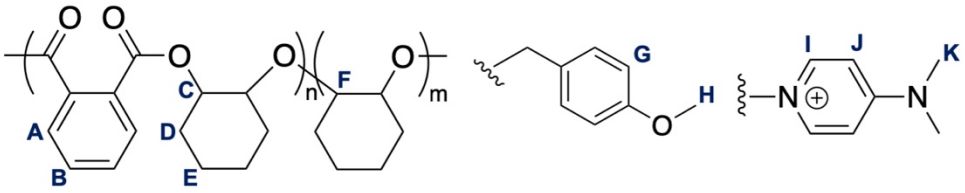

^{1}H NMR (400 MHz, $CDCl_3$, 298 K, ppm): δ = 8.31 (m, 2H, H^{I}), 7.58 (m, 2H, H^{A}), 7.41 (m, 2H, H^{B}), 6.86 (d, 2H, H^{G}), 6.40 (d, 2H, H^{J}) 5.14 (d, 2H, H^{C}), 3.77 (d, 3H, H^{H}), 3.47-3.63 (m, 1H, H^{F}), 2.84 (s, 6H, H^{K}), 2.22 (m, 2H, H^{D}), 1.75 (m, 2H, H^{D}), 1.51 (m, 2H, H^{E}), 1.37 (m, 2H, H^{E}).

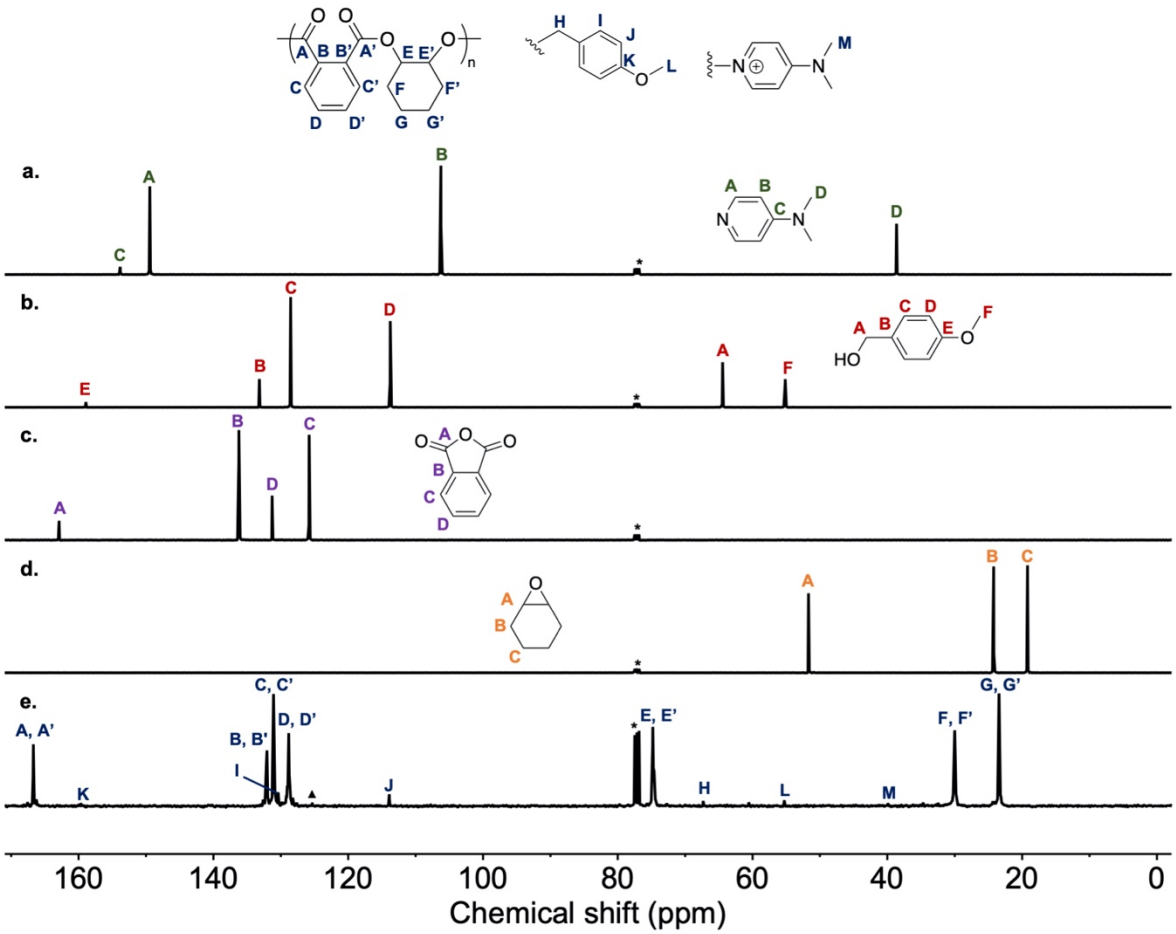

Figure 40. The $^{13}C–\{^{1}H\}$ NMR spectra of a. DMAP, b. 4-MBA, c. PA, d. CHO, e. the precipitated polyester product from the model copolymerisation at 5 h ($CDCl_3$, 101 MHz, 298 K). * = $CHCl_3$, ▲ = toluene.

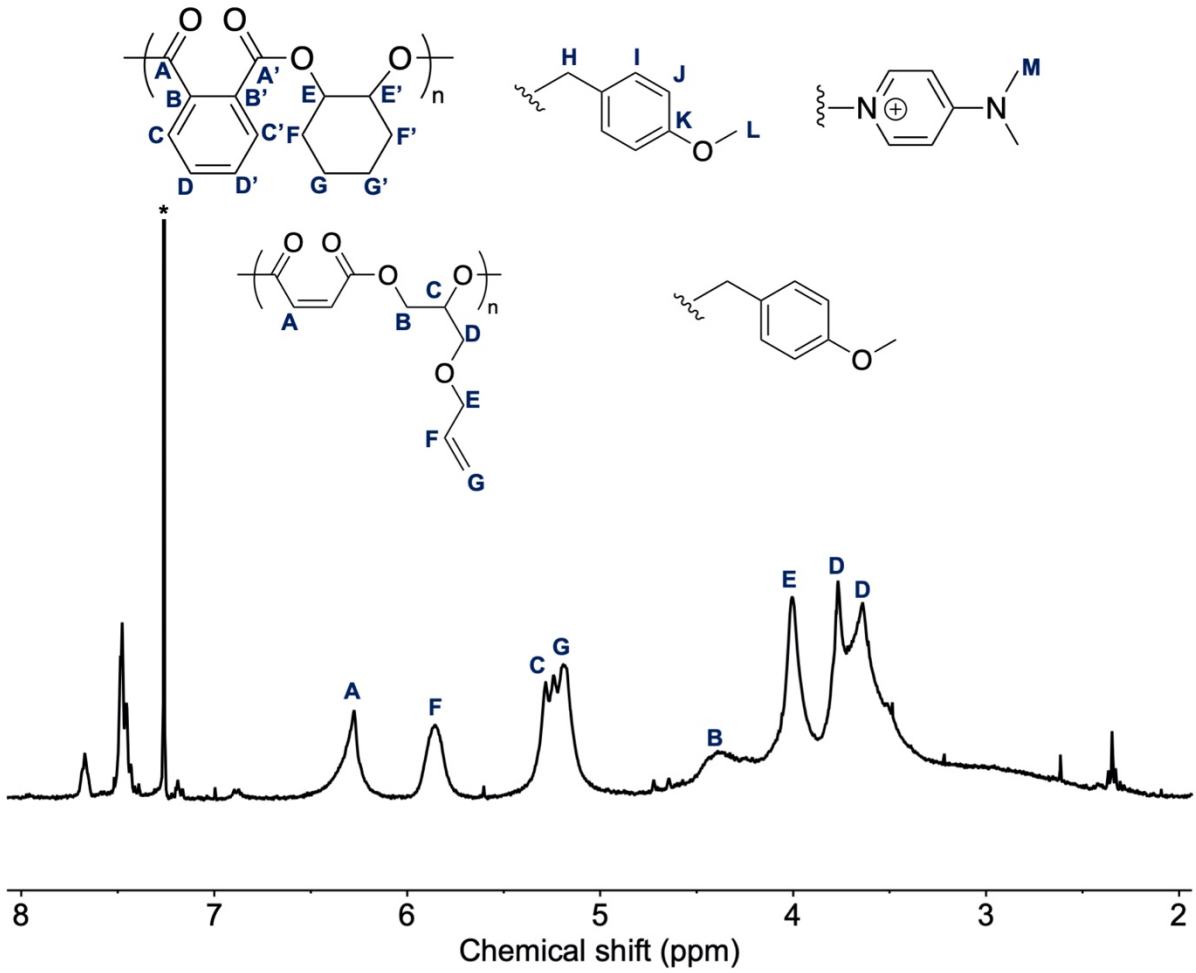

Figure 41. The $^{13}C–\{^1H\}$ NMR spectrum of precipitated (from $CHCl_3$ into methanol/HCl) P(PA-co-CHO) copolymer derived from a copolymerization of PA and CHO using $ZnCl_2$/4-MBA as a catalyst system after 5 h ($CDCl_3$, 101 MHz, 298 K). * = $CHCl_3$.

$^{13}C–\{^1H\}$ NMR (101 MHz, $CDCl_3$, 298 K, ppm): δ = 166.72 (C^A), 166.66 ($C^{A'}$), 159.72 (C^K), 132.14 (C^B), 132.08 ($C^{B'}$) 131.11 (C^C, $C^{C'}$), 130.41 (C^I), 128.83 (C^D, $C^{D'}$), 113.90 (C^J), 74.80 (C^E), 74.65 ($C^{E'}$), 67.34 (C^H), 55.29 (C^L), 39.90 (C^M), 30.04 (C^F, $C^{F'}$), 23.46 (C^G, $C^{G'}$).

2.6 References

1. S. Huijser, E. HosseiniNejad, R. Sablong, C. de Jong, C. E. Koning and R. Duchateau, *Macromolecules*, 2011, **44**, 1132-1139.

2. L. Cui, B.-H. Ren and X.-B. Lu, *J. Polym. Sci.*, 2021, **59**, 1821-1828.

3. W. T. Diment, G. Rosetto, N. Ezaz-Nikpay, R. W. F. Kerr and C. K. Williams, *Green Chem.*, 2023, **25**, 2262-2267.

4. R. C. Jeske, A. M. DiCiccio and G. W. Coates, *J. Am. Chem. Soc.*, 2007, **129**, 11330-11331.

5. R. Xie, Y.-Y. Zhang, G.-W. Yang, X.-F. Zhu, B. Li and G.-P. Wu, *Angew. Chem. Int. Ed.*, 2021, **60**, 19253-19261.

6. R. J. Brotherton, C. J. Weber, C. R. Guibert and J. L. Little, in *Ullmann's Encyclopedia of Industrial Chemistry*, 2000, DOI: https://doi.org/10.1002/14356007.a04_309.

7. *Bretherick's Handbook of Reactive Chemical Hazards (Seventh Edition)*, ed. P. G. Urben, Academic Press, Oxford, 2007, DOI: https://doi.org/10.1016/B978-0-12-372563-9.50033-1, pp. 54-60.

8. C.-M. Chen, X. Xu, H.-Y. Ji, B. Wang, L. Pan, Y. Luo and Y.-S. Li, *Macromolecules*, 2021, **54**, 713-724.

9. X. Dou, X.-H. Liu, B. Wang and Y.-S. Li, *Chin. J. Chem .* 2023, **41**, 83-92.

10. H. Xie, L. Zheng, J. Feng, X. Wang, S. Kuang, L. Zhou, J. Jiang, Y. Xu, Y. Zhao and Z. Xu, *Polym. Chem.*, 2023, **14**, 1630-1638.

11. S. Liu, T. Stettner, R. Klukas, T. Porada, K. Furda, A. M. Fernández and A. Balducci, *ChemElectroChem*, 2022, **9**, e202200711.

12. J. Qiu, B. Charleux and K. Matyjaszewski, *Polimery*, 2022, **46**, 453-460.

13. G. Gee and H. W. Melville, *Trans. Faraday Soc.*, 1944, **40**, 240-251.

14. H.-Y. Ji, B. Wang, L. Pan and Y.-S. Li, *Green Chem.*, 2018, **20**, 641-648.

15. Z. A. Wood, M. K. Assefa and M. E. Fieser, *Chem. Sci.*, 2022, **13**, 10437-10447.

16. J. M. Longo, M. J. Sanford and G. W. Coates, *Chem. Rev.*, 2016, **116**, 15167-15197.

17. W. T. Diment, T. Stößer, R. W. F. Kerr, A. Phanopoulos, C. B. Durr and C. K. Williams, *Catal. Sci.*, 2021, **11**, 1737-1745.

18. A. Kummari, S. Pappuru and D. Chakraborty, *Polym. Chem.*, 2018, **9**, 4052-4062.

19. T. Stößer and C. K. Williams, *Angew. Chem. Int. Ed.*, 2018, **57**, 6337-6341.

20. W. T. Diment and C. K. Williams, *Chem. Sci.*, 2022, **13**, 8543-8549.

21. S. Naumann, P. B. V. Scholten, J. A. Wilson and A. P. Dove, *J. Am. Chem. Soc.*, 2015, **137**, 14439-14445.

22. S. Paul, Y. Zhu, C. Romain, R. Brooks, P. K. Saini and C. K. Williams, *Chem. Commun.*, 2015, **51**, 6459-6479.

23. D. Ryzhakov, G. Printz, B. Jacques, S. Messaoudi, F. Dumas, S. Dagorne and F. Le Bideau, *Polym. Chem.*, 2021, **12**, 2932-2946.

24. Z. Hošťálek, O. Trhlíková, Z. Walterová, T. Martinez, F. Peruch, H. Cramail and J. Merna, *Eur. Polym. J.*, 2017, **88**, 433-447.

25. E. H. Nejad, A. Paoniasari, C. G. W. van Melis, C. E. Koning and R. Duchateau, *Macromolecules*, 2013, **46**, 631-637.

26. X. Zhu and X. Kou, *Chem. Pap.*, 2022, **76**, 2145-2152.

27. R. Mundil, Z. Hošťálek, I. Šeděnková and J. Merna, *Macromol. Res.*, 2015, **23**, 161-166.

28. H. Li, J. Zhao and G. Zhang, *ACS Macro Lett.*, 2017, **6**, 1094-1098.

Chapter 3 – Optimising phthalic anhydride and cyclohexene oxide copolymerisation with metal halide-organobase screening

3.1 Introduction

Lewis pair polymerisation (LPP) uses both a Lewis acid and a Lewis base, either bound in a frustrated pair due to steric hindrance or in a dissociative equilibrium, to cooperatively and synergistically catalyse a polymerisation reaction through the activation of monomers, and control of chain initiation, propagation and transfer.[1,2] A Lewis acid is a species, which possesses relatively low-energy lowest unoccupied molecular orbitals (LUMOs) and therefore tends to accept a pair of electrons. A Lewis base is a species, which possesses relatively high-energy highest occupied molecular orbitals (HOMOs) and therefore tends to donate a pair of electrons. The advantages of using a cooperative, two-component catalytic mechanism given by LPP include the tunability of the catalysts for polymerisation conditions, independent tunability of polymerisation activity and polymer molecular weight, superior control over block copolymerisations and for certain polymerisations kinetic and thermodynamic control and chemoselectivity of monomer functionalities. The ease of fine-tuning Lewis pair catalysts by independently varying the Lewis acid or Lewis base employed respectively has been demonstrated in a range of literature reports on the ring-opening copolymerisation (ROCOP) of anhydrides and epoxides using Lewis pair catalysts.[3]

Initial studies focusing on the tuning of Lewis pair catalysts for anhydride and epoxide ROCOP were carried out in the investigation of well-defined organometallic complexes. In these studies, Lewis acids were well-defined organometallic complexes with complex ligands and so the emphasis of their studies were on fine-tuning the ligand structures rather than wider screening of different Lewis acids. Nevertheless some reports did focus on Lewis acid comparisons. Two reports by Coates and co-workers on the Lewis acidities of salen complexes showed that stronger Lewis acids

had a tendency to minimise undesireable side reactions.[4, 5] They found that an aluminium salen complex more readily promoted a less nucleophilic/basic alkoxide propagating chain end when mediating the copolymerisation of propylene oxide (PO) and a tricyclic anhydride and so minimised the possibility of transesterification and epimerisation reactions compared with more strongly acidic chromium and cobalt analogues. The same observation was made when they modified an aluminium salcy complex with electron-withdrawing and donating groups for the ROCOP of PO and carbic anhydride (CA). The more electron-deficient and therefore strongly acidic complexes mediated polymerisation which gave higher suppression of side reactions and higher alternating selectivity. However, this was complemented with lower rates of polymerisation. Lewis base co-catalysts were also screened for the ROCOP of anhydrides and epoxides using well-defined organometallic catalysts. For example, Duchateau and co-workers screened neutral organobases: 4-(dimethylamino)pyridine (DMAP), *N*-methylimidazole (*N*-Melm), and 1,5,7-triazabicyclododecene (TBD); onium salt bis(triphenylphosphoranylidene)ammonium chloride; and phosphines: trimesitylphosphine ($PMes_3$), tris(2,4,6-trimethoxyphenyl)phosphine (TMPP), tricyclohexylphosphine (PCy_3), triphenylphosphine (PPh_3) alongside a chromium salen catalyst to mediate the ROCOP of cyclohexene oxide (CHO) and phthalic anhydride (PA).[6] The order of catalytic activity for the *N*-heterocyclic nucleophilic co-catalysts was DMAP > *N*-Melm > TBD, while the phosphines saw no clear trend in activity. PPNCl was the most effective co-catalyst, mirroring the results found in studies of epoxide and CO_2 ROCOP.

With the focus on the development of simple catalysts for the ROCOP of anhydrides and epoxides, a wider scope of Lewis acids were screened. Chakraborty and co-

workers screened the simple Lewis acids BEt_3, $Al(CH_3)_3$, Et_2Zn and $^nBu_2Mg$ when paired alongside various Lewis bases for the ROCOP of CHO and PA.[7] While BEt_3 afforded perfectly alternating polyester under the right conditions, the other three Lewis acids gave significant amounts of polyether (15-30%) regardless of other factors in the copolymerisation. BEt_3 also saw a faster polymerisation rate than the others with the catalytic activity ordering being: BEt_3 ⋙ $^nBu_2Mg$ > $Al(CH_3)_3$ > Et_2Zn. The authors attributed BEt_3's superior selectivity and catalytic activity to its mild Lewis acidity. The acidity was strong enough to activate monomers for addition onto the growing chain end but weak enough not to catalyse the homopolymerisation of epoxides. They also noted that the stronger Lewis acids $Al(CH_3)_3$ and Et_2Zn saw stronger coordination with the Lewis base, which decreased the activity at the active site thus promoting undesirable side reactions such as dissociation of the polymer chain and therefore back-biting. Having discovered the use of boron's well-placed Lewis acidity, Zhang and co-workers investigated a series of organoborane Lewis acids which differed in the electron-withdrawing nature and steric bulk of the ligand on the catalytic activity and selectivity as part of a Lewis pair for PO and maleic anhydride (MA) ROCOP.[8] As the steric hindrance and Lewis acidity increased in the series BEt_3, $B(C_6H_5)_3$ and $B(C_6F_5)_3$, the polymerisation rate and selectivity decreased. This confirmed the trend seen by Chakraborty and co-workers. Li and co-workers conducted a similar investigation into zinc alkyl Lewis acids ($ZnEt_2$, $Zn(C_6H_5)_2$ and $Zn(C_6F_5)_2$) paired with simple organobases for the ROCOP of CHO and PA.[3] Interestingly, they found that modifying the Lewis acidity in the series led to little difference in outcome of polymerisation rate or selectivity. Instead, other factors such as the nature of the Lewis base and ratio between the two Lewis pair components were more decisive on the outcome.

The investigation of the effects of different organobases when used alone or paired with simple Lewis acids showed a trend similar to that seen when paired with well-defined organometallic catalysts. Merna and co-workers found PPNCl was the most effective base for catalysing the ROCOP of CHO and PA as a single-component organocatalyst with other quarternary ammonium salts Bu_4NX, triphenylphospine (PPh_3) and 4-Dimethylaminopyridine (DMAP) giving lower conversions and lower molecular weight polymers.[9] In contrast, TBD and DABCO were ineffective at performing the copolymerisation. Chakraborty and co-workers reported that PPNCl gave a significantly higher catalytic activity for the ROCOP of CHO and PA when paired with triethylborane than neutral amine bases did.[7] They attributed this to PPNCl's cationic character which results from fast dissociation of the chloride anion. A more systematic study of the effect of Lewis bases when paired with organoborane Lewis acids on the activities and selectivity for PO and succinic anhydride (SA) ROCOP was conducted by Zhang and co-workers using Lewis bases with a range of basicity: TEA, DBU, MTBD, *t*-BuP_1 and *t*-BuP_2.[10] They found that the catalytic activity increased with basicity when paired with BEt_3: *t*-BuP_2 > *t*-BuP_1 > MTBD > DBU > TEA. Meanwhile, no significant effect was had on the selectivity of the copolymerisation with ester linkages of the afforded polymer remaining above 93%. This was the opposite trend to that seen in a report where organobases were paired with (thio)ureas for the copolymerisation of CHO with PA, which saw bases with lower nucleophilicity give higher catalytic activity (PPNCl > DMAP > DBU).[11] They speculated that this was because a higher basicity led to a stronger interaction with (thio)urea decreasing their ability to attack and ring-open the monomer. PPNCl performed best in catalytic activity from a screen of other quarternary ammonium chloride salts when used without a co-catalyst to

mediate the ROCOP of CHO with PA.[12] However, replacing the chloride with bromide or iodide increased the polymerisation rate up to almost twice as much due to their bulkier nature and thus lower electron affinity and greater tendency to dissociate. To avoid the use of less abundant bromide and iodide salts, the report investigated improving chloride salts. An aminocycloproprenium chloride was employed that showed a greater catalytic activity than PPNCl (though still lower then PPNBr and PPNI). However, it was less commercially available than PPNCl. For this reason, PPNCl still remains the preferred choice of Lewis base.

Overall, literature studies so far have shown some general guidelines for Lewis acid and base selection in the Lewis pair catalysis of anhydride and epoxide ROCOP. For Lewis acids there is a preference for a balance of strong enough acidity to activate a monomer for ring-opening but weak enough acidity to keep the propagating chain from becoming too nucleophilic or basic to encourage transesterification or to homopolymerise the epoxide through cationic polymerisation. For Lewis bases, regardless of the Lewis acid system employed, onium salts which due to their ionic nature can dissociate a strong nucleophile rapidly have seen the most success in improving catalytic activity for the copolymerisation. The choice of Lewis base (with the exception of onium salts) and Lewis acid is also heavily dependent on the choice of the other component. For example, Li and co-workers found that the Lewis pairs $Zn(C_6F_5)_2$/PPh_3 and $B(C_6F_5)_3$/DMAP were inefficient at mediating the ROCOP of CHO and PA despite each component shown to be effective when paired with a different co-component.[3] Moreover, the choice of Lewis pair components weren't the only decisive factors on the selectivity and activity of the copolymerisation. The ratio between Lewis acid and Lewis base, the solvent employed and the purity of the anhydride monomer

can have a decisive impact regardless of the Lewis pair selected.[3, 9] This is expected for complex reaction systems that employ a well-defined, expensive component that requires laborious synthesis rather than multiple simple and inexpensive components. For this reason, investigation of a wider scope of Lewis pairs will only help accumulate the data necessary to draw trends.

The aim of this chapter was to optimise the copolymerisation of PA with CHO established in Chapter 2 by the modification of the simple metal halide Lewis acid and Lewis organobase in the Lewis pair catalyst system. The plan for this chapter was to first fix a simple organobase determined by screening and then screen a range of simple metal halides as Lewis acids. The general reaction conditions would be fixed to those established from the standard polymerisation in the last chapter except for the solvent which had to be changed to accommodate the Lewis acid screen. The effect of different metal halide Lewis acidities on the selectivity and activity of the copolymerisation could be determined and the metal halide(s) and organobase(s) with the best fit for the copolymerisation could be identified.

3.2 Results and discussion

3.2.1 Lewis base screen

In Chapter 2 it was confirmed that the Lewis base employed in the model copolymerisation (DMAP) was a crucial component in the mechanism for the ROCOP of anhydrides and epoxides using the $ZnCl_2$/DMAP Lewis pair catalyst system. To determine the effect of the choice of the Lewis base in the metal halide Lewis pair catalysed ROCOP of anhydrides and epoxides on the catalytic activity, control, and selectivity of the copolymerisation, the ROCOP of PA and CHO was screened using 4-MBA as a chain transfer agent (CTA) and a Lewis pair catalyst system composed of $ZnCl_2$ and a choice of organobase (**Figure 42**). Neutral heterocyclic amines across a range of basicities (determined by the pK_a values of their conjugate acid LB-H^+: pK_aH) were selected to determine if the strength of the base correlated with overall catalytic performance of the Lewis pair. In addition, PPNCl was also screened. A single timepoint screen was used to compare copolymerisations. While it had been determined that the model copolymerisation did not display linear kinetics, limited time and resources prevented performing a kinetic study for each base. Instead, the assumption was taken based on the understanding established in Chapter 2 that the limiting factor for controlled copolymerisation was the Lewis acid's solubility and as the choice of Lewis acid ($ZnCl_2$) would remain the same across the copolymerisation screen, the differences in performance of the copolymerisations would only reflect the choice of Lewis base.

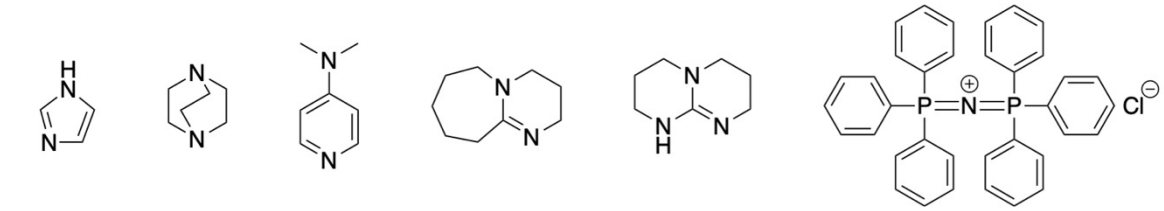

Figure 42. Lewis bases selected for screening. The pk_aH values for the neutral heterocyclic amines are given as found in literature.[13]

As simple metal halide salts were known to have solubility issues, the choice of solvent would be a key factor in screening further Lewis acid options.[14] The ROCOP of anhydrides and epoxides had been conducted in a solvent, in bulk or in a neat amount of the epoxide monomer in literature.[15, 16] It was thought that metal halides would be more susceptible to dissolving in more polar epoxide than in toluene. When a test bulk copolymerisation of the benchmark reaction was conducted, monomer conversion reached 65% after just 30 minutes. However, it then stagnated and did not reach completion within 3 h. It was speculated that this was due to the high viscosity of the reaction mixture which once saturated with resultant polyester impeded further copolymerisation. For this reason, two Lewis base screens were alongside Lewis bases being screened with toluene employed as a solvent in the model copolymerisation (**Table 6**), the Lewis base screen was also performed in a neat amount of the epoxide monomer (**Table 7**).

Table 6. Lewis base screen in toluene. All copolymerisations conducted with $[PA]_0/[CHO]_0/[ZnCl_2]_0/[LB]_0/[4\text{-MBA}]_0$ at 50:50:1:1:1, in toluene (2 mol dm^{-3} monomer concentration in toluene) at 110 °C for 3 h.

Entry	Lewis base	Monomer conversion[a] (%)	Ester linkages[b] (%)	M_n (SEC)[c] ($g \cdot mol^{-1}$)	$Đ_M$
1	PPNCl	90	95	2654	1.20
2	Imidazole	35	87	876	1.35
3	DABCO	49	96	941	1.22
4	DMAP	53	93	1348	1.24
5	DBU	51	95	1586	1.25
6	TBD	32	93	961	1.22

[a]Conversion of CHO calculated from the ^1H NMR spectrum ($CDCl_3$, 400 MHz) of the reaction mixture at 3 h. [b]Percentage of ester linkages determined by the ratio of the integrated height of the ester peak and ether peak in the ^1H NMR spectrum of the precipitated polyester product. [c]Molecular weight as calculated by SEC analysis using THF (0.5% NEt_3) as an eluent with PS standards

Table 7. Lewis base screen in neat CHO. All copolymerisations conducted with $[PA]_0/[CHO]_0/[ZnCl_2]_0/[LB]_0/[4\text{-MBA}]_0$ at 50:100:1:1:1 at 110 °C for 15 min.

Entry	Lewis base	Monomer conversion[a] (%)	Ester linkages[c] (%)	M_n (SEC)[b] ($g \cdot mol^{-1}$)	$Đ_M$
7	PPNCl	53	83	955	1.23
8	Imidazole	15	7	966	1.18
9	DABCO	30	8	667	1.15
10	DMAP	31	12	676	1.16
11	DBU	29	8	1804	4.00
12	TBD	14	5	483	1.36

[a]Conversion of CHO calculated from the ^{1}H NMR spectrum ($CDCl_3$, 400 MHz) of the reaction mixture at the given timepoint. [b]Percentage of ester linkages determined by the ratio of the integrated height of the ester peak and ether peak in the ^{1}H NMR spectrum of the precipitated polyester product. [c]Molecular weight as calculated by SEC analysis using THF (0.5% NEt_3) as an eluent with PS standards.

The copolymerisations were analysed and compared for their monomer conversion by the selected timepoint as a measure of catalytic activity and the portion of ester linkages in the resultant polyester as a measure of selectivity (**Figure 43**). When toluene was used as a solvent, highly alternating polyester (> 87% ester linkages) was afforded with any of the Lewis bases indicating that the choice of Lewis base did not have a significant impact on the selectivity of the catalyst system. However, a dramatic difference was seen when the copolymerisations were run in neat CHO. Only PPNCl achieved a highly alternating polyester (83% ester linkages). In contrast, all the neutral heterocyclic amines screened afforded mostly polyether (5-12% ester linkages). A previous report for the ROCOP of PA and CHO with PPNCl as a single organocatalyst saw a similar trend with a decrease in selectivity when run in bulk (89-92% ester

linkages) compared to when run in toluene (97% ester linkages).[9] They attributed this effect to the increased bulk viscosity and non-homogeneity of the reaction mixture composition. However, this decrease was far less significant than the decrease seen in our work. Additionally, this trend was not reflected when a $Zn(C_6F_5)_2$/DMAP Lewis pair was employed as a catalyst in the bulk or neat epoxide copolymerisation of CHO and PA.[3]

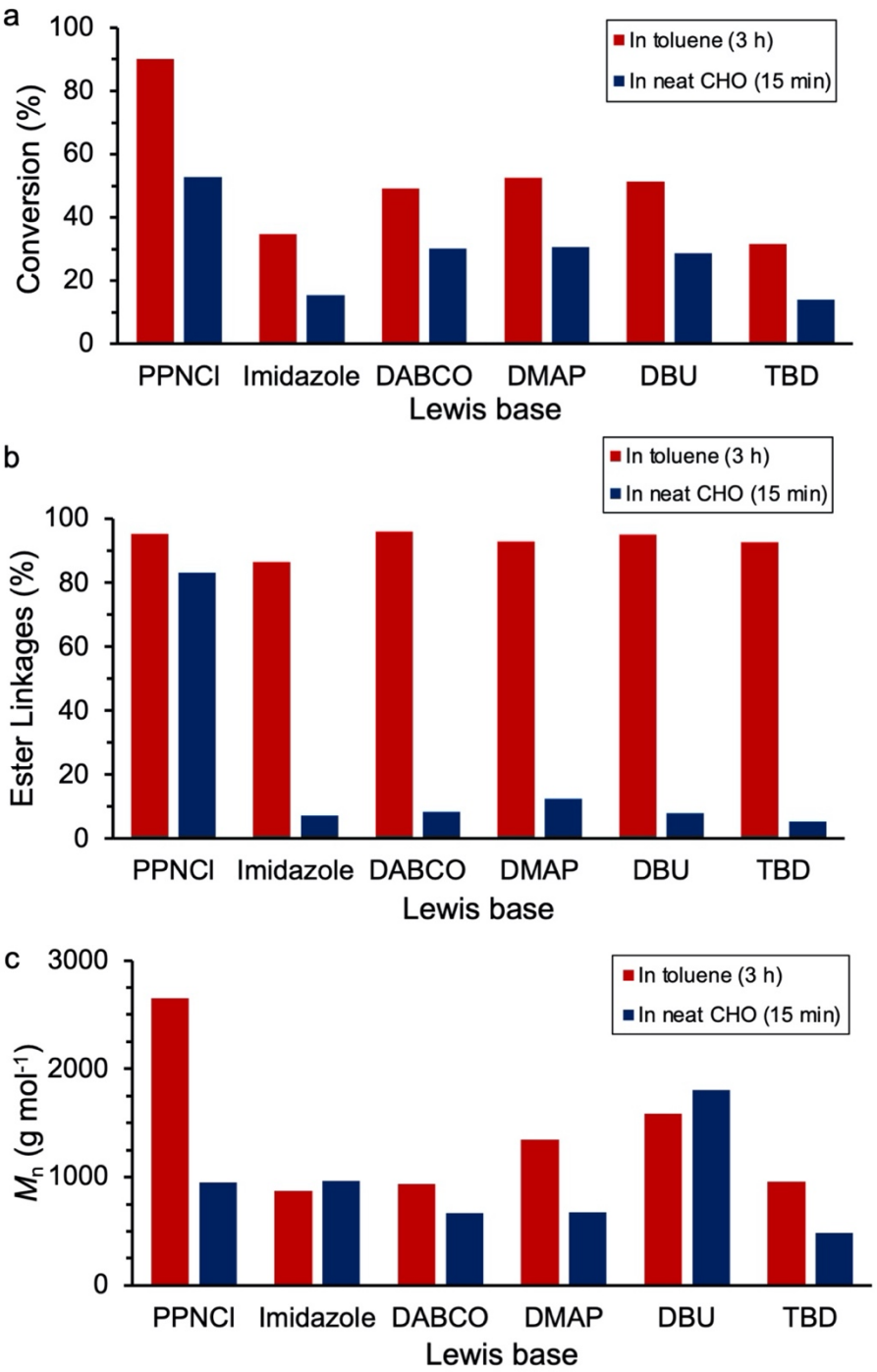

Figure 43. Data from copolymerisation **entries 1-12** where P(PA-co-CHO) was afforded from the ROCOP of PA and CHO mediated by $ZnCl_2$ and a range of Lewis bases in either toluene for 3 h or neat CHO for 15 min. a. Monomer conversion reached by the selected timepoint *vs.* the Lewis base employed. b. The percentage of ester linkages in the P(PA-*co*-CHO) afforded *vs.* the Lewis base employed. c. The number average molecular weight of P(PA-*co*-CHO) afforded *vs.* the Lewis base employed.

As the neutral heterocyclic amines did not afford significant polyester in neat CHO, their monomer conversions could not be usefully compared in the neat CHO reaction conditions. As expected due to the effect of decreased dilution, PPNCl showed a greatly increased polymerisation rate in neat CHO than toluene, achieving a 53% conversion in 15 min with the former conditions *vs*. a 90% conversion in 3 h with the latter conditions. Using toluene as a solvent, the order of the Lewis base's polymerisation rate was shown to be PPNCl > DMAP ≈ DABCO ≈ DBU > TBD ≈ imidazole. PPNCl's superior performance is reflected in literature and has been attributed to its cationic character which results in the faster dissociation of the chloride anion and therefore leads to an increase in the rate of epoxide ring-opening by the nucleophilic anion.[7] For the neutral heterocyclic amine bases, DMAP's superior catalytic activity (53% conversion in 3 h) compared to other neutral heterocyclic amines was a trend also seen across literature.[6, 9, 10] The decrease in polymerisation rate seen by the strongest and weakest base may have indicated that a balance of basicity is required for optimal catalytic performance. This may be because imidazole's weak basicity gave it a low nucleophilicity which hindered its ability to ring-open monomers and TBD's strong basicity allowed it to have a tighter affinity with the Lewis acid, decreasing its acidity and thus hindering its ability to activate an epoxide molecule to allow for ring-opening nucleophilic attack. As copolymerisations were not run to completion and monomer conversions differed significantly, the resultant polyester's number average molecular weight (M_n) could not be compared directly between Lewis acid choices. However, it was notable that PPNCl achieved a respectable molecular weight in toluene having almost reached completion (M_n = 2,654 g·mol^{-1}).

Overall, using different Lewis bases had a significant effect on the catalytic activity of the polymerisation. While the strength of the Lewis base influenced the catalytic activity of the neutral amine bases, a more key factor was the difference in activity achieved between a quarternary onium salt and a neutral organobase with the former showing significantly superior activity. The higher catalytic activity and high selectivity of PPNCl in toluene compared to other Lewis bases, alongside its ability to produce significant polyester when the copolymerisation was run in neat CHO (the preferable conditions for most metal halides) led to it being chosen as the Lewis base to use in the screen of metal halides. In addition to this, it produced clearer MALDI-ToF MS spectra for the polyester afforded than when DMAP was used (as discussed in the previous chapter), which was useful for analysing the polyester microstructure.

3.2.2 Lewis acid solubility

Before conducting a Lewis acid screen, the copolymerisation conditions had to be optimised to accommodate a wide range of metal halide Lewis acids. A test for a range of metal halides was conducted to see which dissolved in a CHO/toluene mix ([CHO] in toluene = 2 mol dm^{-3}, $[LA]_0$:$[CHO]_0$ = 1:50) after an hour at 110 ºC (**Table 8**). Metal halides that either didn't dissolved or saw partial solution were then tested for solubility in pure CHO ($[LA]_0$:$[CHO]_0$ = 1:100]) to replicate the neat epoxide conditions that were previously used in the Lewis base screen. While very few Lewis acids dissolved in the toluene conditions of the standard copolymerisation, YCl_3, $ZnCl_2$, $MgCl_2$, $AuCl_3$, $PdCl_2$, $AlCl_3$, $InCl_3$ and $CuCl_2$ all dissolved in the neat CHO conditions providing a selection of Lewis acids to screen and reaction conditions to screen them with.

Table 8. A solubility screen for metal halide Lewis acids.

Lewis acid	Dissolved in CHO/toluene mix?[a]	Dissolved in CHO?[b]
YCl_3	Yes	-
$ZnCl_2$	Yes	-
$MgCl_2$	No	Yes
$NiCl_2$	No	No
$AuCl_3$	Partially	Yes
$PdCl_2$	No	Yes
$AlCl_3$	Yes	-
$InCl_3$	Yes	-
$CrCl_2$	No	Partially
$CuCl_2$	Partially	Yes
$SrCl_2$	Partially	Partially
$EuCl_3$	Partially	Partially

[a]The metal halide (0.020 mmol) was stirred in a mixture of CHO (101 µL, 1.0 mmol) and toluene (0.5 mL, 4.47 mmol) at 110 ºC for 1 h simulating the conditions of copolymerisation in a solvent. [b]The metal halide (0.020 mmol) was stirred in a mixture of CHO (202 µL, 2.0 mmol) at 110 ºC for 1 h simulating the conditions of copolymerisation in neat epoxide.

3.2.3 Lewis acid metal ion screen

It had been established in literature that the acidity of the Lewis acid can have a significant influence on the selectivity and rate of the copolymerisation. No universal scale of Lewis acidity exists due to the complicated nature of the acid-base interaction. However, certain characteristics can be used as a rough approximation of Lewis acidities. One of the key contributions to the Lewis acidity of a metal salt is the

electronegativity of the central ion. The stronger the electronegativity of the metal ion, the greater its ability to accept a lone pair of electrons and hence the stronger its Lewis acidity. The Pauling scale of electronegativity, which gives the electronegativity of an isolated atom was used as a rough guide determine the Lewis acidity of metal halides selected for the Lewis acid.[17] To determine the effect of the choice of the Lewis acid in the metal halide Lewis pair catalysed ROCOP of anhydrides and epoxides on the catalytic activity, control and selectivity of the copolymerisation, the ROCOP of PA and CHO was screened using 4-MBA as a CTA and a Lewis pair catalyst system composed of PPNCl and a choice of metal halide (**Table 9**). PPNCl had been chosen due to its superior performance in the Lewis base screen.

Table 9. Lewis acid screen. All copolymerisations conducted with $[PA]_0/[CHO]_0/[LA]_0/[PPNCl]_0/[4\text{-}MBA]_0$ at 50:100:1:1:1 at 110 °C for 8 min followed by quenching in an ice bath.

Entry	Lewis acid	Metal ion electronegativity[a]	Monomer conversion[b] (%)	Ester linkages[c] (%)	M_n (SEC)[d] ($g \cdot mol^{-1}$)	$Đ_M$
13[e]	-		28	98	3146	1.14
14	-		52	93	3396	1.11
15	YCl_3	1.22	65	72	1961	1.11
16	$MgCl_2$	1.31	69	85	2994	1.14
17	$AlCl_3$	1.61	55	37	1148	1.18
18	$ZnCl_2$	1.65	31	71	876	1.24
19	$InCl_3$	1.78	50	14	1244	1.28
20	$CuCl_2$	1.90	24	90	945	1.28
21	$PdCl_2$	2.20	72	94	3924	1.13
22	$AuCl_3$	2.54	53	49	2072	1.23

[a]Values taken from the Pauling scale of electronegativity.[17] [b]Conversion of CHO calculated from the ^1H NMR spectrum ($CDCl_3$, 400 MHz) of the reaction mixture at the given timepoint. [c]Percentage of ester linkages determined by the ratio of the integrated height of the ester peak and ether peak in the ^1H NMR spectrum of the precipitated polyester product. [d]Molecular weight as calculated by SEC analysis using THF (0.5% NEt_3) as an eluent with PS standards. [e]4-MBA was omitted from this control copolymerisation.

The copolymerisations were analysed and compared against each other for their monomer conversion by the selected timepoint as a measure of catalytic activity and the portion of ester linkages in the resultant polyester as a measure of selectivity (**Figure 44**). It was expected that metal halides with a high metal electronegativity and therefore high Lewis acidity would promote the cationic homopolymerisation of epoxide

over the alternating copolymerisation of epoxide and anhydride and therefore that Lewis pair catalysts containing them would show poorer selectivity. However, the selectivity of the catalysts did not correspond with the metal halide's central metal ion electronegativity according to the Pauling scale. For example, Lewis acids $CuCl_2$ and $PdCl_2$ saw high ester linkages compared to Lewis acids $AlCl_3$ and $InCl_3$ despite the former two containing more highly electronegative metal ions. This is likely because electronegativity also depends on the chemical environment of the ion. An updated scale of electronegativity of cations, which took into account their oxidation state was determined by Xue and co-workers.[17] Assuming six-coordinated species, their scale of electronegativity gave a better fit for the selectivity of each metal halide: Mg^{2+} (1.23), Zn^{2+} (1.34), Y^{3+} (1.34), Pd^{2+} (1.35), Cu^{2+} (1.37), In^{3+} (1.48), Al^{3+} (1.51), Au^{3+} (1.55). Better selectivity (72-94% ester linkages) was given when metal halides with lower electronegativity ions (Mg^{2+}, Zn^{2+}, Y^{3+}, Pd^{2+}, Cu^{2+}) were employed but selectivity significantly decreased (14-49% ester linkages) for the metal halides with more highly electronegative metal ions (In^{3+}, Al^{3+}, Au^{3+}). Therefore, the number of chloride ligands on the metal halide, and hence the ionisation state, had a determining influence on the selectivity metal halide alongside the nature of the metal atom itself. No Lewis pair catalyst saw improved selectivity over the control PPNCl organocatalyst when used alongside the 4-MBA CTA (98% ester linkages).

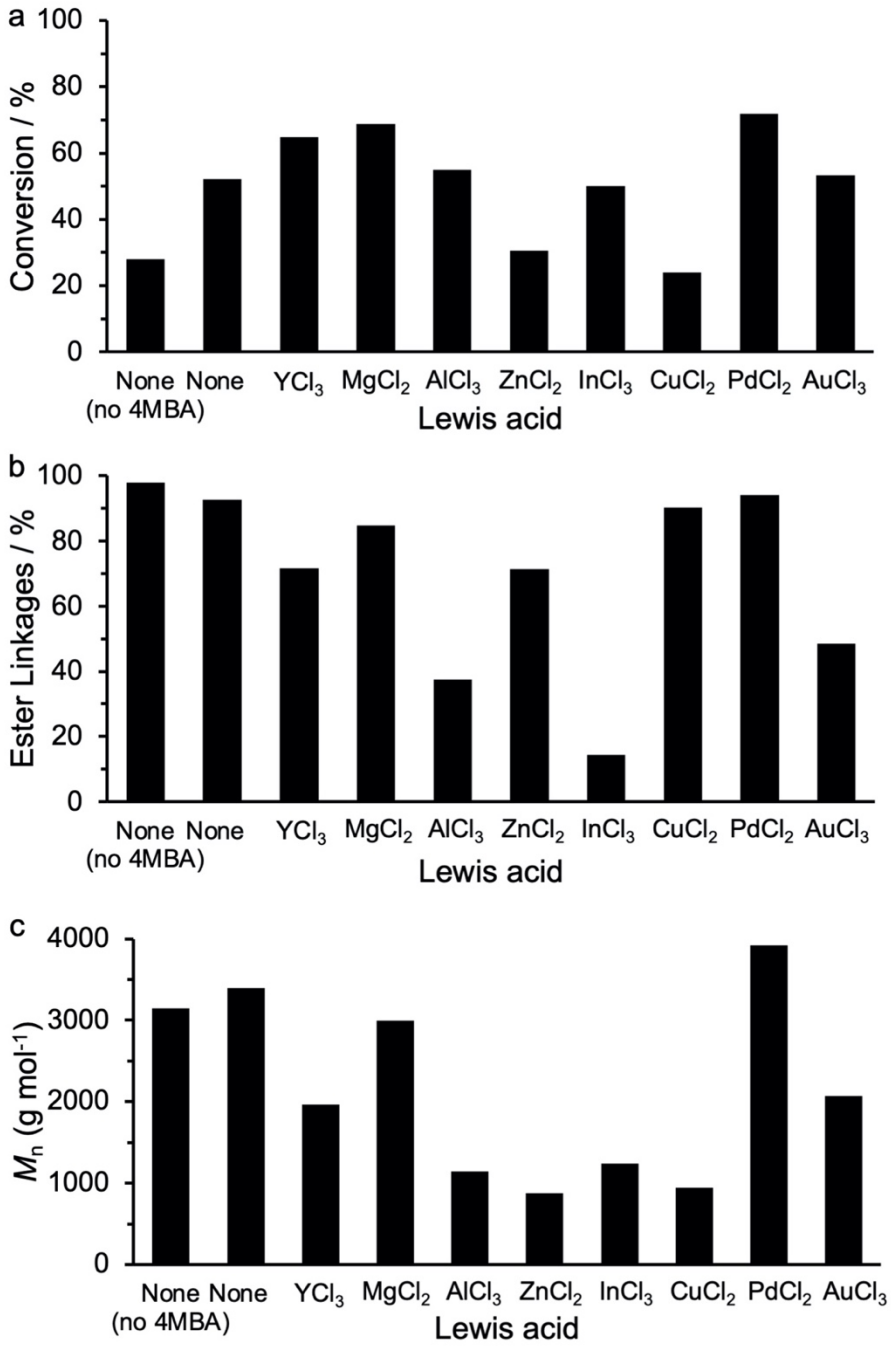

Figure 44. Data from copolymerisation **entries 13-22** where P(PA-co-CHO) was afforded from the ROCOP of PA and CHO mediated by PPNCl and a range of Lewis acids in neat CHO for 8 min. a. Monomer conversion reached by the selected timepoint *vs.* the Lewis base employed. b. The percentage of ester linkages in the P(PA-*co*-CHO) afforded *vs.* the Lewis base employed. c. The number average molecular weight of P(PA-*co*-CHO) afforded *vs.* the Lewis base employed.

Despite the lack of evidence for linear kinetics, an analysis of monomer conversion gave a rough idea for the effect on polymerisation rate by each Lewis acid. Promisingly, the addition of a metal halide Lewis acid in some cases did increase the monomer conversion above that which was achieved with just the Lewis base. This justified the pursuit of these Lewis pairs as potential competitors to alternate simple catalyst systems for anhydride and epoxide ROCOP. No clear trend was seen between the electronegativity of the metal in the metal halide and the monomer conversion at 8 min. $MgCl_2$ and YCl_3, which have metal ions with low electronegativity see higher monomer conversions suggesting that mild Lewis acids tend to give higher catalytic activities. In contrast, when using the Pauling scale, $PdCl_2$'s central metal has a high electronegativity and yet has the highest monomer conversion (72%) or when using the scale corrected for oxidation state, $ZnCl_2$'s central metal has the second lowest electronegativity of the metal halides selected and yet has a low monomer conversion (31%). This suggested that other competing influences played a determining effect on the overall efficiency of the Lewis pair catalysts. The solubility of the metal halide was known to be a determining factor on the copolymerisation's ability to be controlled due to the timeframe taken to dissolve once heated. This would be different for each metal halide and not dependent on its Lewis acidity. The efficiency of the catalyst could also be a result of a more complex understanding of Lewis acidity. Results from literature indicated that mild Lewis acids used in Lewis pair catalysis saw good polymerisation rates as they were able to dissociate from the Lewis base more easily. But this had to be balanced with a Lewis acidity strong enough to activate the monomer rapidly for nucleophilic attack to ring-open it. The ability for the Lewis pair to dissociate also depends on the strength of the Lewis base and the ability for the Lewis acid to activate

the monomer also depends on the ability of the monomer to be ring-opened. Therefore, it is likely that while a general rule on Lewis acidity applies for the selectivity of Lewis pair catalysts, for catalytic activity, the specific conditions play a determining factor on which Lewis acid is most suited to a copolymerisation such as its solubility, the choice of Lewis base and choice of monomer. In this copolymerisation screen, $PdCl_2$ saw the best fit with both the highest monomer conversion after 8 min (72%) and the highest selectivity (88% ester linkages) of all Lewis acids screened.

The effect of the metal halide on the M_n of the afforded polyester was not clear as copolymerisations were not run to the same monomer conversion. Therefore, monomer conversion had to be considered when studying the data. Despite only a slightly lower conversion than $MgCl_2$ (69%), YCl_3 (65%) saw a significantly lower polyester molecular weight. $PdCl_2$ was notable for seeing both the highest conversion (72%) and highest afforded polyester molecular weight (M_n = 3,924 g·mol^{-1}). $MgCl_2$ also saw a high conversion (69%) and high afforded polyester molecular weight (M_n = 2,994 g·mol^{-1}). Overall, the screen highlighted three Lewis acids which showed high catalytic activity and good selectivity: $PdCl_2$, $MgCl_2$ and YCl_3. However, given the influences of solubility on the performance of each Lewis acid, which the single timepoint screen could not account for a more detailed kinetic investigation of these Lewis acids was needed.

3.2.4 Lewis acid ligand screen

The nature of the ligand has a contributing factor to a metal halide's Lewis acidity.[4, 5] To determine the effect of the choice of the ligand in the metal halide Lewis pair catalysed ROCOP of anhydrides and epoxides on the catalytic activity, control and selectivity of the copolymerisation, the ROCOP of PA and CHO was screened using

4-MBA as a CTA and a Lewis pair catalyst system composed of PPNCl and a choice of metal salt with different ligands (**Table 10**). Bromide and iodide ions allowed for a comparison of copolymerisation effects when the electronegativity of the metal halide was changed. Magnesium acetate was also tested alongside the metal halides as a contrasting comparison as no mention of it being tested in such a Lewis pair was found in literature.

Table 10. Lewis acid ligand screen. All copolymerisations conducted with $[PA]_0/[CHO]_0/[LA]_0/[PPNCl]_0/[4\text{-MBA}]_0$ at 50:100:1:1:1 at 110 °C for 8 min followed by quenching in an ice bath.

Entry	Lewis acid	Monomer conversion[a] (%)	Ester linkages[b] (%)	M_n (SEC)[c] ($g \cdot mol^{-1}$)	$Đ_M$
23	$MgBr_2$	59	90	1859	1.14
24	MgI_2	65	92	1892	1.17
25	$Mg(OAc)_2$	66	93	3259	1.19
26	$PdBr_2$	73	93	3360	1.14

[a]Conversion of CHO calculated from the ^{1}H NMR spectrum ($CDCl_3$, 400 MHz) of the reaction mixture at the given timepoint. [b]Percentage of ester linkages determined by the ratio of the integrated height of the ester peak and ether peak in the ^{1}H NMR spectrum of the precipitated polyester product. [c]Molecular weight as calculated by SEC analysis using THF (0.5% NEt_3) as an eluent with PS standards.

The copolymerisations were analysed and compared against each other for their monomer conversion by the selected timepoint as a measure of catalytic activity and the portion of ester linkages in the resultant polyester as a measure of selectivity (**Figure 45**). For the magnesium salts, the selectivity of the Lewis pair catalysts was improved by changing the halide ligand from a chloride (85% ester linkages) to a bromide (90% ester linkages) to an iodide (92% ester linkages) or from a halide to an

acetate ligand (93% ester linkages). This trend was reflected in the comparison between palladium chloride (92%) and bromide (93%). This trend was likely seen because stronger Lewis acids promoted the homopolymerisation of epoxides leading to a lower degree of alternation in the polyesters afforded. Bromide, iodide and acetate ions were progressively less electron withdrawing, promoting relatively higher electron density on the metal ion compared to chloride and thus lowering the Lewis acidity of the overall complex. In contrast, changing the ligand in the metal halide had little significant effect on monomer conversion and therefore no conclusions could be drawn especially considering the unknown and therefore possibly non-linear kinetics of the copolymerisations.

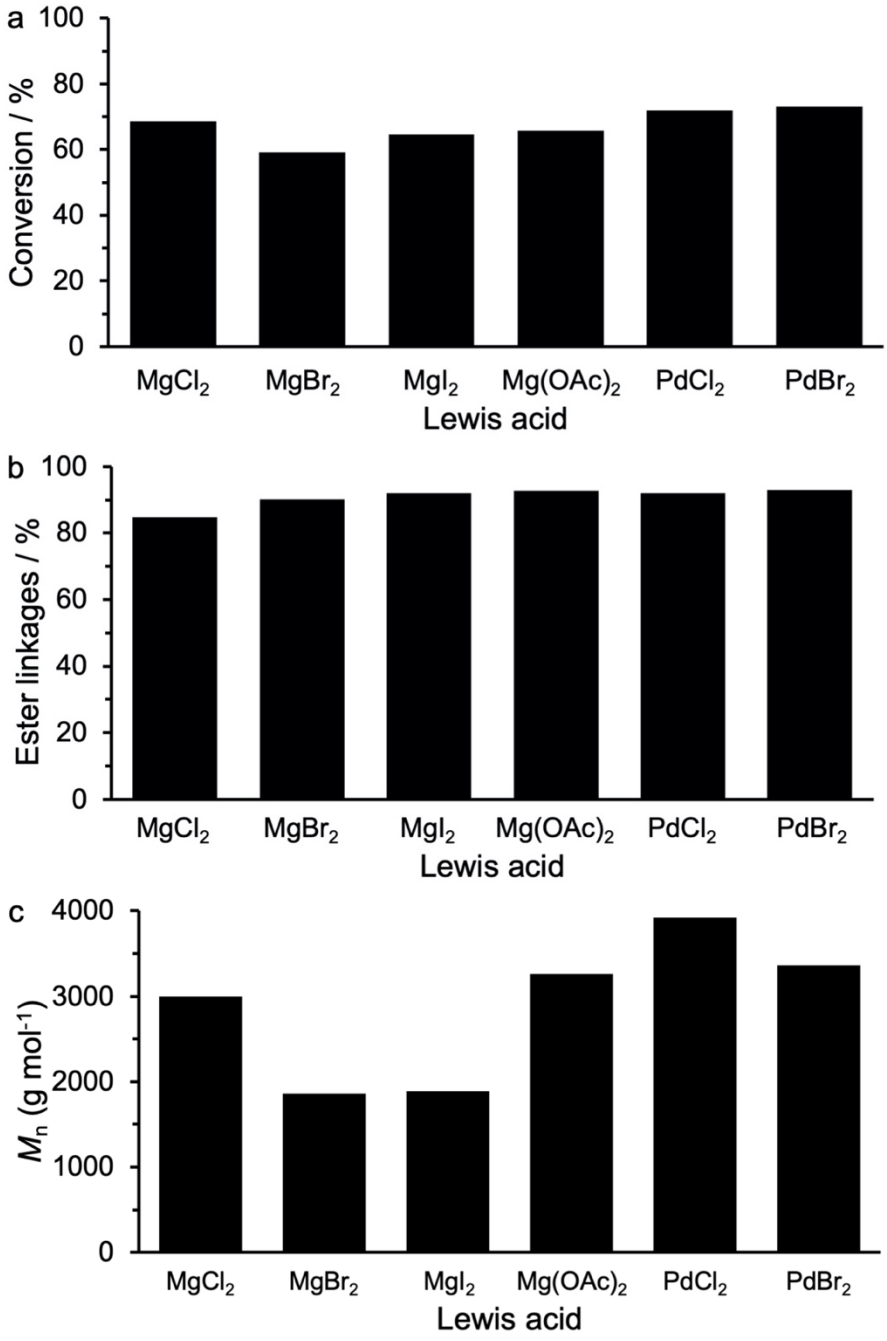

Figure 45. Data from copolymerisation **entries 16, 21, 23-26** where P(PA-co-CHO) was afforded from the ROCOP of PA and CHO mediated by PPNCl and a range of Lewis acids in neat CHO for 8 min. a. Monomer conversion reached by the selected timepoint *vs.* the Lewis base employed. b. The percentage of ester linkages in the P(PA-*co*-CHO) afforded *vs.* the Lewis base employed. c. The number average molecular weight of P(PA-*co*-CHO) afforded *vs.* the Lewis base employed.

The choice of ligand had a significant effect on the M_n of the polyester produced. $MgBr_2$ and MgI_2 gave polyester with almost two thirds the length (M_n = 1,900 g·mol^{-1}) of polyester chains produced by $MgCl_2$ (M_n = 3,000 g·mol^{-1}). It was thought that this was due to the nature of bromide and iodide ions, which can stabilise the negative charge more easily than chloride ions and therefore were better leaving groups. Therefore, they were more likely to dissociate or be displaced from the metal centre and act as copolymerisation initiators or CTAs than the chloride ions, increasing the amount of initiators or CTAs overall and thus shorter polymer chains. No significant effect was seen for palladium halides. Acetate ions are worse leaving groups than halide ions and so acetate was least able to be displaced and act as an initiator or CTA leading to the highest chain length polyester (M_n = 3,300 g·mol^{-1}). Overall, the effect of replacing the chloride ligand with bromide or iodide in the ROCOP of CHO and PA using metal halide Lewis pair catalysts resulted in a comparable polymerisation rate, only a slight increase in alternating nature of the polyester produced and a significant decrease in molecular weight of the polyester produced. Using an acetate ion saw comparable behaviour to the chloride ion.

3.2.5 Kinetics of the best Lewis acids

To determine if the ROCOP of PA and CHO using a Lewis pair catalyst containing the best performing Lewis acids from the Lewis acid screen were controlled, copolymerisations with Lewis acids YCl_3 (**Entry 15**), $MgCl_2$ (**Entry 16**) and $PdCl_2$ (**Entry 21**) were tested in kinetic studies with 5 timepoints across 10 minutes. PPNCl was employed as a Lewis base and the copolymerisations were run in neat CHO (2:1 ratio of CHO with PA) with 4-MBA included. A control copolymerisation was also run with no Lewis acid present (**Entry 14**).

Kinetic analysis demonstrated non-linear kinetics for all four copolymerisations (**Figure 46**). This was unexpected for the control copolymerisation without a Lewis acid employed, as it had been hypothesised in Chapter 2 that the contributing factor to the uncontrolled nature of the system was the Lewis acid's solubility and/or the introduction of its chloride ligands as initiators or CTAs into the copolymerisation through displacement over time. This finding did not match the literature reports that PPNCl gave linear kinetic plots when used as an organocatalyst for the ROCOP of PA and CHO (though this study was conducted in a toluene solution).[9] A plausible explanation for this difference may be that unlike in large amounts of toluene, PPNCl takes a significant amount of time to dissolve in small amounts of CHO once heated relative to the time taken for the copolymerisation to reach completion. YCl_3 saw the fastest polymerisation rate with an overall order of: YCl_3 > $PdCl_2$ > $MgCl_2$ > no Lewis acid.

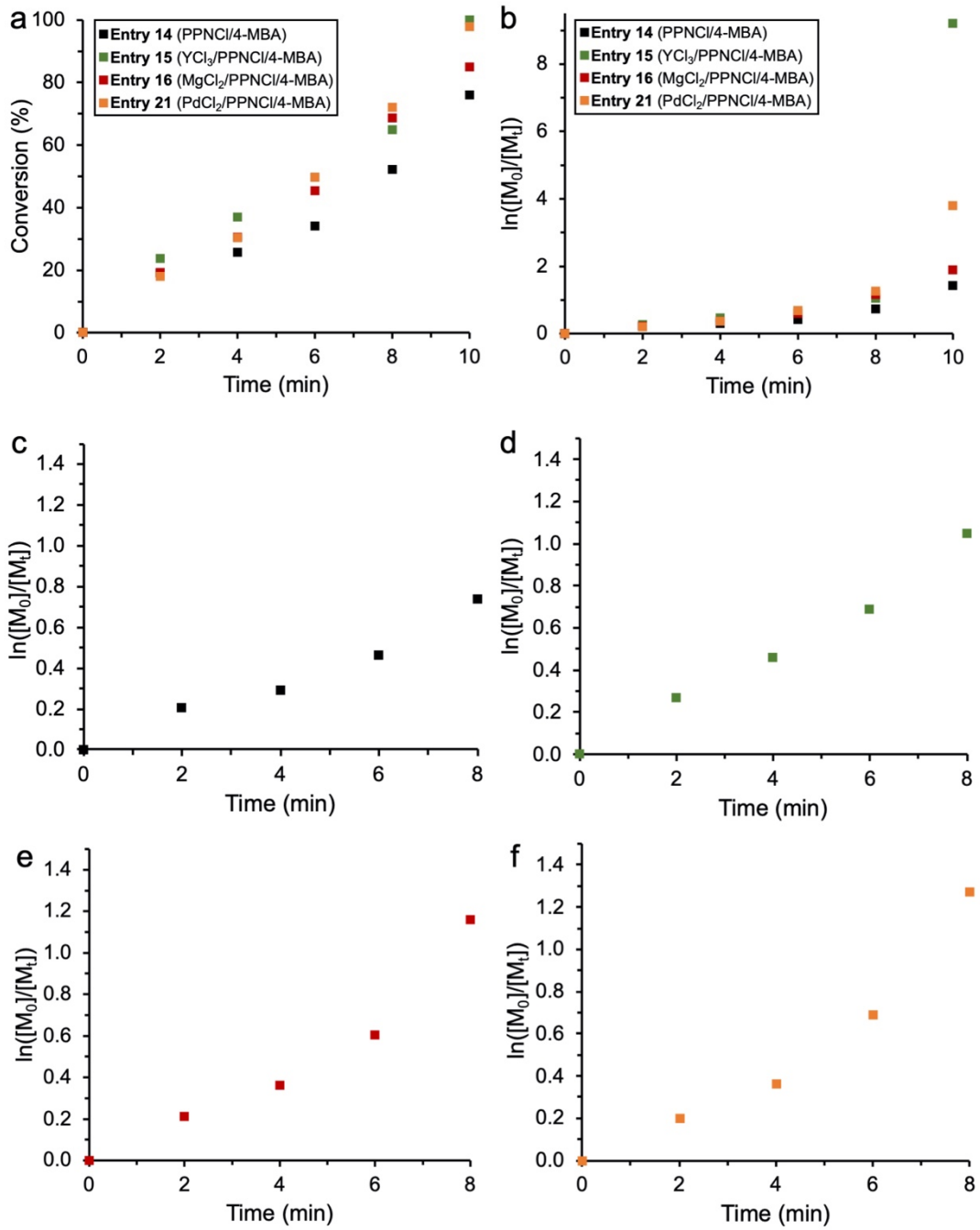

Figure 46. Data from copolymerisation **entries 14-16** and **21** in which P(PA-co-CHO) was afforded from the ROCOP of PA and CHO mediated by PPNCl and a Lewis acid (or no Lewis acid in the case of the control) in neat CHO for 15 min. a. Monomer conversion *vs.* time plot with for all entries combined (up to 10 min). b. Kinetic plot for all entries combined (up to 10 min). c. Kinetic plot for **Entry 27** (up to 8 min). d. Kinetic plot for **Entry 28** (up to 8 min). e. Kinetic plot for **Entry 29** (up to 8 min). f. Kinetic plot for **Entry 30** (up to 8 min).

Plots of monomer conversion against the M_n of afforded polyester were not linear and instead showed that an induction period existed at the start of each copolymerisation where initiation dominated over propagation (**Figure 47**). This was likely due to the time taken for the copolymerisation to heat to reaction temperature and thus allow all the initiating species to form a propagating chain through reactions with the monomers. All copolymerisations afforded different molecular weight polyesters. YCl_3 produced the shortest chains followed by $MgCl_2$. $PdCl_2$ and no Lewis acid both produced respectable molecular weight polyesters (M_n ~ 5,000 $g \cdot mol^{-1}$). The control copolymerisation without a Lewis acid did not reach completion and so would have likely achieved an even higher molecular weight for the afforded polyester.

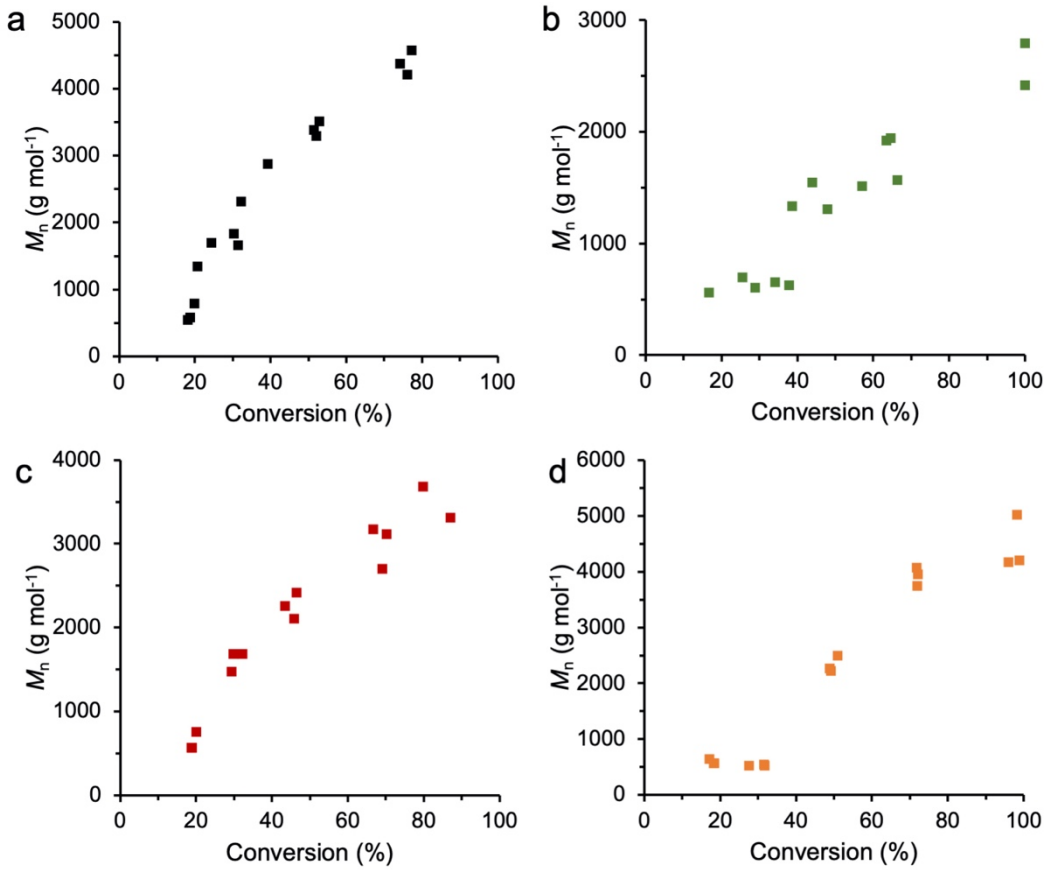

Figure 47. A comparison of monomer conversion vs number average molecular weight (M_n) of afforded polyester for each copolymerisation a. **Entries 14** (no Lewis acid), b. **Entry 15** (YCl_3), c. **Entry 16** ($MgCl_2$), d. **Entry 21** ($PdCl_2$).

3.3 Conclusions

The optimisation of the model copolymerisation for the ROCOP of PA and CHO using a simple metal halide-based Lewis pair catalyst established in Chapter 2 was explored. In accordance with literature reports of previous catalysts employed for the ROCOP of anhydrides and epoxides, it was found that manipulating the Lewis acid, Lewis base and solvent had an effect on the outcome of the copolymerisation. Screening different Lewis bases confirmed the superiority of PPNCl over neutral heterocyclic amines for both selectivity and catalytic activity widely acknowledged in literature due to its cationic nature and hence the rapid dissociation of its chloride to act as a nucleophile for epoxide ring-opening. By running copolymerisations in neat CHO rather than toluene, polymerisation rates dramatically increased from completion in 5 h to completion in 10 min due to the lower dilution effects from using a small amount of excess monomer rather than large amounts of solvent. In addition to this, metal halides had higher solubilities in the polar monomer than relatively apolar solvent.

A screen of Lewis acids found three metal halides which showed a catalytic activity higher than the controls and good selectivity: YCl_3, $MgCl_2$ and $PdCl_2$. In general, milder Lewis acids saw higher selectivities but no trend could be made between Lewis acidity and catalytic activity. This was either due to the catalytic activity being dependent on a good match between the Lewis acidity of the metal halide and the Lewis base strength or because the difference in solubility timeframe of the metal halides played a determining factor on their polymerisation rate. Meanwhile, manipulating the nature of the halide ligand from a chloride to a bromide or iodide had a far less significant impact on selectivity than manipulating the choice of metal centre. No significant change in catalytic activity came from changing the halide ligand's nature but a large

decrease in polymer chain length was afforded from bromide and iodide salts due to their greater ability to be displaced from the metal. Kinetic analysis showed the true order of catalytic activity for the best performing Lewis acids to be: YCl_3 > $PdCl_2$ > $MgCl_2$. Copolymerisations did not show a controlled nature as seen with the model copolymerisation in Chapter 2 but this included the control without Lewis acid which suggested the reaction conditions were responsible for this. As suggested in Chapter 2, a solution to this could be pre-heating the Lewis acid and Lewis base in solvent before the monomer is added and using a THF salt of the Lewis acid to increase its solubility. Another solution when running the copolymerisations in neat epoxide conditions could be to increase the amount of epoxide from a 2:1 ratio to a 5:1 ratio of $[CHO]_0$:$[PA]_0$ to increase the amount of solvent present (though this is expected to decrease the rate of polymerisation). Nevertheless, these findings show the potential a wide-range of metal halide benchtop reagents can play as part of simple Lewis pair catalyst systems as a low-cost, industrial viable route to affording polyesters.

3.4 Experimental details

3.4.1 General considerations

All reagents for the copolymerisations were stored in a nitrogen-filled glovebox. Dry toluene, chloroform and dichloromethane were obtained from a SPS system, degassed by three freeze-pump-thaw cycles and stored over activated 3 Å or 4 Å molecular sieves in a nitrogen-filled glovebox nitrogen. Before use in an air-free reaction, all glassware was dried in the oven at 180 °C overnight.

3.4.2 Instruments

3.4.2.1 NMR Spectrometer

^{1}H NMR and ^{13}C–{^{1}H} NMR spectra were recorded at 298 K on an Ascend Bruker 400 spectrometer equipped with a BBFO smart probe operating at 400 MHz and 101 MHz respectively. Chemical shifts on the 1H NMR spectra were referenced to the solvent residual proton resonance signals: δ 7.26 ppm for d_1–CDCl3. The data obtained was processed and analysed using MestReNova 12.0.3 software.

3.4.2.2 Size exclusion chromatography

Size exclusion chromatography (SEC) in THF was performed on an Agilent 1260 Infinity II LC system equipped with a Wyatt Optilab T-rEX differential refractive index detector, an Agilent guard column (PLGel 5 μM, 50 × 7.5 mm) and two Agilent Mixed-C columns (PLGel 5 μM, 300 × 7.5 mm). The mobile phase was THF (HPLC grade) at flow rate of 1.0^{-1} mL·min. Number average molecular weights (M_n), weight average molecular weights (M_w) and dispersities ($Đ_M = M_w/M_n$) were determined using Wyatt ASTRA v7.1.3 software against poly(styrene) (PS) standards.

3.4.2.3 Centrifuge

Ohaus FC5706 Frontier Centrifuge Multi 230V.

3.4.3 Materials

Zinc chloride anhydrous (anhydrous, 98+%) and 4-methoxybenzyl alcohol (dissolved in dry dichloromethane, dried over CaH_2, distilled under nitrogen, degassed and stored under an inert atmosphere, 98%) were purchased from Alfa Aesar. 4-dimethylaminopyridine (dried over molecular sieves, ≥99%), palladium (II) chloride (anhydrous), magnesium chloride (anhydrous, ≥98%), palladium (II) bromide (99%, anhydrous), magnesium acetate (≥98%), gold (III) chloride (anhydrous, 99.99%), aluminium (III) chloride (anhydrous, 99.999%), yttrium (III) chloride (anhydrous, 99.99%), toluene (99.8%), methanol (99.8%), phthalic anhydride (≥99%), bis(triphenylphosphine)iminium chloride (97%), chloroform (≥99%), tetrahydrofuran (HPLC grade, ≥99.9%, inhibitor-free), triethylamine (≥99.5%) and calcium hydride (95%) were purchased from Sigma Aldrich. Magnesium iodide (anhydrous, 99.997%) and indium (III) chloride (anhydrous, ≥99.999%) were purchased from VWR. Magnesium bromide (anhydrous, 98%), cyclohexene oxide (98%) and dichloromethane (≥99.5%) were purchased from Acros Organics. Hydrochloric acid (37%) and copper (II) chloride (anhydrous, 99.995%) were purchased from Fisher Scientific. Deuterated chloroform (dried over CaH_2 and distilled under nitrogen twice, degassed and stored under an inert atmosphere, 98%) was purchased from Apollo Scientific. Unless stated otherwise, all chemicals and compounds were used as received.

3.4.4 Monomer preparation

Given the ease by which monomer impurities can disrupt anhydride and epoxide ring-opening copolymerisation, it was important to stringently purify and dry the phthalic anhydride and cyclohexene oxide comonomers.

Phthalic anhydride (20 g) was stirred in dry toluene (500 mL) and then cannula filtered under nitrogen. Toluene was then removed under reduced pressure before the solid was recrystallised in dry chloroform. The crystals were then sublimed twice in a nitrogen filled sublimation chamber under reduced pressure and heat (80 ºC). The resultant white crystals (~ 5 g) were analysed with ^{1}H NMR and ^{13}C–{^{1}H} NMR spectroscopy to determine the purity.

Cyclohexene oxide (200 mL) was stirred over CaH_2 and distilled under nitrogen twice followed by degassing through freeze-pump thawing thrice. The resultant colourless liquid was analysed with ^{1}H NMR and ^{13}C–{^{1}H} NMR spectroscopy to determine the purity.

3.4.5 Copolymerisation procedures

3.4.5.1 Lewis base screen (in toluene)

In a nitrogen-filled glove box, a 7 mL teflon-sealed vial with a magnetic stirrer bar was primed with zinc chloride (2.7 mg, 0.020 mmol), an organobase (0.020 mmol), phthalic anhydride (148 mg, 1.0 mmol) and a stock solution of 4-methoxybenzyl alcohol (2.5 µL, 0.020 mmol), cyclohexene oxide (101 µL, 1.0 mmol) and toluene (0.5 mL, 4.47 mmol). The vial was stirred and heated to 110 ºC for 3 h after which the vial was quenched in an ice bath and then opened to air. $CDCl_3$ was added and a sample taken for ^{1}H NMR and ^{13}C–{^{1}H} NMR analysis. A sample was also taken and diluted in

tetrahydrofuran (1 mL) for SEC analysis. The polymer was crashed out of the remaining reaction mixture by precipitation into a MeOH/HCl mixture cooled using liquid nitrogen. Polymers were dried under reduced pressure at 60 ºC

3.4.5.2 Lewis base screen (in neat epoxide)

In a nitrogen-filled glove box, a 7 mL teflon-sealed vial with a magnetic stirrer bar was primed with zinc chloride (2.7 mg, 0.020 mmol), an organobase (0.020 mmol), phthalic anhydride (148 mg, 1.0 mmol) and a stock solution of 4-methoxybenzyl alcohol (2.5 µL, 0.020 mmol) and cyclohexene oxide (202 µL, 2.0 mmol). The vial was stirred and heated to 110 ºC for 15 min after which the vial was quenched in an ice bath and then opened to air. $CDCl_3$ was added and a sample taken for ^{1}H NMR and $^{13}C–\{^{1}H\}$ NMR analysis. A sample was also taken and diluted in tetrahydrofuran (1 mL) for SEC analysis. The polymer was crashed out of the remaining reaction mixture by precipitation into a MeOH/HCl mixture cooled using liquid nitrogen. Polymers were dried under reduced pressure at 60 ºC.

3.4.5.3 Lewis acid screen

In a nitrogen-filled glove box, a 7 mL teflon-sealed vial with a magnetic stirrer bar was primed with a metal halide (0.024 mmol), bis(triphenylphosphine)iminium chloride (13.8 mg, 0.024 mmol), phthalic anhydride (178 mg, 1.2 mmol) and a stock solution of 4-methoxybenzyl alcohol (3.0 µL, 0.024 mmol) and cyclohexene oxide (243 µL, 2.4 mmol). The vial was stirred and heated to 110 ºC for 8 min after which the vial was quenched in an ice bath and then opened to air. $CDCl_3$ was added and a sample taken for ^{1}H NMR and $^{13}C–\{^{1}H\}$ NMR analysis. A sample was also taken and diluted in tetrahydrofuran (1 mL) for SEC analysis. The polymer was crashed out of the

remaining reaction mixture by precipitation into a MeOH/HCl mixture cooled using liquid nitrogen. Polymers were dried under reduced pressure at 60 ºC.

3.5 Appendix

3.5.1 Data for kinetic runs

3.5.1.1 PPNCl only kinetic run

Table 11. Kinetic study of **Entry 14** (no Lewis acid). Conducted with $[PA]_0/[CHO]_0/[PPNCl]_0/[4\text{-MBA}]_0$ at 50:100:1:1 at 110 °C.

Entry	Time (min)	Monomer conversion[a] (%)	M_n (SEC)[b] ($g \cdot mol^{-1}$)	$Đ_M$
1	2	19	848	1.34
2	4	26	1563	1.12
3	6	37	2340	1.11
4	8	52	3396	1.11
5	10	76	4385	1.12

[a]Conversion of CHO calculated from the ^1H NMR spectrum ($CDCl_3$, 400 MHz) of the reaction mixture at the given timepoint. [b]Molecular weight as calculated by SEC analysis using THF (0.5% NEt_3) as an eluent with PS standards.

3.5.1.2 YCl_3/PPNCl kinetic run

Table 12. Kinetic study of **Entry 15** (with YCl_3). Conducted with $[PA]_0/[CHO]_0/[YCl_3]_0/[PPNCl]_0/[4\text{-MBA}]_0$ at 50:100:1:1:1 at 110 °C.

Entry	Time (min)	Monomer conversion[a] (%)	M_n (SEC)[b] ($g \cdot mol^{-1}$)	$Đ_M$
1	2	24	621	1.25
2	4	37	872	1.29
3	6	50	1459	1.18
4	8	65	1812	1.12
5	10	99	2607	1.14

[a]Conversion of CHO calculated from the ^1H NMR spectrum ($CDCl_3$, 400 MHz) of the reaction mixture at the given timepoint. [b]Molecular weight as calculated by SEC analysis using THF (0.5% NEt_3) as an eluent with PS standards.

3.5.1.3 $MgCl_2$/PPNCl kinetic run

Table 13. Kinetic study of **Entry 16** (with $MgCl_2$). Conducted with $[PA]_0/[CHO]_0/[MgCl_2]_0/[PPNCl]_0/[4\text{-}MBA]_0$ at 50:100:1:1:1 at 110 °C.

Entry	Time (min)	Monomer conversion[a] (%)	M_n (SEC)[b] ($g \cdot mol^{-1}$)	$Đ_M$
1	2	19	626	1.32
2	4	30	1614	1.12
3	6	45	2259	1.14
4	8	69	2994	1.14
5	10	85	3492	1.13

[a]Conversion of CHO calculated from the ^1H NMR spectrum ($CDCl_3$, 400 MHz) of the reaction mixture at the given timepoint. [b]Molecular weight as calculated by SEC analysis using THF (0.5% NEt_3) as an eluent with PS standards.

3.5.1.4 $PdCl_2$/PPNCl kinetic run

Table 14. Kinetic study of **Entry 16** (with $PdCl_2$). Conducted with $[PA]_0/[CHO]_0/[PdCl_2]_0/[PPNCl]_0/[4\text{-}MBA]_0$ at 50:100:1:1:1 at 110 °C.

Entry	Time (min)	Monomer conversion[a] (%)	M_n (SEC)[b] ($g \cdot mol^{-1}$)	$Đ_M$
1	2	18	595	1.32
2	4	30	533	1.12
3	6	50	2326	1.19
4	8	72	3924	1.13
5	10	98	4466	1.13

[a]Conversion of CHO calculated from the ^1H NMR spectrum ($CDCl_3$, 400 MHz) of the reaction mixture at the given timepoint. [b]Molecular weight as calculated by SEC analysis using THF (0.5% NEt_3) as an eluent with PS standards.

3.5.2 Bulk copolymerisation of CHO and PA with $ZnCl_2$/DMAP

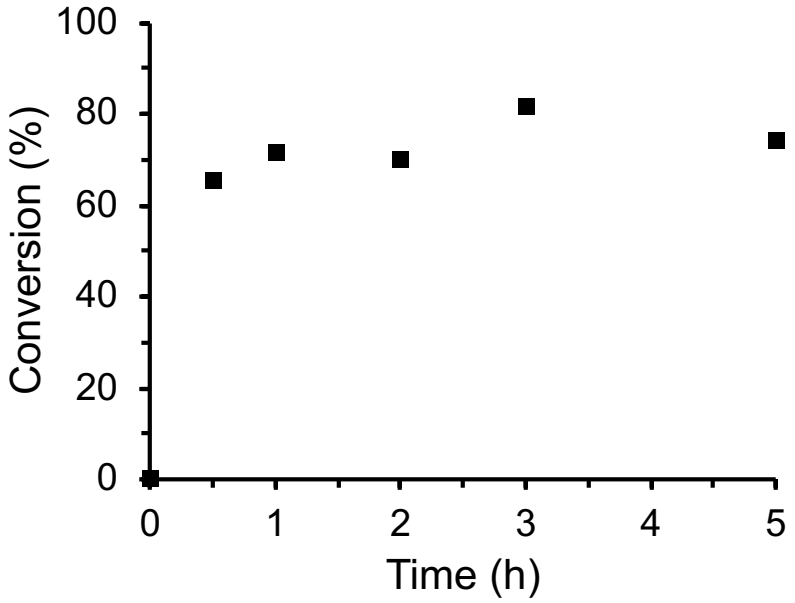

Figure 48. Monomer conversion vs. time plot with for the ROCOP of PA and CHO by $ZnCl_2$/DMAP in bulk conditions. $[PA]_0:[CHO]_0:[ZnCl2]_0:[DMAP]_0:[4\text{-}MBA]_0$ = 50:50:1:1:1.

3.5.3 SEC traces

3.5.3.1 Lewis base screen in toluene

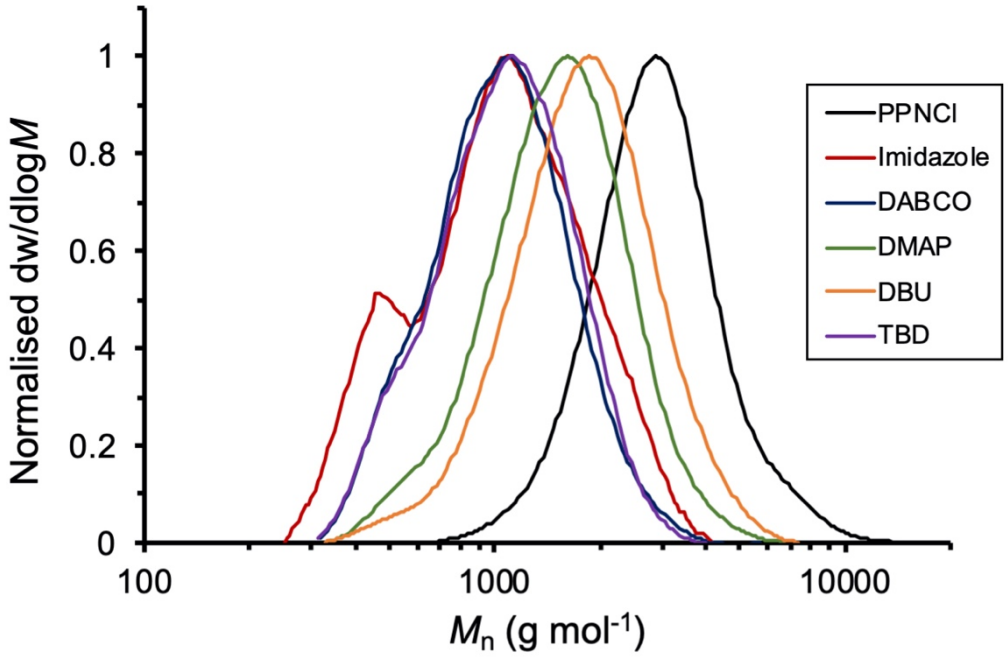

Figure 49. The size exclusion chromatograms of the molecular weight distribution of the P(PA-co-CHO) copolymer derived from each copolymerization run in the Lewis base screen in toluene (**Entries 1-6**). Molecular weight was determined against poly(styrene) standards using tetrahydrofuran (THF) (0.5% NEt_3) as an eluent.

3.5.3.2 Lewis base screen in neat CHO

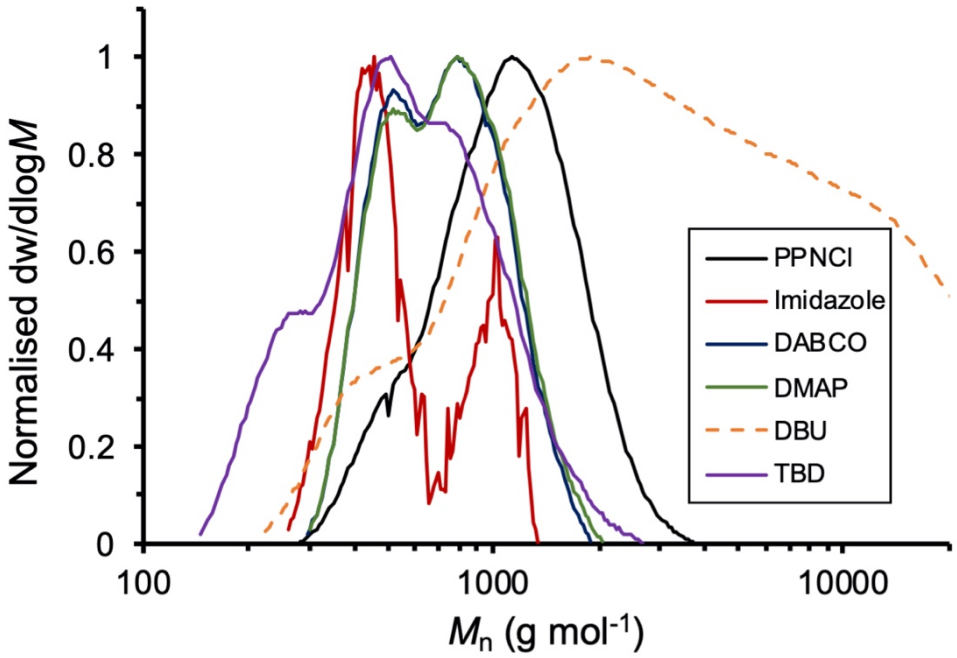

Figure 50. The size exclusion chromatograms of the molecular weight distribution of the P(PA-co-CHO) copolymer derived from each copolymerization run in the Lewis base screen in neat CHO (**Entries 7-12**). Molecular weight was determined against poly(styrene) standards using tetrahydrofuran (THF) (0.5% NEt_3) as an eluent.

3.5.3.3 Lewis acid metal screen

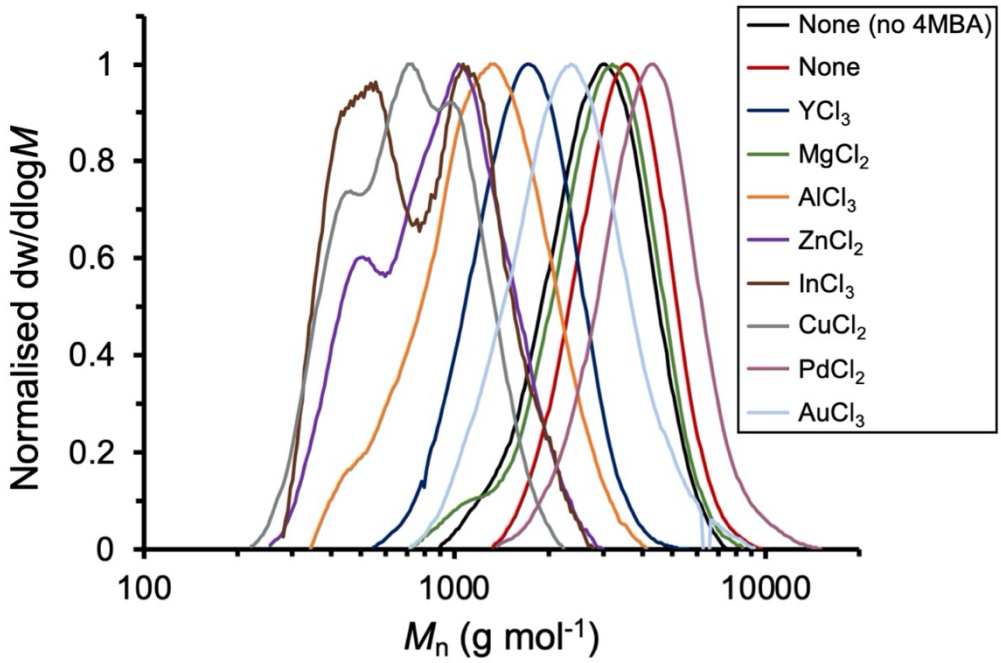

Figure 51. The size exclusion chromatograms of the molecular weight distribution of the P(PA-co-CHO) copolymer derived from each copolymerization run in the Lewis acid metal screen (**Entries 13-22**). Molecular weight was determined against poly(styrene) standards using tetrahydrofuran (THF) (0.5% NEt_3) as an eluent.

3.5.3.4 Lewis acid ligand screen

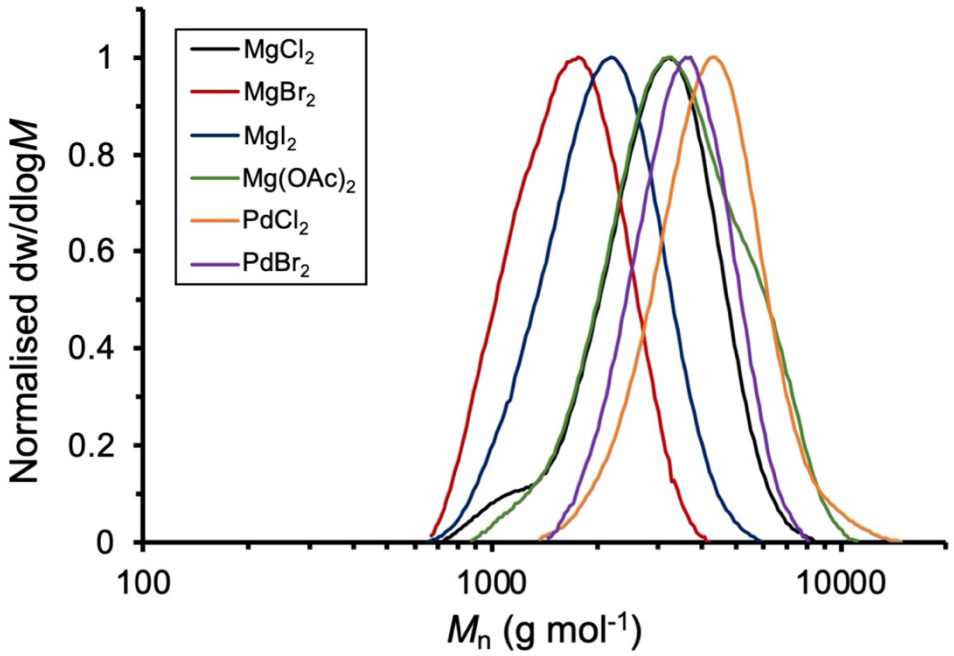

Figure 52. The size exclusion chromatograms of the molecular weight distribution of the P(PA-co-CHO) copolymer derived from each copolymerization run in the Lewis acid ligand screen (**Entries 16, 21, 23-26**). Molecular weight was determined against poly(styrene) standards using tetrahydrofuran (THF) (0.5% NEt_3) as an eluent.

3.6 References

1. M. L. McGraw and E. Y. X. Chen, *Macromolecules*, 2020, **53**, 6102-6122.
2. M. Hong, J. Chen and E. Y. X. Chen, *Chem. Rev.*, 2018, **118**, 10551-10616.
3. H.-Y. Ji, B. Wang, L. Pan and Y.-S. Li, *Green Chem.*, 2018, **20**, 641-648.
4. N. J. Van Zee and G. W. Coates, *Angew. Chem. Int. Ed.*, 2015, **54**, 2665-2668.
5. N. J. Van Zee, M. J. Sanford and G. W. Coates, *J. Am. Chem. Soc.*, 2016, **138**, 2755-2761.
6. E. Hosseini Nejad, C. G. W. van Melis, T. J. Vermeer, C. E. Koning and R. Duchateau, *Macromolecules*, 2012, **45**, 1770-1776.
7. A. Kummari, S. Pappuru and D. Chakraborty, *Polym. Chem.*, 2018, **9**, 4052-4062.
8. L.-F. Hu, C.-J. Zhang, H.-L. Wu, J.-L. Yang, B. Liu, H.-Y. Duan and X.-H. Zhang, *Macromolecules*, 2018, **51**, 3126-3134.
9. Z. Hošťálek, O. Trhlíková, Z. Walterová, T. Martinez, F. Peruch, H. Cramail and J. Merna, *Eur. Polym. J.*, 2017, **88**, 433-447.
10. L.-F. Hu, D.-J. Chen, J.-L. Yang and X.-H. Zhang, *Molecules*, 2020, **25**, 253.
11. L. Lin, J. Liang, Y. Xu, S. Wang, M. Xiao, L. Sun and Y. Meng, *Green Chem.*, 2019, **21**, 2469-2477.
12. J. Xu, P. Zhang, Y. Yuan and N. Hadjichristidis, *Angew. Chem. Int. Ed.*, 2023, **62**, e202218891.

13. S. Tshepelevitsh, A. Kütt, M. Lõkov, I. Kaljurand, J. Saame, A. Heering, P. G. Plieger, R. Vianello and I. Leito, *Eur. J. Org. Chem.*, 2019, **2019**, 6735-6748.

14. S. Naumann, P. B. V. Scholten, J. A. Wilson and A. P. Dove, *J. Am. Chem. Soc.*, 2015, **137**, 14439-14445.

15. J. M. Longo, M. J. Sanford and G. W. Coates, *Chem. Rev.*, 2016, **116**, 15167-15197.

16. D. Ryzhakov, G. Printz, B. Jacques, S. Messaoudi, F. Dumas, S. Dagorne and F. Le Bideau, *Polym. Chem.*, 2021, **12**, 2932-2946.

17. K. Li and D. Xue, *J. Phys. Chem. A*, 2006, **110**, 11332-11337.

Chapter 4 – Structurally diverse polyesters from the copolymerisation of anhydrides and epoxides mediated by a metal halide-organobase catalyst

4.1 Introduction

A key advantage of ring-opening copolymerisation (ROCOP) over step-growth polymerisation (SGP) or ring-opening polymerisation (ROP) as a method for synthesising polyesters is that it can incorporate a wide-range of functionalised monomers.[1, 2] Not only are desired functionalities accessible from commercial reagents without requiring laborious synthetic procedures, but functionalities that ROP struggles to accommodate due to their tendency to decrease ring-strain needed to drive ROP forwards can also be incorporated into the backbone of the polymer in the ROCOP of anhydrides and epoxides.[3, 4] In 2016, a review by Coates and co-workers highlighted that 20 anhydrides and 20 epoxides had been reported as monomers for ROCOP in literature giving a theoretical potential of 400 different polyester structures.[1] Therefore a multitude of possible polymer properties and performances are available from the ROCOP of anhydrides and epoxides simply by changing either one or both monomers in the copolymerisation.

Both epoxides and anhydrides can be classified by their side chains and number of rings, both of which affect the resultant polyester's properties. Several considerations have governed the choices of anhydride and epoxide monomers focused on in previous research. The crystallinity and thermal properties of a given polyester are important when considering its potential applications.[5] These can be affected by the polymer backbone structure and the length and rigidity of the epoxide sidechains. For example, by manipulating the choice of the monomer, the glass transition temperatures (T_g) of polyesters afforded by the ROCOP of anhydrides with epoxides have been reported in the range of –44 °C to 184 °C.[6, 7] Interest has extended beyond aliphatic polyesters to semiaromatic polyesters, synthesised from bulky, multi-ringed

monomers, as these typically give superior thermal properties (*e.g.* T_g > 100 °C) to the latter. In addition to this, unsaturated polyesters are desirable as their unsaturated moieties can be modified in post-polymerisation to give polyesters desireable for applications including resins, composite materials, biomedical devices, and drug delivery.[8] Many functionalities such as hydroxyl, primary or secondary amines, carboxylic acid, or other protonic functional groups cannot be introduced before copolymerisation as they can function as chain transfer agents during copolymerisation or even deactivate the catalyst in the case of excessively protonic functional groups.[9] The final consideration for monomer choice is a desire for monomers to be renewably sourced. This is important for the development of sustainable polymers as an alternative to current commodity plastics, which are typically sourced from limited fossil-fuel resources. Many epoxides and anhydrides can be renewably sourced with their copolymerisations to afford renewably-sourced or partially renewably-sourced polyesters having been reported extensively.[1]

The three most extensively studied monomers for ROCOP have been propylene oxide (PO), cyclohexene oxide (CHO) and phthalic anhydride (PA) due to their simple nature and universal ability to be copolymerised by catalyst systems.[1, 10] However, these monomers lack the full range of desirable functionalities previously discussed. To test the industrial-viability for a catalyst system, it is useful to demonstrate its versatility in copolymerising a wide range of monomers especially those with functionalities that can be post-polymerised, can improve the thermal properties of the polyester and are renewably sourced.

Maleic anhydride (MA) is an inexpensive anhydride commercially produced in large quantities from the vapour-phase oxidation of benzene or butane/butene. It also has

the potential to be sourced sustainably from the oxidation of sugar-derived furfaldehyde.[11, 12] Thanks to its unsaturated moiety, it has drawn a lot of interest for copolymerisation to produce maleate or fumurate units in unsaturated polyesters suitable for post-polymerisation modifications. Despite this, it has been a challenge to copolymerise due to its tendency to crosslink at high temperature or deprotonation of the active α-proton in the presence of certain catalysts. Initial reports on copolymerisations with MA using early ROCOP catalysts showed these difficulties.[13-15] Even when Coates and co-workers applied the highly efficient zinc β-diketiminate acetate ((BDI)ZnOAc) complex to the ROCOP of MA and propylene oxide (PO), a low conversion (5% after 15 h) and significant ether linkages (86%) was achieved.[8] Only when a chromium salen complex was applied was perfectly alternating polyester afforded from the ROCOP of MA and an epoxide. A broad range of epoxides were successful with high catalytic activity in mild conditions (TOF ≤ 50 h^{-1}, 45 °C). However, Duchateau and co-workers found that ROCOP of MA and styrene oxide (SO) performed with a chromium salen complex in the absence of a co-catalyst led to a failed reaction producing only a hard, crosslinked solid that was insoluble in organic solvents formed.[16] Similar results were found using the simple organocatalyst bis(triphenylphosphine)iminium chloride (PPNCl) to mediate the ROCOP of MA with either PO or cyclohexene oxide (CHO).[17] Zhang and co-workers found success with a simple catalyst system by using the Lewis pair catalyst of triethylborane (BEt_3) and tetraphenylphosphonium bromide (PPh_4Br), which saw the copolymerisation of MA and PO produce perfectly alternating polyester with good activity in mild conditions (TOF = 102 h^{-1}, 45 °C).[18] Perfectly alternating polyester was also produced with good activities from the copolymerisation of MA with phenyl glycidyl ether (PGE) and

epichlorohydrin (ECH). A range of organoborane-based simple Lewis pair catalysts were reported giving different catalytic activities but not affecting selectivity. Alkali metal carboxylate (AMC) Lewis pair catalysts mediated the copolymerisation of MA with PO giving a perfectly alternating polyester and with CHO giving a polyester with significant ether linkages (30.2%).[19] Copolymerisations were conducted at 80 °C to avoid crosslinking but this led to a lower polymerisation rate. The KOAc catalyst was used alongside 18-crown-6 to improve the polymerisation rate but still gave a low catalytic activity (TOF = 19.7 h^{-1}). The application of protic acid diphenyl phosphate (DPP) and organobase 4-dimethylaminopyridine (DMAP) as a Lewis pair to mediate the ROCOP of MA with CHO was unsuccessful giving only polyether.[20]

Unsaturated bi- or tricyclic-based monomers are particularly interesting as these can both increase the T_g of an anhydride-epoxide copolymer above 100 ºC and introduce reactive olefin moieties into the backbone for post-polymerisation functionalisation. Coates and co-workers demonstrated this by affording polyesters with T_g with tuneable T_g between 66 ºC and 184 ºC aluminium salen or iron aminotriphenolate complexes paired with PPNCl to mediate the copolymerisation of PO with different tricyclic anhydrides some of which had been derived from Diels-Alder adducts of maleic anhydride and renewable terpenes.[7, 21] Using a heterometallic dinuclear aluminium and potassium complex, Williams and co-workers achieved the ROCOP of CHO and a sterically-hindered tricyclic anhydride with an impressively high catalytic activity (TOF = 288 h^{-1}, 100 °C).[22] Not every well-defined metal complex was able to catalyse these bulky anhydrides so easily. A report into ROCOP of anhydrides and epoxides mediated by yttrium β-diketiminate complexes found the copolymerisation of tricyclic anhydride carbic anhydride (CA) with epoxides CHO and 1-butylene oxide (BO) as sluggish with

significant polyether formation.[23] Simple Lewis pair catalyst system BEt_3/PPNCl was able to effectively mediate the ROCOP of CA with a wide range of epoxides giving good catalytic activities (TOF ≤ 267 h^{-1}, 80 °C).[24] The AMC KOAc mediated the copolymerisation of CA and CHO, PO, SO or vinyl-cyclohexene oxide (VCHO) to afford perfectly alternating polyester but with low activities characteristic of AMC catalysts (1.0 h^{-1} ≤ TOF ≤ 4.4 h^{-1}, 110 °C).[19] Weems and co-workers achieved the ROCOP of CA with bulky epoxide limonene oxide (LO) to afford robust polyesters suitable for 3D printing using a simple catalyst system of a thiourea paired with 1,8-diazabicyclo[5,4,0]-7-undecene (DBU) with good selectivity (97% ether linkages) and a catalytic turnover frequency of 6.25 h^{-1}.

Limonene oxide has generated a lot of interest as a bulky epoxide, which has a pendant alkene moiety. Additionally, it is sourced renewably from *R*-limonene, a naturally occurring terpene found in citrus fruits. This interest has existed since the revival of research into epoxide and anhydride ROCOP with Coates and co-workers successfully copolymerising LO and diglycolic anhydride (DGA) mediated by (BDI)ZnOAc.[25] However, the copolymerisation required high temperatures and a significantly longer reaction time (TOF = 30.7 h^{-1}, 70 °C) than the other epoxides reported. This was because limonene oxide sterically inhibited the carboxylate chain end attack.[26] The copolymerisation of MA and LO was also reported (TOF = 4.6 h^{-1}, 60 °C). A T_g = 62 °C was reported for the polyester of MA and LO. Duchateau and co-workers used a chromium salen complex with PPNCl to catalyse the copolymerisation of LO and PA with a reasonable catalytic activity at higher temperature (TOF = 78.3 h^{-1}, 130 °C).[27] No homopolymerisation of LO occurred as expected from the bulky nature of the epoxide. Williams and co-workers reported a polyester with a T_g of 112 ºC from

the copolymerisation of LO and PA mediated by an iron and potassium heterodinuclear complex catalyst.[28] However, this was lower than the T_g given by polyesters synthesised from PA with CHO and PA (T_g = 136 ºC) with menthane oxide (MO), another bio-derived terpene-based epoxide, and PA (T_g = 177 ºC).

Considering that this thesis has established an effective catalyst system for the ROCOP of CHO and PA, there was need to demonstrate its versatility in copolymerising other monomers. 4 anhydrides and 4 epoxides were selected for this monomer screen with potentially 16 possible polyesters to be synthesised. The anhydrides selected were PA, CA, MA and itaconic anhydride (IA) (**Figure 53**). IA is structurally similar to MA and can be renewably sourced from fungi and contains a pendant alkene moiety for post-polymerisation functionalisation. It has been demonstrated to be able to tune T_g through crosslinking its units in the resultant polyester from its copolymerisation with BO.[29] The epoxides selected were CHO, LO, ECH and allyl glycidyl ether (AGE) (**Figure 53**). ECH and AGE contain a chloride and allyl pendant functionality respectively, which can be modified post-polymerisation. To compare monomer combinations, the $PdCl_2$/PPNCl Lewis pair catalyst established in the previous chapter was employed alongside the 4-MBA chain transfer agent to mediate each copolymerisation in excess epoxide for 8 minutes. While a controlled copolymerisation has not been demonstrated with the system, the monomer conversion after the set timepoint was considered a good comparison of polymerisation rates given that the only change between the copolymerisation set-ups was the choice of monomers. Fourteen of the sixteen monomer combinations were known to have been copolymerised with different catalyst systems in literature. The

copolymerisations of IA with AGE and LO respectively had not been reported on at all in literature likely due to the limited focus given to IA previously.

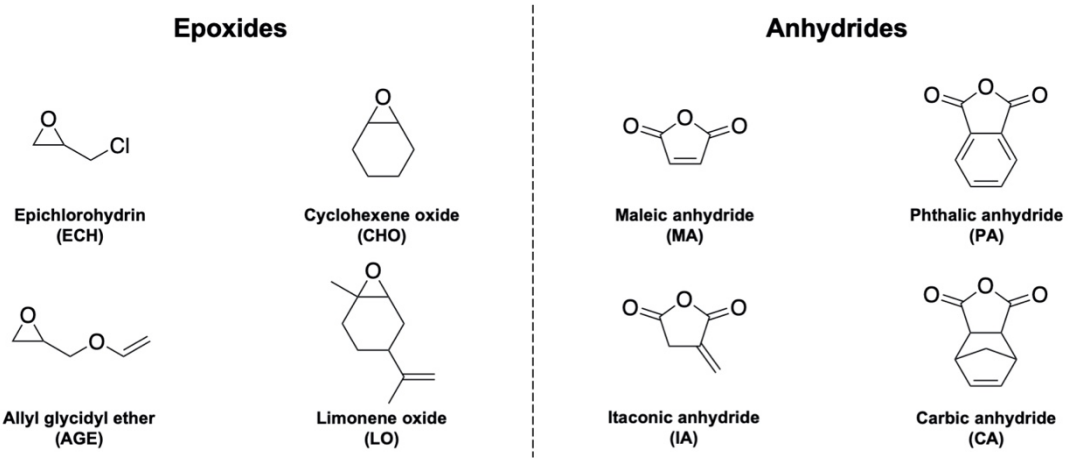

Figure 53. The chemical structures of the eight monomers screened in this chapter.

4.2 Results

4.2.1 Phthalic anhydride screen

The copolymerisations of the different epoxides CHO, ECH, AGE and LO with PA were compared first as PA was a simple anhydride (**Table 15**). Copolymerisations were mediated by the $PdCl_2$/PPNCl Lewis pair catalyst system established in the previous chapter.

Table 15. A screen of epoxides copolymerised with PA. All copolymerisations conducted with $[PA]_0/[Epoxide]_0/[PdCl_2]_0/[PPNCl]_0/[4\text{-MBA}]_0$ at 50:100:1:1:1 at 110 °C for 8 min.

Entry	Anhydride	Epoxide	Monomer conversion[a] (%)	M_n (SEC)[b] (g·mol^{-1})	$Đ_M$	Ester linkages[c] (%)
1	PA	CHO	72	3924	1.13	94
2	PA	ECH	94	4998	1.22	98
3	PA	AGE	94	6029	1.57	93
4	PA	LO	10	802	1.14	-

[a]Conversion of CHO calculated from the ^{1}H NMR spectrum ($CDCl_3$, 400 MHz) of the reaction mixture at the given timepoint. [b]Molecular weight as calculated by SEC analysis using THF (0.5% NEt_3) as an eluent with PS standards. [c]Percentage of ester linkages determined by the ratio of the integrated height of the ester peak and ether peak in the ^{1}H NMR spectrum of the precipitated polyester product.

All four epoxides were successfully copolymerised with PA using the $PdCl_2$/PPNCl catalyst system to afford P(PA-*co*-CHO), P(PA-*co*-ECH), P(PA-*co*-AGE) and P(PA-*co*-LO) (see sections 4.5.1.1-4.5.1.4 for characterisation spectra). This demonstrated that the system could accommodate a wide range of electronics and sterics in epoxide functional groups such as the less bulky, electron withdrawing group in ECH or more bulky groups of CHO and LO. As expected, the less bulky epoxides ECH and AGE

were copolymerised with the highest yields within 8 min. It was proposed that LO's bulky structure contributed to steric hinderance, which led to a significantly reduced polymerisation rate due to the increased difficulties of a nucleophile ring-opening the monomer. This is in accordance with the lower rates of copolymerisation with anhydrides seen for it compared to other epoxides in literature.[25, 26] The catalyst system also demonstrated high selectivity for the copolymerisations of PA with CHO, ECH and AGE. These results indicated therefore that changing the functional group on the epoxide had a greater effect on the polymerisation rate than on selectivity for the monomers selected. The polymer yield attained from the copolymerisation of LO with PA was too low to give an accurate measurement of ester linkages using NMR analysis. Interestingly, the copolymerisation of AGE gave a significantly large dispersity of 1.57. It was not known exactly why such a high dispersity had been attained. Typically, high dispersities indicate the presence of unwanted side reactions which can abruptly terminate a propagating chain. However, there was no indication found in literature that AGE was more susceptible to this than other epoxides. Instead, dispersities for anhydride-epoxide copolymers varied depending on the catalyst system employed.

4.2.2. Maleic and itaconic anhydride screen

Maleic and itaconic anhydride are both monomers possessing unsaturated moieties that can be easily functionalised after incorporation into a polyester. Each respective anhydride was copolymerised with epoxides CHO, LO, ECH or AGE using the $PdCl_2$/PPNCl Lewis pair catalyst system alongside 4-MBA (**Table 16**).

Table 16. A screen of epoxides copolymerised with MA and IA. All copolymerisations conducted with $[Anhydride]_0/[Epoxide]_0/[PdCl_2]_0/[PPNCl]_0/[4\text{-}MBA]_0$ at 50:100:1:1:1 at 110 °C for 8 min.

Entry	Anhydride	Epoxide	Monomer conversion[a] (%)	M_n (SEC)[b] (g·mol^{-1})	$Đ_M$	Ester linkages[c] (%)
5	MA	CHO	26	942	1.02	-
6	MA	ECH	28	1309	1.14	-
7	MA	AGE	10	620	1.14	-
8	MA	LO	0	-	-	-
9	IA	CHO	28	906	1.03	-
10	IA	ECH	34	909	1.03	-
11	IA	AGE	0	-	-	-
12	IA	LO	0	-	-	-

[a]Conversion of CHO calculated from the ^{1}H NMR spectrum ($CDCl_3$, 400 MHz) of the reaction mixture at the given timepoint. [b]Molecular weight as calculated by SEC analysis using THF (0.5% NEt_3) as an eluent with PS standards. [c]Percentage of ester linkages determined by the ratio of the integrated height of the ester peak and ether peak in the ^{1}H NMR spectrum of the precipitated polyester product.

Five of the eight copolymerisations were successful producing P(MA-*co*-CHO), P(MA-*co*-ECH), P(MA-*co*-AGE), P(IA-*co*-CHO), and P(IA-*co*-ECH) (see sections 4.5.1.5-4.5.1.9 for characterisation spectra). Copolymerisations using MA and IA gave significantly lower polymerisation rates than those using PA and some (MA with LO and IA with AGE or LO) did not copolymerise at all. In the case of MA this reflected its difficulty to copolymerise reported in literature. Given IA's similar structure it was assumed that this suffered similar difficulties to MA. Nevertheless, the success of some of the copolymerisations, which produced polyester rather than crosslinked, insoluble solids suggested the catalyst system could be tuned to accommodate both monomers.

Interestingly, in comparison with copolymerisations with PA, AGE gave a lower polymerisation rate with MA than ECH and CHO. ECH's superior polymerisation rate was likely due to its electron-withdrawing chloride group which activates the epoxide further by increasing its electrophilicity and thereby tendency to be attacked by a nucleophile, as inferred by previous reports on ECH copolymerisation with anhydrides.[30] Copolymerisations with IA saw polyester afforded with both itaconic and citraconic repeating units (Appendix sections **4.5.1.8** and **4.5.1.9**). It was known that above its melting point (66–68 ºC), itaconic anhydride isomerises into citraconic anhydride.[31] In a similar manner to a previously run copolymerisation of IA with ECH at 100 ºC, it was thought that this isomerisation had occurred here leading to the copolymerisation of both anhydride isomers with the epoxide.[32] In all cases of successful copolymerisation, small oligomers were afforded due to the low monomer conversion achieved in 8 min. Polyester yields were too low to give an accurate measurement of ester linkages using NMR analysis and so the selectivity of the copolymerisations could not be determined.

4.2.3. Carbic anhydride screen

Carbic anhydride possesses an unsaturated moiety that can be functionalised after incorporation into a polyester and a bulky tricyclic structure ideal for enhancing the material properties of the afforded polyester. The anhydride was copolymerised with epoxides CHO, LO, ECH or AGE with the copolymerisations mediated by the $PdCl_2$/PPNCl Lewis pair catalyst system established in the previous chapter (**Table 17**).

Table 17. A screen of epoxides copolymerised with MA and IA. All copolymerisations conducted with $[Anhydride]_0/[Epoxide]_0/[PdCl_2]_0/[PPNCl]_0/[4\text{-}MBA]_0$ at 50:100:1:1:1 at 110 °C for 8 min.

Entry	Anhydride	Epoxide	Monomer conversion[a] (%)	M_n (SEC)[b] (g·mol^{-1})	$Đ_M$	Ester linkages[c] (%)
13	CA	CHO	16	909	1.03	-
14	CA	ECH	91	1778	1.35	*
15	CA	AGE	39	2730	1.10	*
16	CA	LO	0	-	-	-

[a]Conversion of CHO calculated from the ^{1}H NMR spectrum ($CDCl_3$, 400 MHz) of the reaction mixture at the given timepoint. [b]Molecular weight as calculated by SEC analysis using THF (0.5% NEt_3) as an eluent with PS standards. [c]Percentage of ester linkages determined by the ratio of the integrated height of the ester peak and ether peak in the ^{1}H NMR spectrum of the precipitated polyester product. *Ether peak is obscured by overlapping peaks.

Despite the bulky nature of carbic anhydride, the monomer successfully copolymerised with epoxides CHO, ECH and AGE to afford P(CA-*co*-CHO), P(CA-*co*-ECH), and P(CA-*co*-AGE) (see sections 4.5.1.10-4.5.1.12 for characterisation spectra). The steric hindrance of both the LO and CA monomers were suspected to have prevented the monomer pair from copolymerising using the $PdCl_2$/PPNCl catalyst system. Steric hinderance from bulky functionalities was also likely responsible for the low monomer conversion seen for the copolymerisation of CA and CHO after 8 min. ECH gave the fastest polymerisation rate of any epoxide with CA by a significant difference. As seen with its copolymerisation with MA and IA, this was likely due to its electron-poor nature increasing the likelihood of ring-opening. Interestingly, despite reaching a similar degree of conversion and the molar mass of the repeating units being very similar, the copolymerisation of ECH and CA afforded significantly shorter polyester chains than

those of ECH and PA. The moderate dispersity of 1.35 may indicate that this result was because of unwanted side reactions. However, the decrease in polyester length is too significant to be simply explained by transesterification and back-biting reactions affording shorter chains. The polyester molar mass achieved after just 39% monomer conversion for the copolymerisation of CA and AGE showed promise for affording a high molecular weight polyester if the copolymerisation had been run to completion. Due to overlapping peaks in the ^{1}H NMR spectrum it was not possible to obtain a measurement of ester linkages using NMR analysis and so the selectivity of the copolymerisations could not be determined.

4.3 Conclusions

The ability for the optimised $PdCl_2$/PPNCl Lewis pair catalyst system established in Chapter 3 to copolymerise a range of epoxide and anhydride monomers were investigated to determine the catalyst system's versatility. Overall, the $PdCl_2$/PPNCl catalyst system optimised in the previous chapter was successful in affording polyester from twelve copolymerisations from sixteen attempted. This showed the competitively versatile nature of the catalyst system. The catalyst system was generally less active for copolymerisations using MA and IA monomers but more active for copolymerisations using PA and CA. In future, copolymerisations for the former two monomers would need to be run to a longer timepoint to allow them to reach conversion so that the polyesters could be more rigorously characterised. Where copolymerisations neared completion in 8 min, oligomeric molecular weights were afforded between M_n = 1,000-6,000 g·mol^{-1}. Where selectivity could be determined, highly alternating polyester structures were observed. In some cases, monomer combinations were copolymerised with higher activities and/or affording higher molecular weight polyesters than the standard PA and CHO pairing. Notably, the catalyst system was efficient in affording unsaturated polyesters P(PA-*co*-ECH) (94% conversion in 8 min, M_n = 4,998 g·mol^{-1}), P(PA-*co*-AGE) (94% conversion in 8 min, M_n = 6,029 g·mol^{-1}), P(CA-*co*-ECH) (91% conversion in 8 min, M_n = 1,778 g·mol^{-1}), and P(CA-*co*-AGE) (38% conversion in 8 min, M_n = 2,730 g·mol^{-1}). These unsaturated polyesters have the potential to be suited to a range of applications with the latter two polyesters having been successfully reported in literature to undergo post-polymerisation functionalisation of the norbornene alkene moieties through click chemistry to install desired functional groups on the polyester or through thiol-ene

cross-linking to produce 3D printed structures.[33, 34] Further work would be needed to determine what thermal properties (e.g. T_g) could be achieved through thermal analysis using the $PdCl_2$/PPNCl catalyst system. One of the advantages of Lewis pair catalysts is that their Lewis acid-base interaction which is key to conversion rates and selectivity can be modified by changing the Lewis acid or base as was demonstrated in the previous chapter. Monomer combinations that were slow or did not produce polyester at all could re-run with different Lewis acids such as $MgCl_2$ or YCl_3 to determine if they were able to access copolymerisations of monomer combinations that $PdCl_2$ was unable to.

4.4 Experimental details

4.4.1 General considerations

All reagents for the copolymerisations were stored in a nitrogen-filled glovebox. Dry toluene, chloroform and dichloromethane were obtained from a SPS system, degassed by three freeze-pump-thaw cycles, and stored over activated 3 Å or 4 Å molecular sieves in a nitrogen-filled glovebox nitrogen. Before use in an air-free reaction, all glassware was dried in the oven at 180 °C overnight.

4.4.2 Instruments

4.4.2.1 NMR Spectrometer

^{1}H NMR and ^{13}C–{^{1}H} NMR spectra were recorded at 298 K on an Ascend Bruker 400 spectrometer equipped with a BBFO smart probe operating at 400 MHz and 101 MHz respectively. Chemical shifts on the ^{1}H NMR spectra were referenced to the solvent residual proton resonance signals: δ 7.26 ppm for d_1–$CDCl_3$. The data obtained was processed and analysed using MestReNova 12.0.3 software.

4.4.2.2 Size exclusion chromatography

Size exclusion chromatography (SEC) in THF was performed on an Agilent 1260 Infinity II LC system equipped with a Wyatt Optilab T-rEX differential refractive index detector, an Agilent guard column (PLGel 5 μM, 50 × 7.5 mm) and two Agilent Mixed-C columns (PLGel 5 μM, 300 × 7.5 mm). The mobile phase was THF (HPLC grade) at flow rate of 1.0^{-1} mL·min. Number average molecular weights (M_n), weight average molecular weights (M_w) and dispersities ($Đ_M = M_w/M_n$) were determined using Wyatt ASTRA v7.1.3 software against poly(styrene) (PS) standards.

4.4.2.3 Centrifuge

Ohaus FC5706 Frontier Centrifuge Multi 230V.

4.4.3 Materials

4-methoxybenzyl alcohol (dissolved in dry dichloromethane, dried over CaH_2, distilled under nitrogen, degassed and stored under an inert atmosphere, 98%) was purchased from Alfa Aesar. Palladium (II) chloride (anhydrous), maleic anhydride (99%), itaconic anhydride (95%), epichlorohydrin (≥99%), allyl glycidyl ether (≥99%), limonene oxide (mixture of *cis* and *trans*, 97%), toluene (99.8%), methanol (99.8%), phthalic anhydride (≥99%), bis(triphenylphosphine)iminium chloride (97%), chloroform (≥99%), tetrahydrofuran (HPLC grade, ≥99.9%, inhibitor-free), triethylamine (≥99.5%) and calcium hydride (95%) were purchased from Sigma Aldrich. Cyclohexene oxide (98%) and dichloromethane (≥99.5%) were purchased from Acros Organics. Hydrochloric acid (37%) and carbic anhydride (>99%) were purchased from Fisher Scientific. Deuterated chloroform (dried over CaH_2 and distilled under nitrogen twice, degassed and stored under an inert atmosphere, 98%) was purchased from Apollo Scientific. Unless stated otherwise, all chemicals and compounds were used as received.

4.4.4 Monomer preparation

Given the ease by which monomer impurities can disrupt anhydride and epoxide ring-opening copolymerisation, it was important to stringently purify and dry the phthalic anhydride and cyclohexene oxide comonomers.

The anhydrides (20 g) were stirred in dry toluene (500 mL) and then cannula filtered under nitrogen. Toluene was then removed under reduced pressure before the solid

was recrystallised in dry chloroform. The crystals were then sublimed twice in a nitrogen filled sublimation chamber under reduced pressure and heat (80 ºC). The resultant white crystals (~ 5 g) were analysed with ^{1}H NMR and $^{13}C–\{^{1}H\}$ NMR spectroscopy to determine the purity. The purity of the anhydrides determined by NMR spectroscopy was found to be PA (99.5%), MA (100%), IA (100%), and CA (100%).

Cyclohexene oxide, allyl glycidyl ether and epichlorohydrin, limonene oxide (25 mL) were each respectively stirred over CaH_2 and distilled under nitrogen (in the case of cyclohexene oxide, allyl glycidyl ether and epichlorohydrin) or under reduced pressure (in the case of limonene oxide) twice followed by degassing through freeze-pump thawing thrice. The resultant colourless liquid was analysed with ^{1}H NMR and $^{13}C–\{^{1}H\}$ NMR spectroscopy to determine the purity. The purity of the anhydrides determined by NMR spectroscopy was found to be CHO (100 %), ECH (99.9%), AGE (100%), and LO (100%).

4.4.5 General copolymerisation procedure

In a nitrogen-filled glove box, a 7 mL teflon-sealed vial with a magnetic stirrer bar was primed with palladium chloride (2.8 mg, 0.016 mmol), bis(triphenylphosphine)iminium chloride (9.2 mg, 0.016 mmol), anhydride (0.8 mmol) and a stock solution of a chosen multiple amount of 4-methoxybenzyl alcohol (2.0 µL, 0.016 mmol) and epoxide (1.6 mmol) respectively. The vial was stirred and heated to 110 ºC for 8 min after which the vial was quenched in an ice bath and then opened to air. $CDCl_3$ was added and a sample taken for ^{1}H NMR and $^{13}C–\{^{1}H\}$ NMR analysis. A sample was also taken and diluted in tetrahydrofuran (1 mL) for SEC analysis. The polymer was crashed out of the

remaining reaction mixture by precipitation into a MeOH/HCl mixture cooled using liquid nitrogen. Polymers were dried under reduced pressure at 60 ºC.

4.5 Appendix

4.5.1 Polymer characterisation

For all the successful copolymerisations, a ^{1}H NMR spectrum of the precipitated polymer is given alongside a SEC spectrum of the polymer. In cases where the polymer was afforded in sufficient quantity, a $^{13}C–\{^{1}H\}$ NMR spectra of the precipitated polyester is given. Yields given were calculated based on the conversion seen in the ^{1}H NMR crude spectrum for each copolymerisation.

4.5.1.1 Poly(PA-*co*-CHO)

The afforded polyester was a cream-white solid (yield = 142 mg). ^{1}H NMR and ^{13}C–{^{1}H} NMR characterisation were confirmed by previous literature reports for the polyester's synthesis.[35]

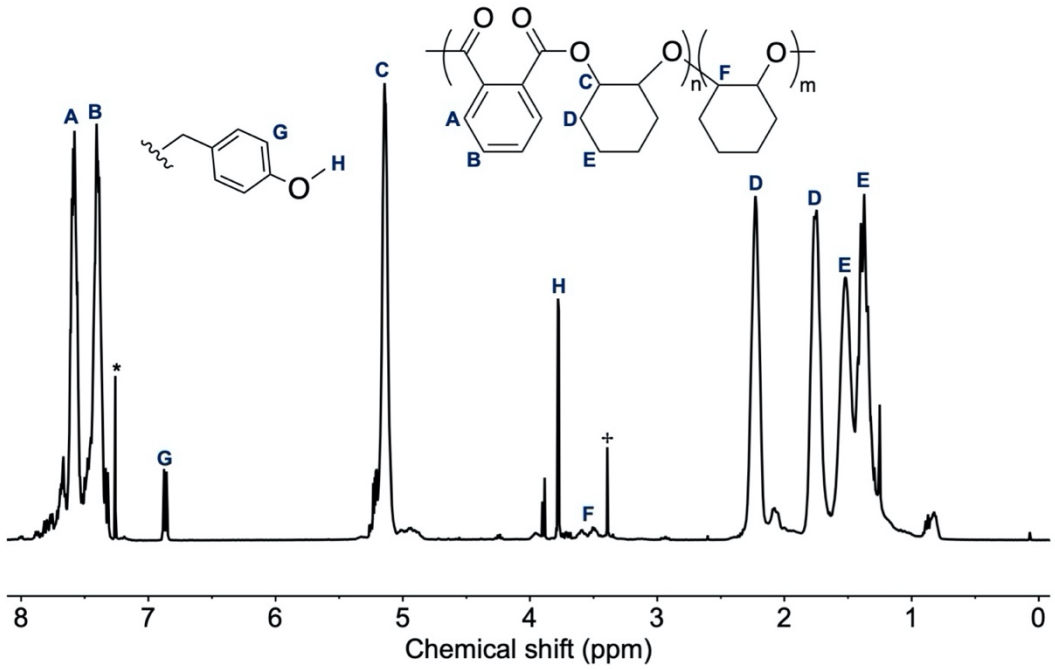

Figure 54. The ^{1}H NMR spectrum of precipitated (from $CHCl_3$ into methanol/HCl) P(PA-co-CHO) copolymer derived from a copolymerization of PA and CHO using $PdCl_2$/PPNCl/4-MBA as a catalyst system ($[PA]_0/[CHO]_0/[PdCl_2]_0/[PPNCl]_0/[4\text{-MBA}]_0$ = 50:100:1:1:1) after 8 min ($CDCl_3$, 400 MHz, 298 K). $^{+}$ = methanol, * = $CHCl_3$.

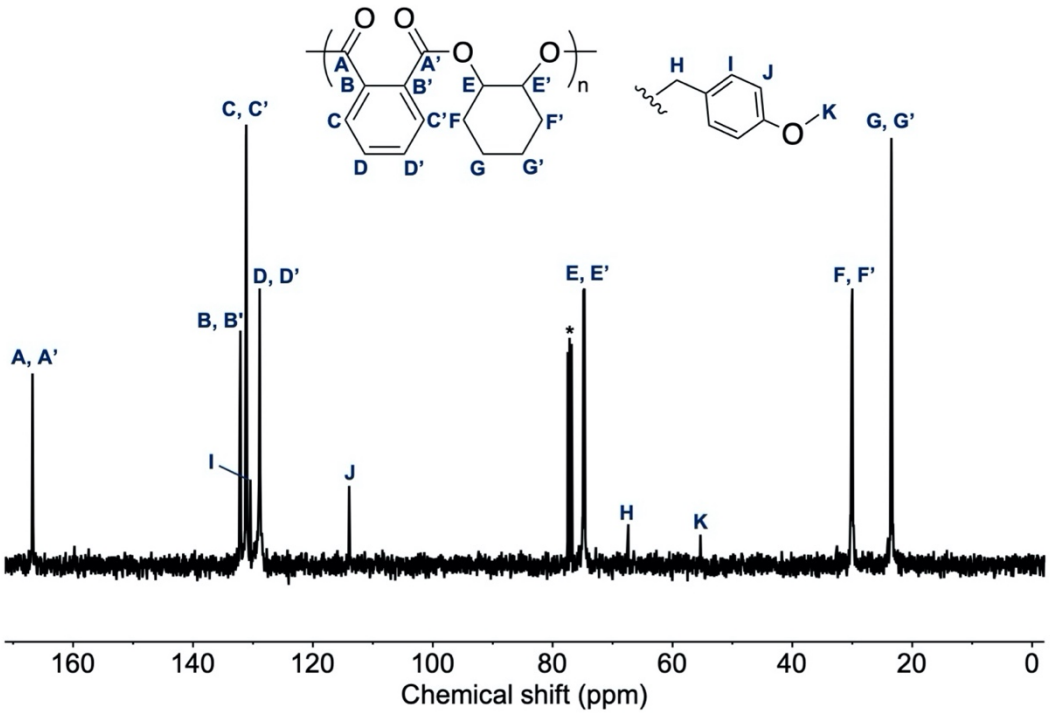

Figure 55. The $^{13}C–\{^{1}H\}$ NMR spectrum of precipitated (from $CHCl_3$ into methanol/HCl) P(PA-co-CHO) copolymer derived from a copolymerization of PA and CHO using $PdCl_2$/PPNCl/4-MBA as a catalyst system ($[PA]_0/[CHO]_0/[PdCl_2]_0/[PPNCl]_0/[4\text{-}MBA]_0$ = 50:100:1:1:1) after 8 min ($CDCl_3$, 101 MHz, 298 K). * = $CHCl_3$.

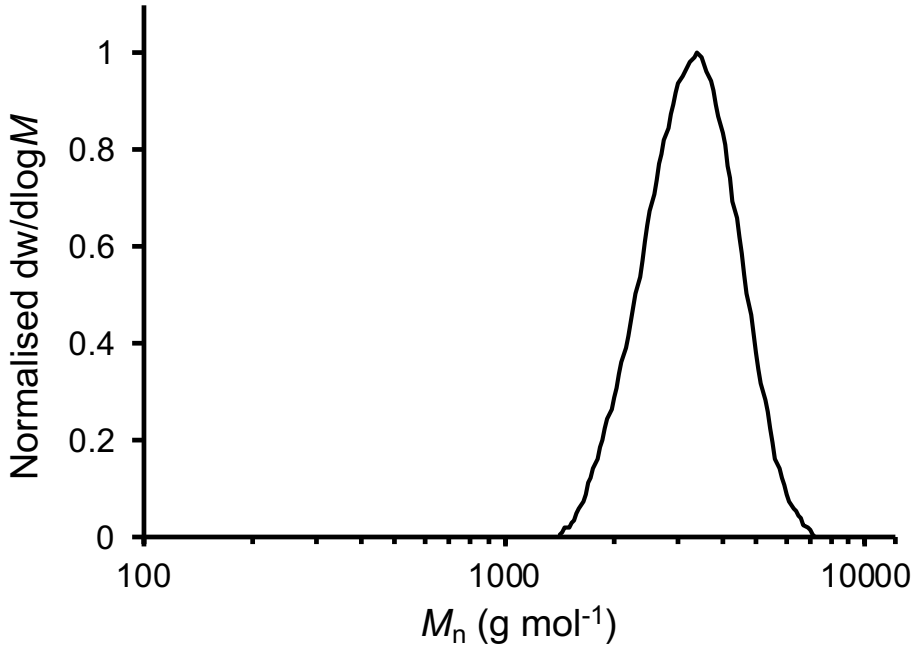

Figure 56. The size exclusion chromatogram of the molecular weight distribution of the P(PA-co-CHO) copolymer derived from the copolymerization of PA and CHO using $PdCl_2$/PPNCl/4-MBA as a catalyst system ($[PA]_0/[CHO]_0/[PdCl_2]_0/[PPNCl]_0/[4\text{-MBA}]_0$ = 50:100:1:1:1) after 8 min. Molecular weight was determined against poly(styrene) standards using tetrahydrofuran (THF) (0.5% NEt_3) as an eluent.

4.5.1.2 Poly(PA-*co*-ECH)

The afforded polyester was a cream-white solid (yield = 181 mg). ^{1}H NMR and ^{13}C–{^{1}H} NMR characterisation were confirmed by previous literature reports for the polyester's synthesis.[30]

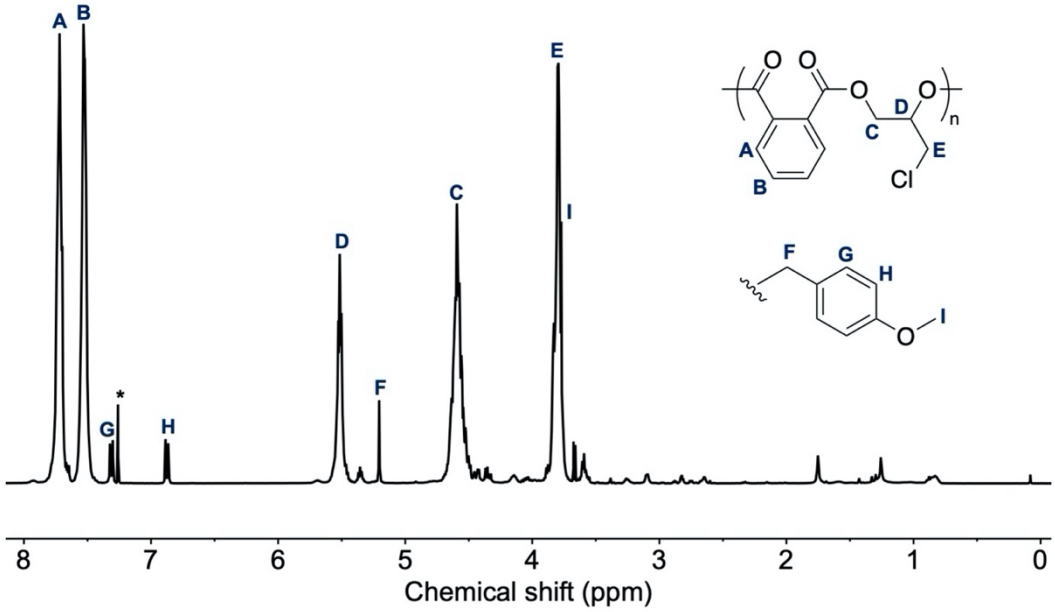

Figure 57. The ^{1}H NMR spectrum of precipitated (from $CHCl_3$ into methanol/HCl) P(PA-co-ECH) copolymer derived from a copolymerization of PA and ECH using $PdCl_2$/PPNCl/4-MBA as a catalyst system ($[PA]_0/[ECH]_0/[PdCl_2]_0/[PPNCl]_0/[4\text{-}MBA]_0$ = 50:100:1:1:1) after 8 min ($CDCl_3$, 400 MHz, 298 K). * = $CHCl_3$.

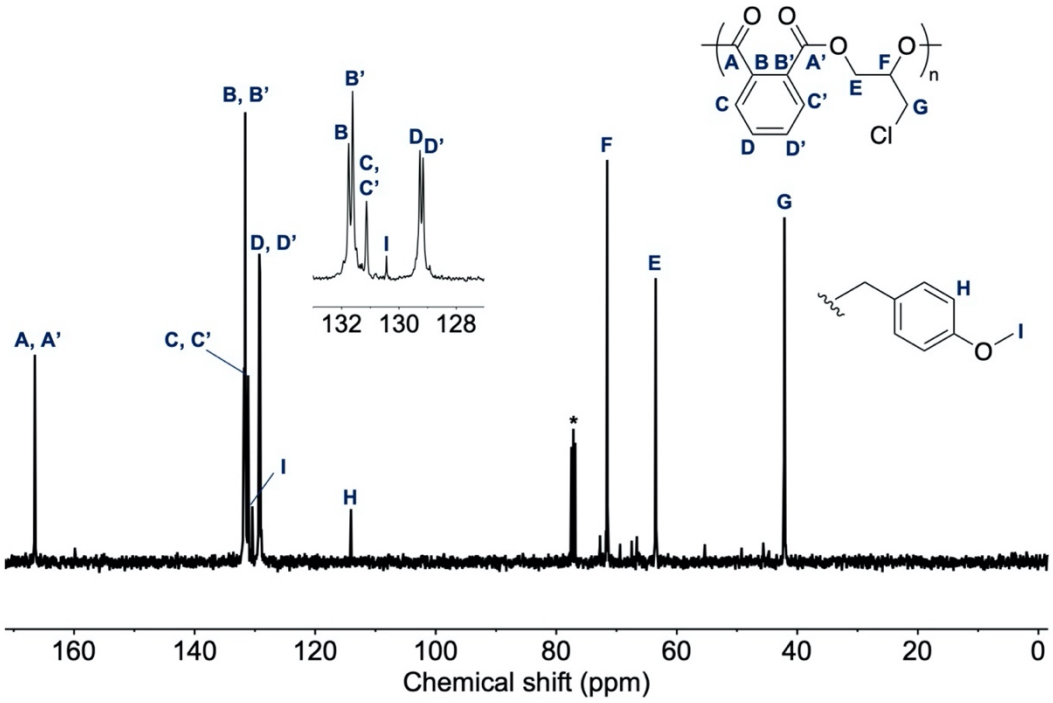

Figure 58. The $^{13}C–\{^{1}H\}$ NMR spectrum of precipitated (from $CHCl_3$ into methanol/HCl) P(PA-co-ECH) copolymer derived from a copolymerization of PA and ECH using $PdCl_2$/PPNCl/4-MBA as a catalyst system ($[PA]_0/[ECH]_0/[PdCl_2]_0/[PPNCl]_0/[4\text{-MBA}]_0$ = 50:100:1:1:1) after 8 min ($CDCl_3$, 101 MHz, 298 K). * = $CHCl_3$.

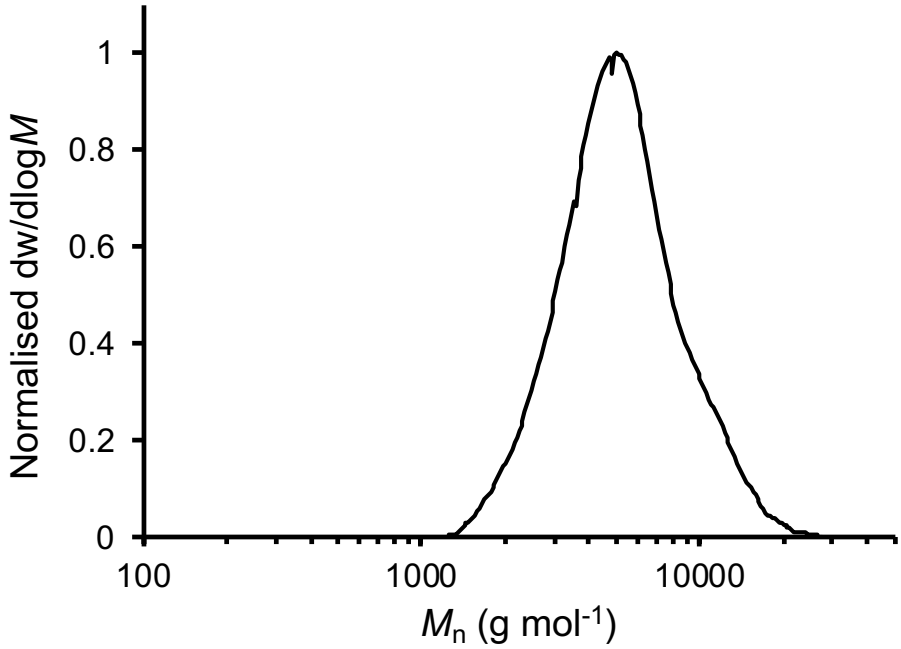

Figure 59. The size exclusion chromatogram of the molecular weight distribution of the P(PA-co-ECH) copolymer derived from the copolymerization of PA and ECH using $PdCl_2$/PPNCl/4-MBA as a catalyst system ($[PA]_0/[ECH]_0/[PdCl_2]_0/[PPNCl]_0/[4\text{-}MBA]_0$ = 50:100:1:1:1) after 8 min. Molecular weight was determined against poly(styrene) standards using tetrahydrofuran (THF) (0.5% NEt_3) as an eluent.

4.5.1.3 Poly(PA-*co*-AGE)

The afforded polyester was a cream-white solid (yield = 197 mg). ^{1}H NMR characterisation was confirmed by previous literature reports for the polyester's synthesis.[36]

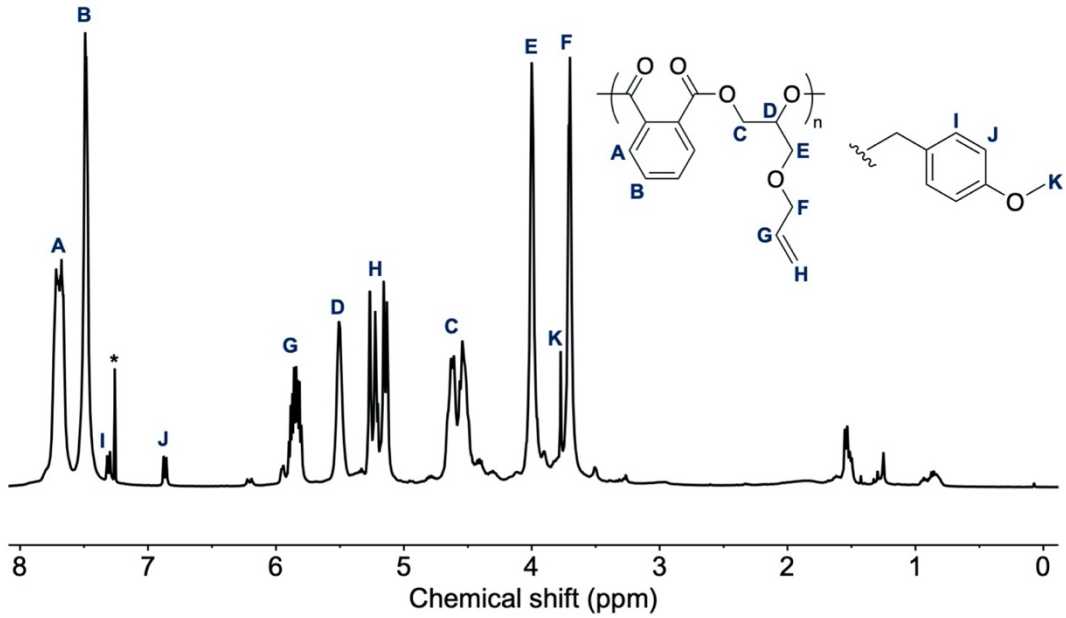

Figure 60. The ^{1}H NMR spectrum of precipitated (from $CHCl_3$ into methanol/HCl) P(PA-*co*-AGE) copolymer derived from a copolymerization of PA and AGE using $PdCl_2$/PPNCl/4-MBA as a catalyst system ($[PA]_0/[AGE]_0/[PdCl_2]_0/[PPNCl]_0/[4\text{-MBA}]_0$ = 50:100:1:1:1) after 8 min ($CDCl_3$, 400 MHz, 298 K). * = $CHCl_3$.

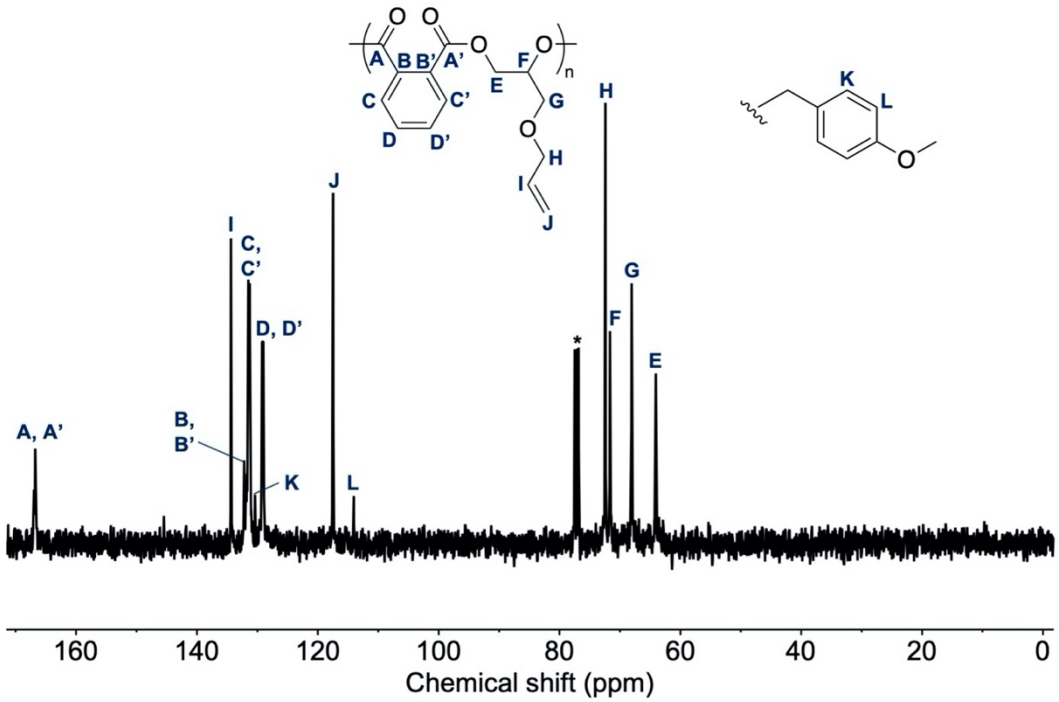

Figure 61. The $^{13}C–\{^{1}H\}$ NMR spectrum of precipitated (from $CHCl_3$ into methanol/HCl) P(PA-co-AGE) copolymer derived from a copolymerization of PA and AGE using $PdCl_2$/PPNCl/4-MBA as a catalyst system ($[PA]_0/[AGE]_0/[PdCl_2]_0/[PPNCl]_0/[4\text{-MBA}]_0$ = 50:100:1:1:1) after 8 min ($CDCl_3$, 101 MHz, 298 K). * = $CHCl_3$.

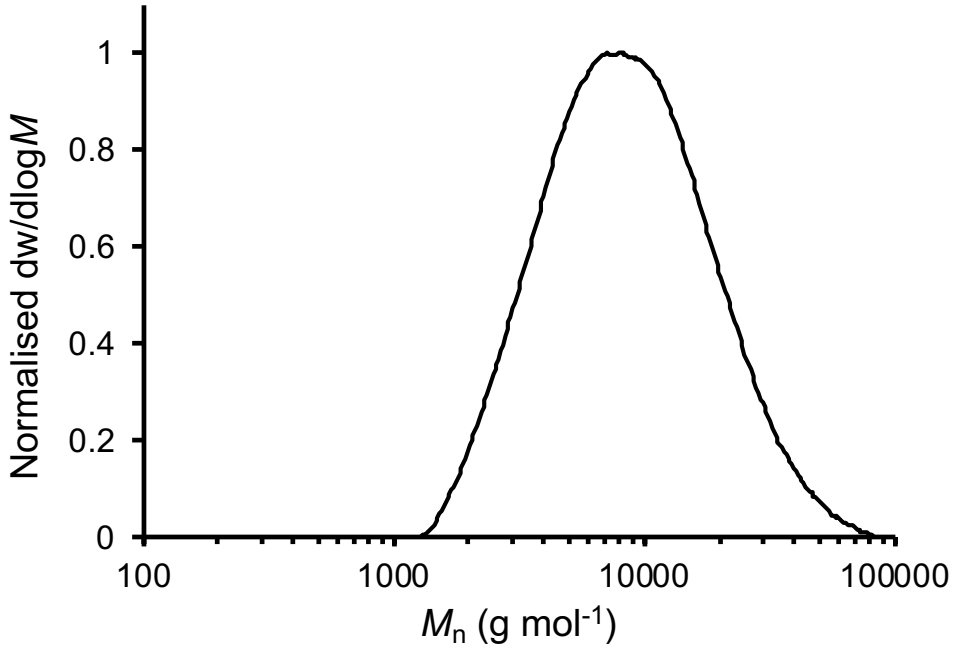

Figure 62. The size exclusion chromatogram of the molecular weight distribution of the P(PA-co-AGE) copolymer derived from the copolymerization of PA and AGE using $PdCl_2$/PPNCl/4-MBA as a catalyst system ($[PA]_0/[AGE]_0/[PdCl_2]_0/[PPNCl]_0/[4\text{-}MBA]_0$ = 50:100:1:1:1) after 8 min. Molecular weight was determined against poly(styrene) standards using tetrahydrofuran (THF) (0.5% NEt_3) as an eluent.

4.5.1.4 Poly(PA-*co*-LO)

The afforded polyester was a cream-white solid (yield = 24 mg). ^{1}H NMR characterisation was confirmed by previous literature reports for the polyester's synthesis.[27]

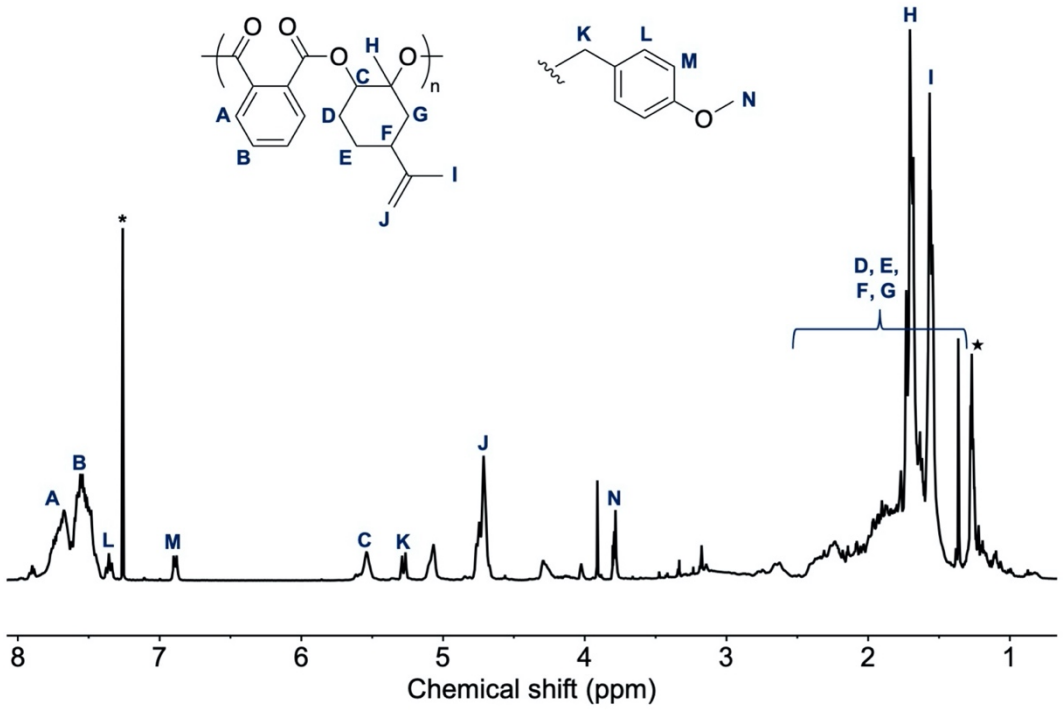

Figure 63. The ^{1}H NMR spectrum of precipitated (from $CHCl_3$ into methanol/HCl) P(PA-co-LO) copolymer derived from a copolymerization of PA and LO using $PdCl_2$/PPNCl/4-MBA as a catalyst system ($[PA]_0/[LO]_0/[PdCl_2]_0/[PPNCl]_0/[4\text{-}MBA]_0$ = 50:100:1:1:1) after 8 min ($CDCl_3$, 400 MHz, 298 K).* = $CHCl_3$.

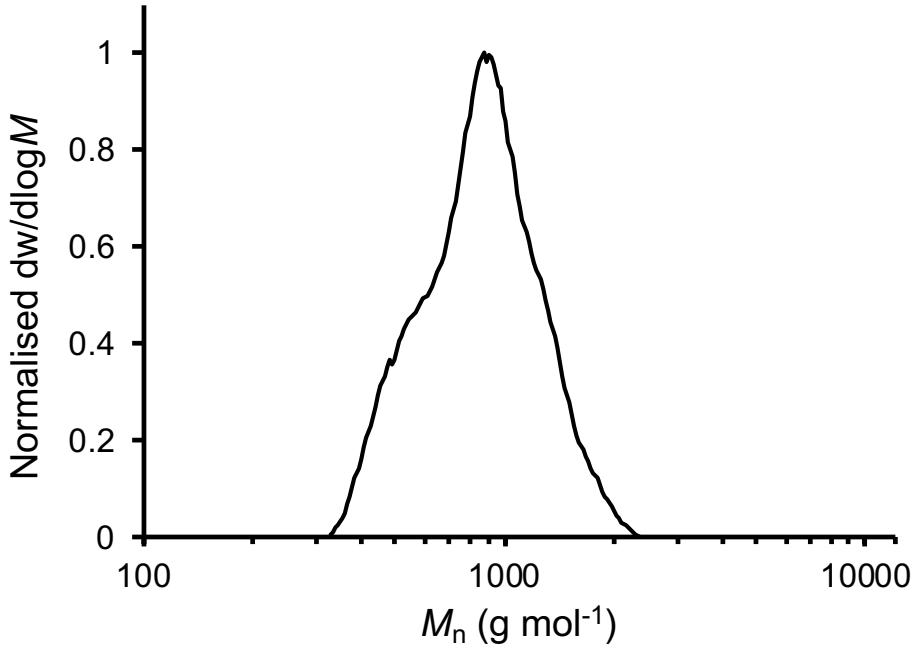

Figure 64. The size exclusion chromatogram of the molecular weight distribution of the P(PA-co-LO) copolymer derived from the copolymerization of PA and LO using $PdCl_2$/PPNCl/4-MBA as a catalyst system ($[PA]_0/[LO]_0/[PdCl_2]_0/[PPNCl]_0/[4\text{-MBA}]_0$ = 50:100:1:1:1) after 8 min. Molecular weight was determined against poly(styrene) standards using tetrahydrofuran (THF) (0.5% NEt_3) as an eluent.

4.5.1.5 Poly(MA-*co*-CHO)

The afforded polyester was a cream-white solid (yield = 41 mg). ^{1}H NMR and ^{13}C–{^{1}H} NMR characterisation were confirmed by previous literature reports for the polyester's synthesis.[37, 38]

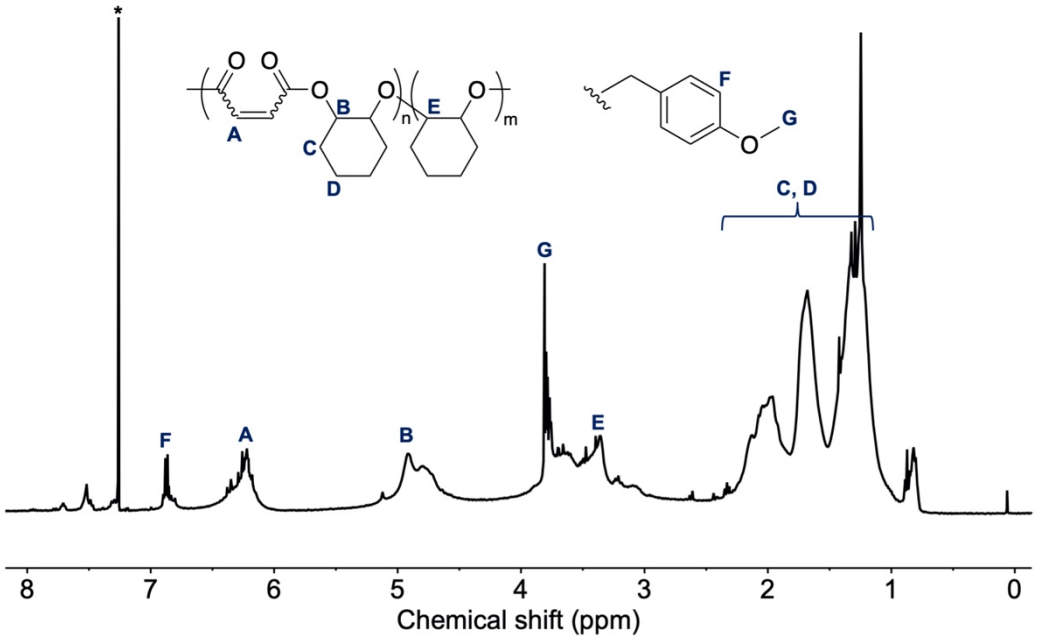

Figure 65. The ^{1}H NMR spectrum of precipitated (from $CHCl_3$ into methanol/HCl) P(MA-co-CHO) copolymer derived from a copolymerization of MA and CHO using $PdCl_2$/PPNCl/4-MBA as a catalyst system ($[MA]_0/[CHO]_0/[PdCl_2]_0/[PPNCl]_0/[4\text{-MBA}]_0$ = 50:100:1:1:1) after 8 min ($CDCl_3$, 400 MHz, 298 K). * = $CHCl_3$.

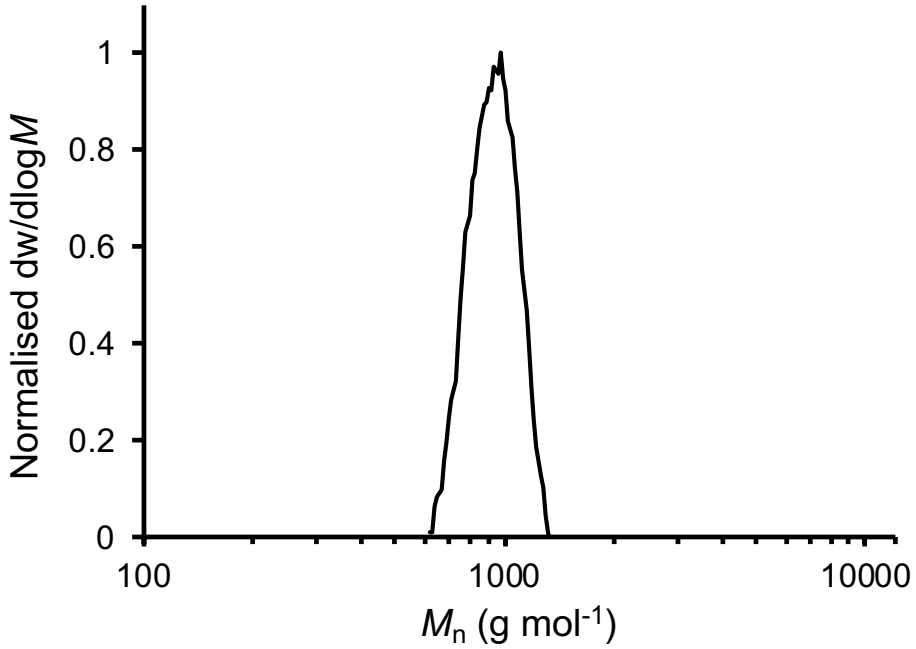

Figure 66. The size exclusion chromatogram of the molecular weight distribution of the P(MA-co-CHO) copolymer derived from the copolymerization of MA and CHO using $PdCl_2$/PPNCl/4-MBA as a catalyst system ($[MA]_0/[CHO]_0/[PdCl_2]_0/[PPNCl]_0/[4\text{-}MBA]_0$ = 50:100:1:1:1) after 8 min. Molecular weight was determined against poly(styrene) standards using tetrahydrofuran (THF) (0.5% NEt_3) as an eluent.

4.5.1.6 Poly(MA-*co*-ECH)

The afforded polyester was a cream-white solid (yield = 43 mg). ^{1}H NMR characterisation was confirmed by previous literature reports for the polyester's synthesis.[8]

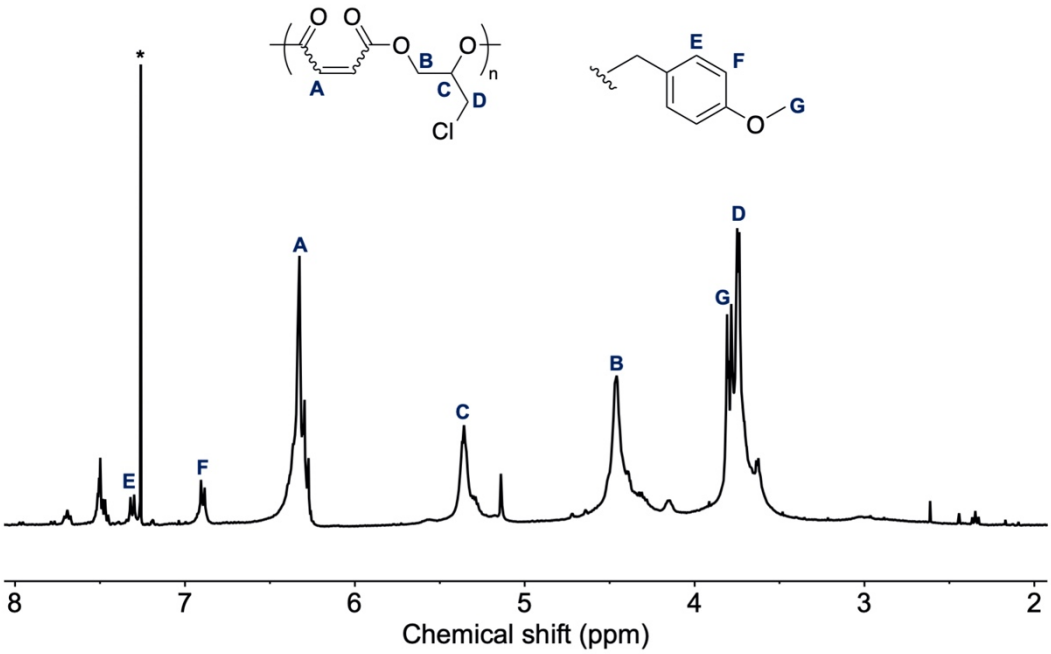

Figure 67. The ^{1}H NMR spectrum of precipitated (from $CHCl_3$ into methanol/HCl) P(MA-co-ECH) copolymer derived from a copolymerization of MA and ECH using $PdCl_2$/PPNCl/4-MBA as a catalyst system ($[MA]_0/[ECH]_0/[PdCl_2]_0/[PPNCl]_0/[4\text{-}MBA]_0$ = 50:100:1:1:1) after 8 min ($CDCl_3$, 400 MHz, 298 K). * = $CHCl_3$.

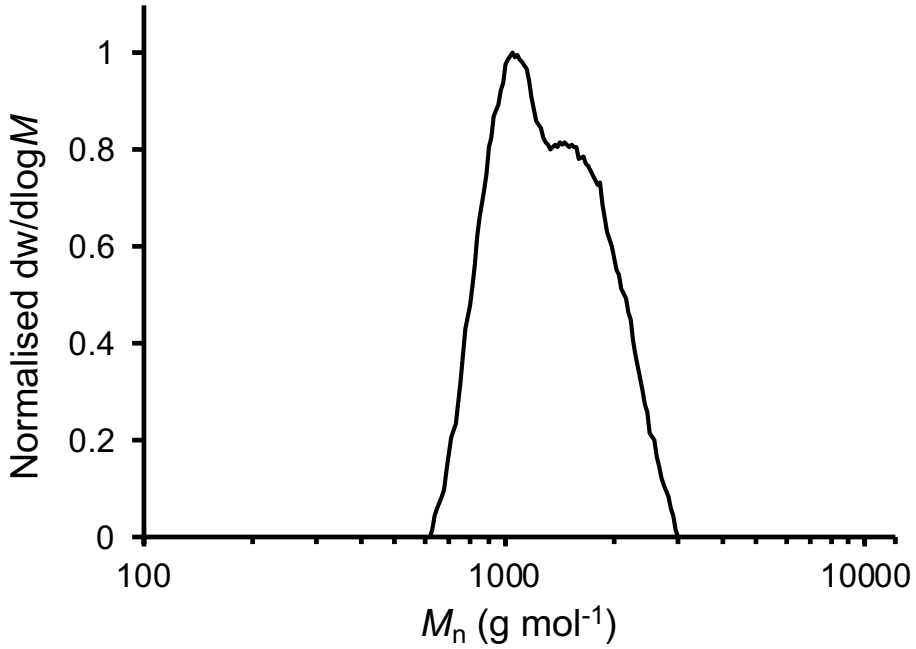

Figure 68. The size exclusion chromatogram of the molecular weight distribution of the P(MA-co-ECH) copolymer derived from the copolymerization of MA and ECH using $PdCl_2$/PPNCl/4-MBA as a catalyst system ($[MA]_0/[ECH]_0/[PdCl_2]_0/[PPNCl]_0/[4\text{-}MBA]_0$ = 50:100:1:1:1) after 8 min. Molecular weight was determined against poly(styrene) standards using tetrahydrofuran (THF) (0.5% NEt_3) as an eluent.

4.5.1.7 Poly(MA-*co*-AGE)

The afforded polyester was a cream-white solid (yield = 17 mg). ^{1}H NMR characterisation was confirmed by previous literature reports for the polyester's synthesis.[8]

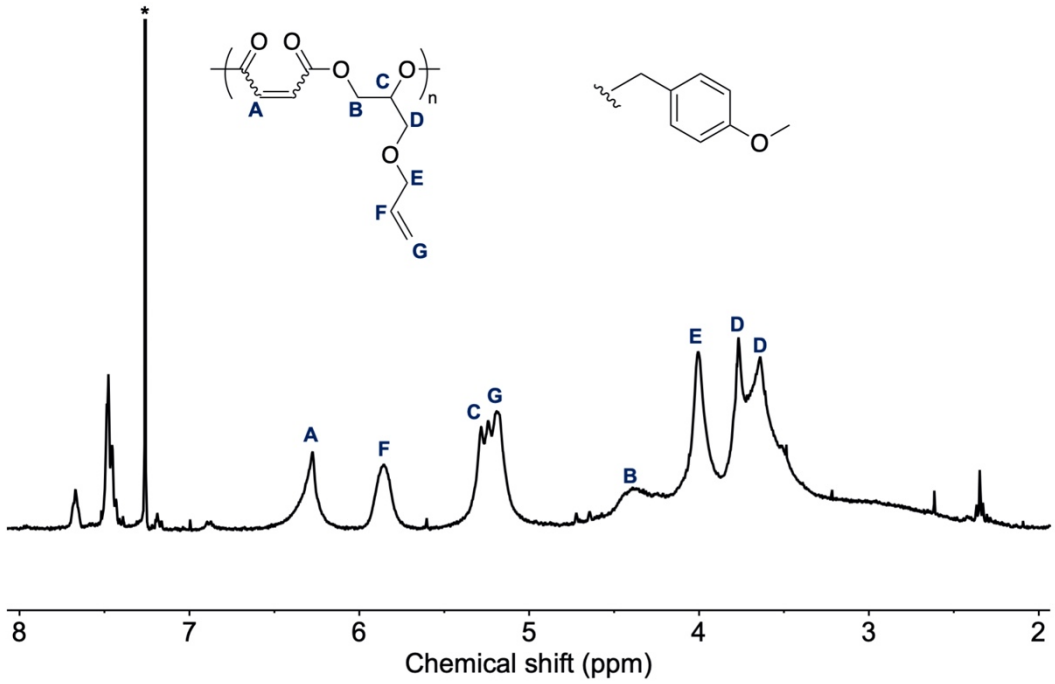

Figure 69. The ^{1}H NMR spectrum of precipitated (from $CHCl_3$ into methanol/HCl) P(MA-co-AGE) copolymer derived from a copolymerization of MA and AGE using $PdCl_2$/PPNCl/4-MBA as a catalyst system ($[MA]_0/[AGE]_0/[PdCl_2]_0/[PPNCl]_0/[4\text{-}MBA]_0$ = 50:100:1:1:1) after 8 min ($CDCl_3$, 400 MHz, 298 K). * = $CHCl_3$.

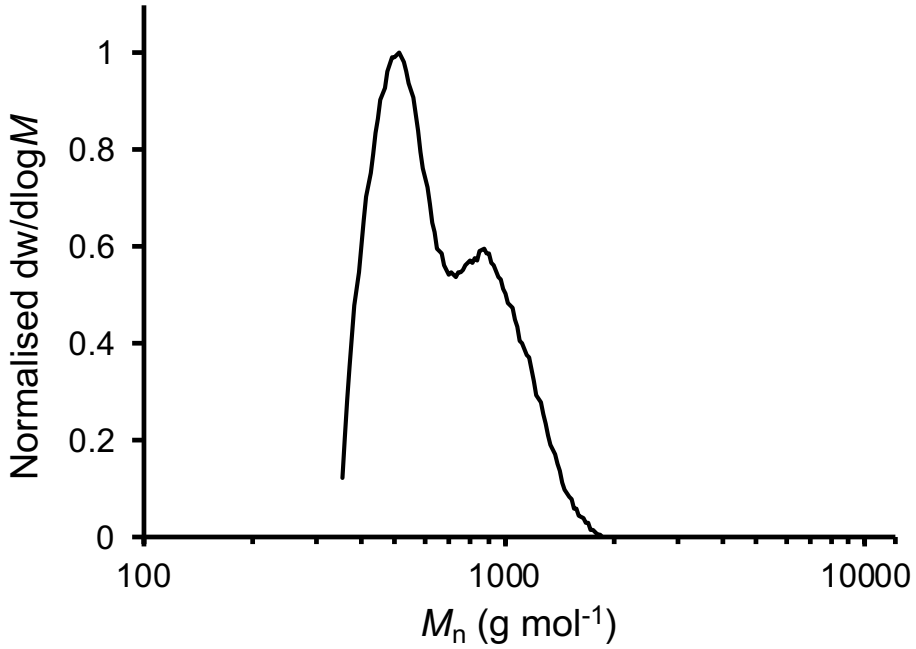

Figure 70. The size exclusion chromatogram of the molecular weight distribution of the P(MA-co-AGE) copolymer derived from the copolymerization of MA and AGE using $PdCl_2$/PPNCl/4-MBA as a catalyst system ($[MA]_0/[AGE]_0/[PdCl_2]_0/[PPNCl]_0/[4\text{-}MBA]_0$ = 50:100:1:1:1) after 8 min. Molecular weight was determined against poly(styrene) standards using tetrahydrofuran (THF) (0.5% NEt_3) as an eluent.

4.5.1.8 Poly(IA-*co*-CHO)

The afforded polyester was a cream-white solid (yield = 47 mg). ^{1}H NMR characterisation was confirmed by previous literature reports for the polyester's synthesis.[32]

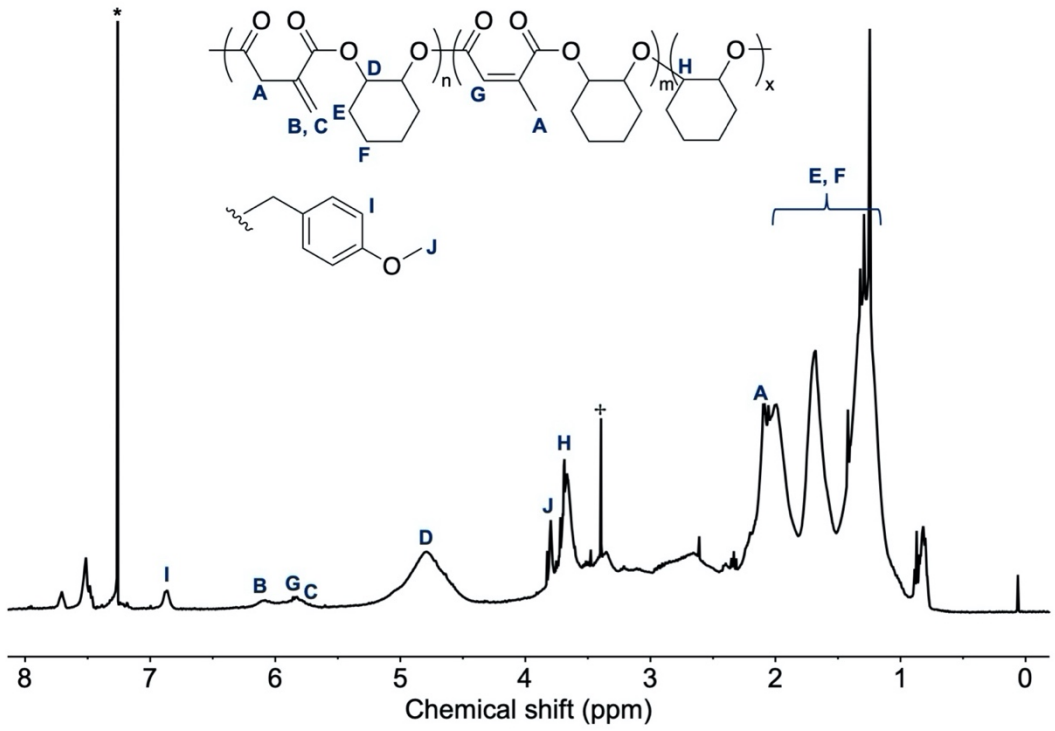

Figure 71. The ^{1}H NMR spectrum of precipitated (from $CHCl_3$ into methanol/HCl) P(IA-co-CHO) copolymer derived from a copolymerization of IA and CHO using $PdCl_2$/PPNCl/4-MBA as a catalyst system ($[IA]_0/[CHO]_0/[PdCl_2]_0/[PPNCl]_0/[4\text{-MBA}]_0$ = 50:100:1:1:1) after 8 min ($CDCl_3$, 400 MHz, 298 K). $^{+}$ = methanol, * = $CHCl_3$.

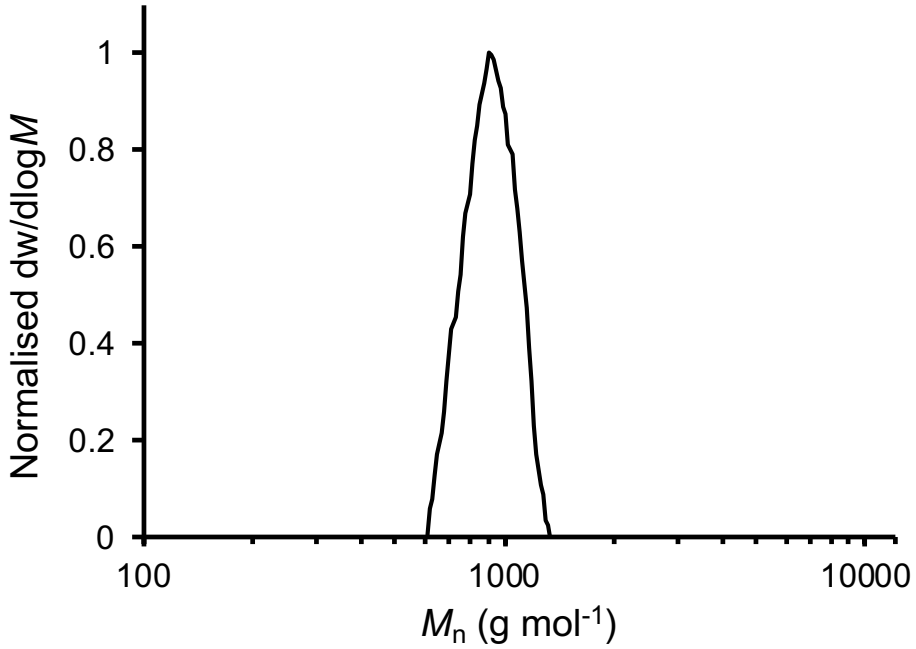

Figure 72. The size exclusion chromatogram of the molecular weight distribution of the P(IA-co-CHO) copolymer derived from the copolymerization of IA and CHO using $PdCl_2$/PPNCl/4-MBA as a catalyst system ($[IA]_0/[CHO]_0/[PdCl_2]_0/[PPNCl]_0/[4\text{-}MBA]_0$ = 50:100:1:1:1) after 8 min. Molecular weight was determined against poly(styrene) standards using tetrahydrofuran (THF) (0.5% NEt_3) as an eluent.

4.5.1.9 Poly(IA-*co*-ECH)

The afforded polyester was a cream-white solid (yield = 56 mg). ^{1}H NMR and ^{13}C–{^{1}H} NMR characterisation was confirmed by previous literature reports for the polyester's synthesis.[32]

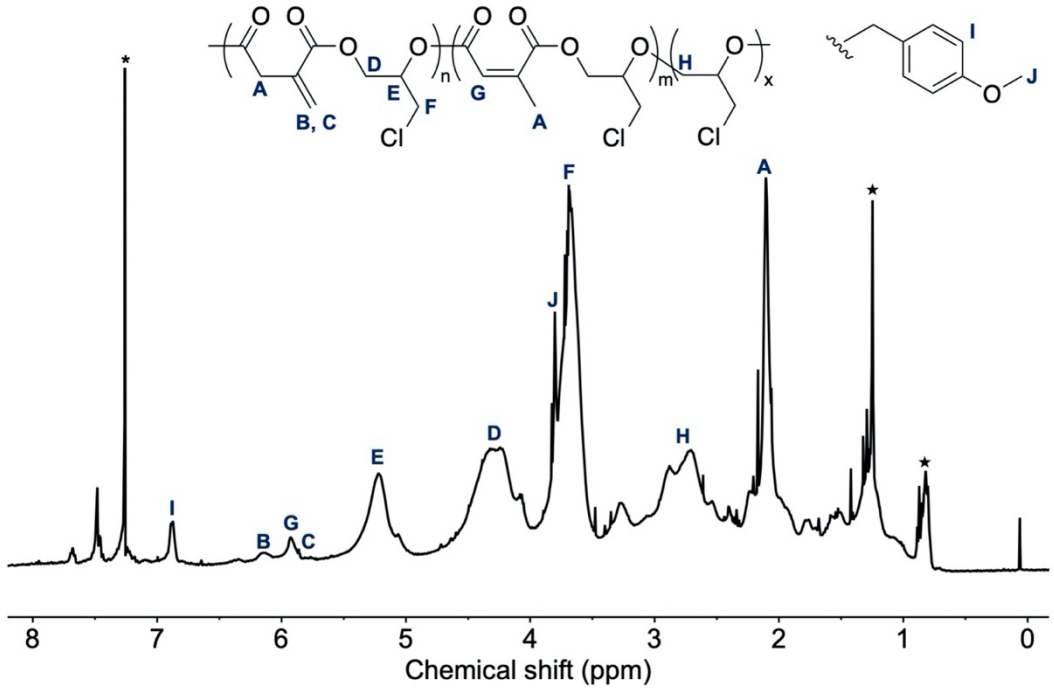

Figure 73. The ^{1}H NMR spectrum of precipitated (from $CHCl_3$ into methanol/HCl) P(IA-co-ECH) copolymer derived from a copolymerization of IA and ECH using $PdCl_2$/PPNCl/4-MBA as a catalyst system ($[IA]_0/[ECH]_0/[PdCl_2]_0/[PPNCl]_0/[4\text{-}MBA]_0$ = 50:100:1:1:1) after 8 min ($CDCl_3$, 400 MHz, 298 K). * = $CHCl_3$.

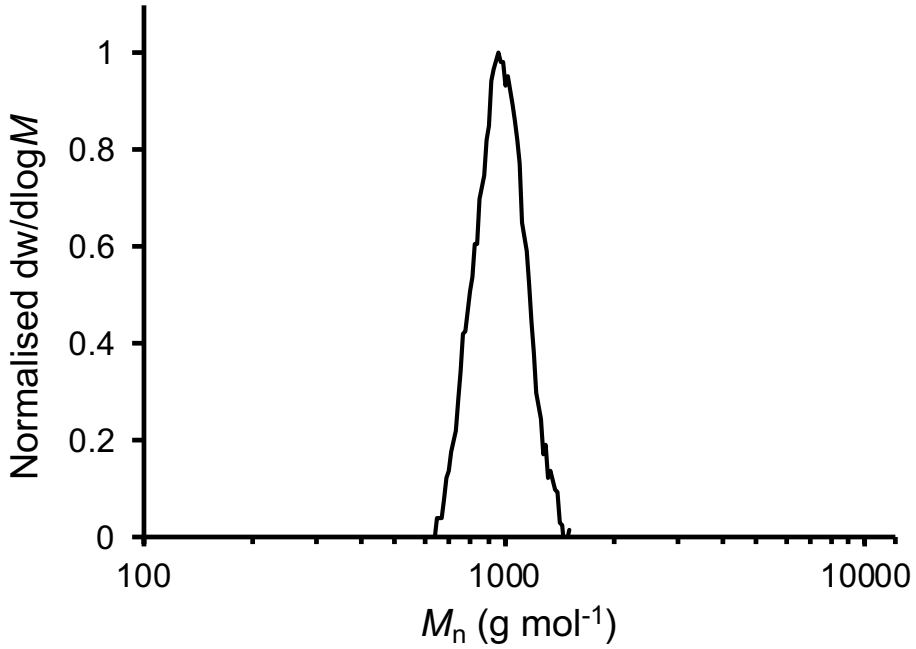

Figure 74. The size exclusion chromatogram of the molecular weight distribution of the P(IA-co-ECH) copolymer derived from the copolymerization of IA and ECH using $PdCl_2$/PPNCl/4-MBA as a catalyst system ($[IA]_0/[ECH]_0/[PdCl_2]_0/[PPNCl]_0/[4\text{-}MBA]_0$ = 50:100:1:1:1) after 8 min. Molecular weight was determined against poly(styrene) standards using tetrahydrofuran (THF) (0.5% NEt_3) as an eluent.

4.5.1.10 Poly(CA-*co*-CHO)

The afforded polyester was a cream-white solid (yield = 34 mg). ^{1}H NMR characterisation was confirmed by previous literature reports for the polyester's synthesis.[33]

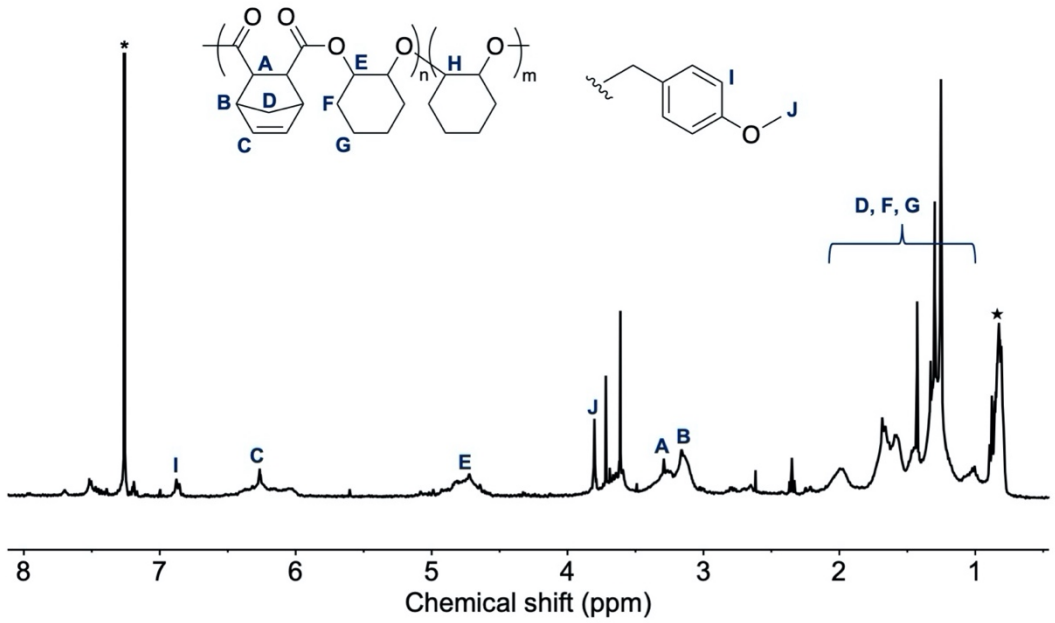

Figure 75. The ^{1}H NMR spectrum of precipitated (from $CHCl_3$ into methanol/HCl) P(CA-co-CHO) copolymer derived from a copolymerization of CA and CHO using $PdCl_2$/PPNCl/4-MBA as a catalyst system ($[CA]_0/[CHO]_0/[PdCl_2]_0/[PPNCl]_0/[4\text{-}MBA]_0$ = 50:100:1:1:1) after 8 min ($CDCl_3$, 400 MHz, 298 K). * = $CHCl_3$.

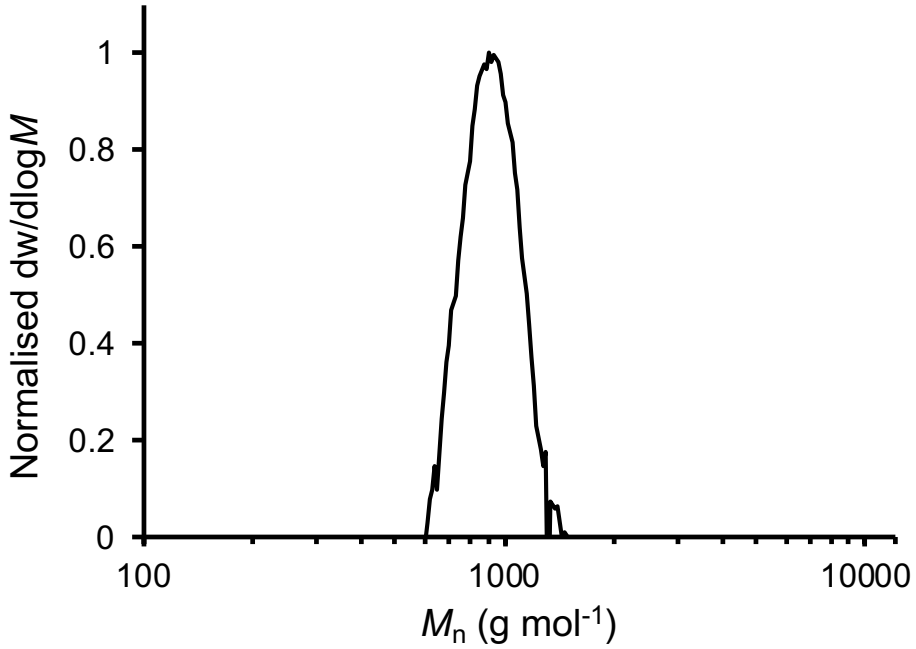

Figure 76. The size exclusion chromatogram of the molecular weight distribution of the P(CA-co-CHO) copolymer derived from the copolymerization of CA and CHO using $PdCl_2$/PPNCl/4-MBA as a catalyst system ($[CA]_0/[CHO]_0/[PdCl_2]_0/[PPNCl]_0/[4\text{-MBA}]_0$ = 50:100:1:1:1) after 8 min. Molecular weight was determined against poly(styrene) standards using tetrahydrofuran (THF) (0.5% NEt_3) as an eluent.

4.5.1.11 Poly(CA-*co*-ECH)

The afforded polyester was a cream-white solid (yield = 187 mg). ^{1}H NMR and ^{13}C–{^{1}H} NMR characterisation were confirmed by previous literature reports for the polyester's synthesis.[33]

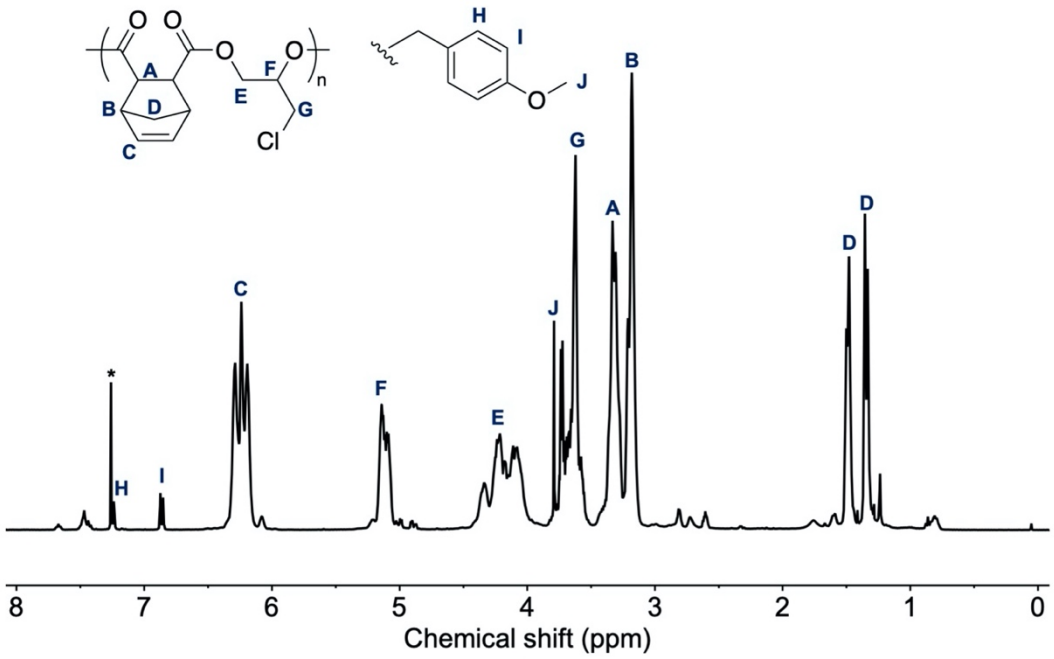

Figure 77. The ^{1}H NMR spectrum of precipitated (from $CHCl_3$ into methanol/HCl) P(CA-co-ECH) copolymer derived from a copolymerization of CA and ECH using $PdCl_2$/PPNCl/4-MBA as a catalyst system ($[CA]_0/[ECH]_0/[PdCl_2]_0/[PPNCl]_0/[4\text{-}MBA]_0$ = 50:100:1:1:1) after 8 min ($CDCl_3$, 400 MHz, 298 K). * = $CHCl_3$.

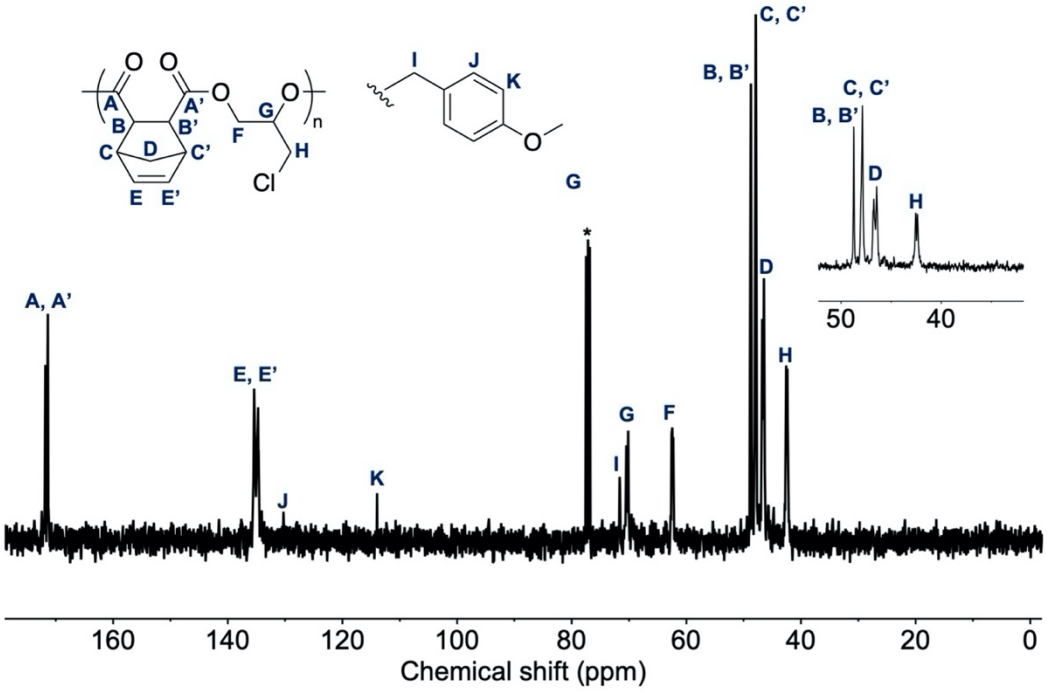

Figure 78. The $^{13}C–\{^{1}H\}$ NMR spectrum of precipitated (from $CHCl_3$ into methanol/HCl) P(CA-co-ECH) copolymer derived from a copolymerization of CA and ECH using $PdCl_2$/PPNCl/4-MBA as a catalyst system ($[CA]_0/[ECH]_0/[PdCl_2]_0/[PPNCl]_0/[4\text{-MBA}]_0$ = 50:100:1:1:1) after 8 min ($CDCl_3$, 101 MHz, 298 K). * = $CHCl_3$.

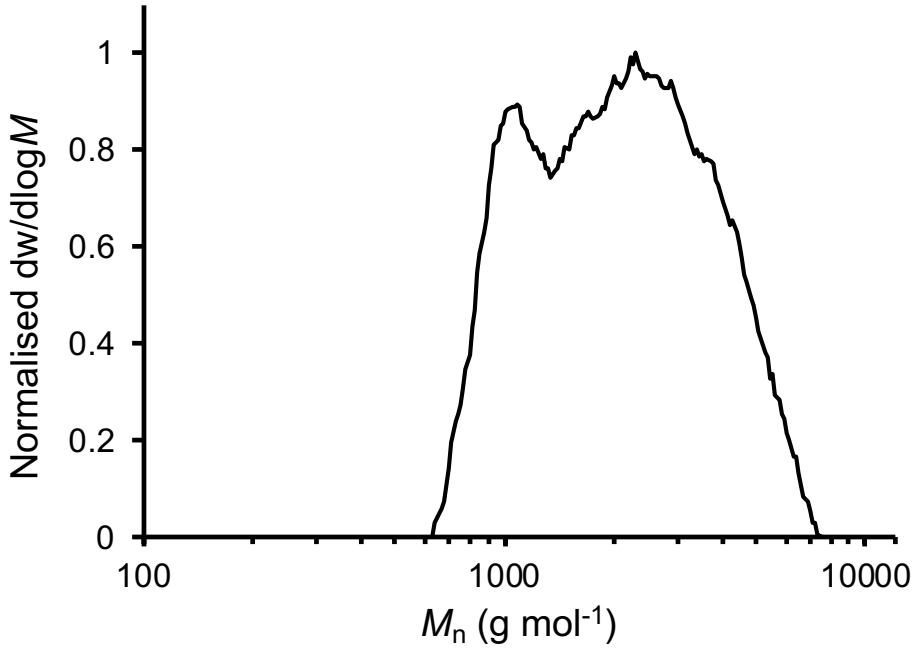

Figure 79. The size exclusion chromatogram of the molecular weight distribution of the P(CA-co-ECH) copolymer derived from the copolymerization of CA and ECH using $PdCl_2$/PPNCl/4-MBA as a catalyst system ($[CA]_0/[ECH]_0/[PdCl_2]_0/[PPNCl]_0/[4\text{-}MBA]_0$ = 50:100:1:1:1) after 8 min. Molecular weight was determined against poly(styrene) standards using tetrahydrofuran (THF) (0.5% NEt_3) as an eluent.

4.5.1.12 Poly(CA-*co*-AGE)

The afforded polyester was a cream-white solid (yield = 87 mg). ^{1}H NMR characterisation was confirmed by previous literature reports for the polyester's synthesis.[33]

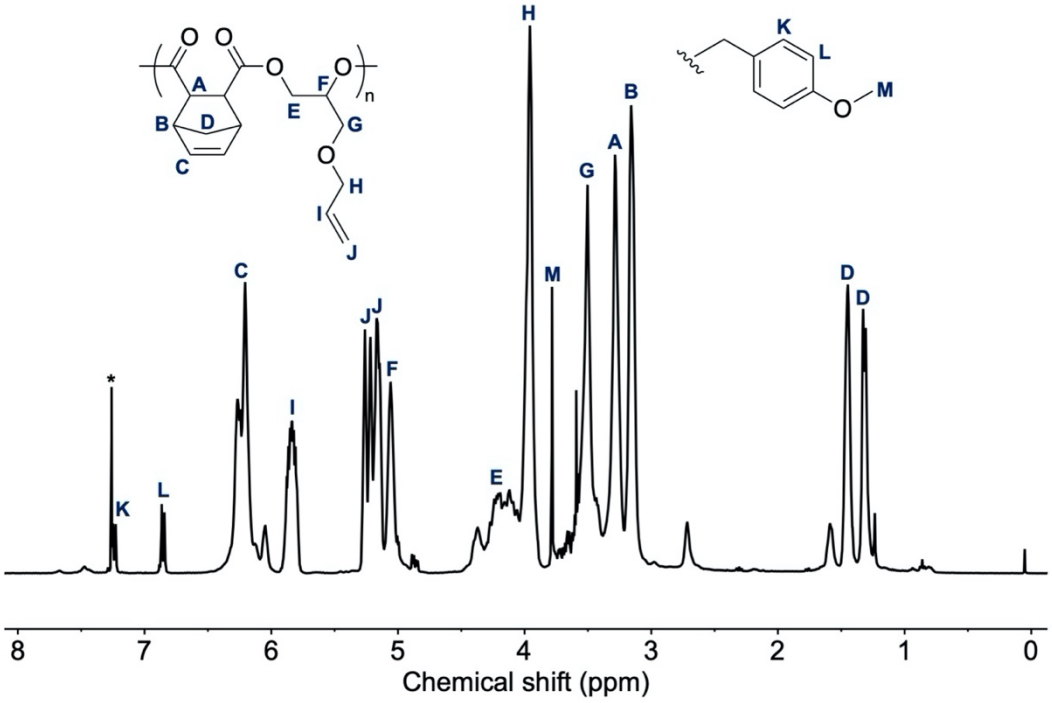

Figure 80. The ^{1}H NMR spectrum of precipitated (from $CHCl_3$ into methanol/HCl) P(CA-co-AGE) copolymer derived from a copolymerization of CA and AGE using $PdCl_2$/PPNCl/4-MBA as a catalyst system ($[CA]_0/[AGE]_0/[PdCl_2]_0/[PPNCl]_0/[4\text{-MBA}]_0$ = 50:100:1:1:1) after 8 min ($CDCl_3$, 400 MHz, 298 K). * = $CHCl_3$.

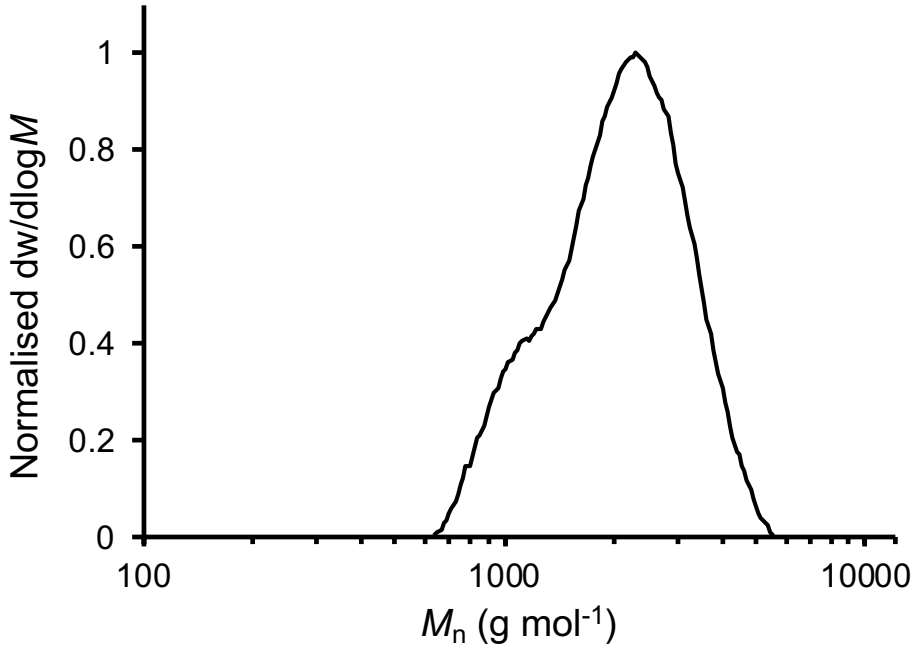

Figure 81. The size exclusion chromatogram of the molecular weight distribution of the P(CA-co-AGE) copolymer derived from the copolymerization of CA and AGE using $PdCl_2$/PPNCl/4-MBA as a catalyst system ($[CA]_0/[AGE]_0/[PdCl_2]_0/[PPNCl]_0/[4\text{-MBA}]_0$ = 50:100:1:1:1) after 8 min. Molecular weight was determined against poly(styrene) standards using tetrahydrofuran (THF) (0.5% NEt_3) as an eluent.

4.5 References

1. J. M. Longo, M. J. Sanford and G. W. Coates, *Chem. Rev.*, 2016, **116**, 15167-15197.

2. S. Paul, Y. Zhu, C. Romain, R. Brooks, P. K. Saini and C. K. Williams, *Chem. Commun.*, 2015, **51**, 6459-6479.

3. P. Olsén, K. Odelius and A.-C. Albertsson, *Biomacromolecules*, 2016, **17**, 699-709.

4. C. K. Williams, *Chem. Soc. Rev.*, 2007, **36**, 1573-1580.

5. L. Sangroniz, Y.-J. Jang, M. A. Hillmyer and A. J. Müller, *J. Chem. Phys.*, 2023, **159**.

6. U. Biermann, A. Sehlinger, M. A. R. Meier and J. O. Metzger, *Eur. J. Lipid Sci. Technol.*, 2016, **118**, 104-110.

7. M. J. Sanford, L. Peña Carrodeguas, N. J. Van Zee, A. W. Kleij and G. W. Coates, *Macromolecules*, 2016, **49**, 6394-6400.

8. A. M. DiCiccio and G. W. Coates, *J. Am. Chem. Soc.*, 2011, **133**, 10724-10727.

9. N. Yi, T. T. D. Chen, J. Unruangsri, Y. Zhu and C. K. Williams, *Chem Sci*, 2019, **10**, 9974-9980.

10. D. Ryzhakov, G. Printz, B. Jacques, S. Messaoudi, F. Dumas, S. Dagorne and F. Le Bideau, *Polymer Chemistry*, 2021, **12**, 2932-2946.

11. Y. Lou, S. Marinkovic, B. Estrine, W. Qiang and G. Enderlin, *ACS Omega*, 2020, **5**, 2561-2568.

12. X. Li, J. Ko and Y. Zhang, *ChemSusChem*, 2018, **11**, 612-618.

13. Z. Hua, G. Qi and S. Chen, *J. Appl. Polym. Sci.*, 2004, **93**, 1788-1792.

14. W. Kuran and A. Niestochowski, *Polym. Bull.*, 1980, **2**, 411-416.

15. H. S. Suh, J. Y. Ha, J. H. Yoon, C.-S. Ha, H. Suh and I. Kim, *React. Funct. Polym.*, 2010, **70**, 288-293.

16. E. Hosseini Nejad, A. Paoniasari, C. E. Koning and R. Duchateau, *Polym. Chem.*, 2012, **3**, 1308-1313.

17. Z. Hošťálek, O. Trhlíková, Z. Walterová, T. Martinez, F. Peruch, H. Cramail and J. Merna, *Eur. Polym. J.*, 2017, **88**, 433-447.

18. L.-F. Hu, C.-J. Zhang, H.-L. Wu, J.-L. Yang, B. Liu, H.-Y. Duan and X.-H. Zhang, *Macromolecules*, 2018, **51**, 3126-3134.

19. C.-M. Chen, X. Xu, H.-Y. Ji, B. Wang, L. Pan, Y. Luo and Y.-S. Li, *Macromolecules*, 2021, **54**, 713-724.

20. X. Zhu and X. Kou, *Chem. Pap.*, 2022, **76**, 2145-2152.

21. N. J. Van Zee and G. W. Coates, *Angew. Chem. Int. Ed.*, 2015, **54**, 2665-2668.

22. W. T. Diment, G. L. Gregory, R. W. F. Kerr, A. Phanopoulos, A. Buchard and C. K. Williams, *ACS Catal.*, 2021, **11**, 12532-12542.

23. Y. Manjarrez, M. D. C. L. Cheng-Tan and M. E. Fieser, *Inorg. Chem.*, 2022, **61**, 7088-7094.

24. H.-Y. Ji, X.-L. Chen, B. Wang, L. Pan and Y.-S. Li, *Green Chem.*, 2018, **20**, 3963-3973.

25. R. C. Jeske, A. M. DiCiccio and G. W. Coates, *J. Am. Chem. Soc.*, 2007, **129**, 11330-11331.

26. L. Peña Carrodeguas, C. Martín and A. W. Kleij, *Macromolecules*, 2017, **50**, 5337-5345.

27. E. H. Nejad, A. Paoniasari, C. G. W. van Melis, C. E. Koning and R. Duchateau, *Macromolecules*, 2013, **46**, 631-637.

28. W. T. Diment, G. Rosetto, N. Ezaz-Nikpay, R. W. F. Kerr and C. K. Williams, *Green Chem.*, 2023, **25**, 2262-2267.

29. A. Takasu, M. Ito, Y. Inai, T. Hirabayashi and Y. Nishimura, *Polym. J.*, 1999, **31**, 961-969.

30. A. M. DiCiccio, J. M. Longo, G. G. Rodríguez-Calero and G. W. Coates, *J. Am. Chem. Soc.*, 2016, **138**, 7107-7113.

31. M. C. Galanti and A. V. Galanti, *J. Org. Chem.,* 1982, **47**, 1572-1574.

32. M. N. D. Haslewood, T. J. Farmer and M. North, *J. Polym. Sci.*, 2023, **61**, 311-322.

33. R. Baumgartner, Z. Song, Y. Zhang and J. Cheng, *Polym. Chem.*, 2015, **6**, 3586-3590.

34. D. Merckle, O. King and A. C. Weems, *ACS Sustain. Chem. Eng.*, 2023, **11**, 2219-2228.

35. A. Kummari, S. Pappuru and D. Chakraborty, *Polym. Chem.*, 2018, **9**, 4052-4062.

36. G. Si, L. Zhang, B. Han, Z. Duan, B. Li, J. Dong, X. Li and B. Liu, *Polym. Chem.*, 2015, **6**, 6372-6377.

37. L.-y. Wu, D.-d. Fan, X.-q. Lü and R. Lu, *Chin. J. Polym. Sci.*, 2014, **32**, 768-777.

38. J. Liu, Y.-Y. Bao, Y. Liu, W.-M. Ren and X.-B. Lu, *Polym. Chem.*, 2013, **4**, 1439-1444.

Chapter 5 – Conclusion

The aim of this thesis was to investigate the use of Lewis pair catalysts composed of metal halide salts and organobases in the ring-opening copolymerisation (ROCOP) of anhydrides and epoxides. This was intended to address the need for simple catalyst systems to afford polyesters by using low-cost, common, benchtop components in ROCOP catalysis without additional synthesis. This was realised by gaining an understanding of the nature of a model metal halide Lewis pair catalysed copolymerisation and its efficiency for a benchmark ROCOP (Chapter 2). Later, the Lewis pair catalyst system was optimised (Chapter 3) and the catalyst system's versatility was finally explored, affording a range of desirable polyesters (Chapter 4).

The effective copolymerisation of phthalic anhydride (PA) and cyclohexene oxide (CHO) in toluene by a $ZnCl_2$/DMAP Lewis pair alongside an alcohol chain-transfer agent (CTA) was demonstrated in Chapter 2. A monomer conversion of 93% in 5 h was obtained to afford highly alternating (95% ester linkages) P(PA-*co*-CHO). The polyester afforded possessed a narrow dispersity ($Đ_M$ = 1.20) and the employment of a chain transfer agent led to a unimodal molecular weight distribution. However, upon kinetic analysis, the copolymerisation was found to have an accelerating rate instead of the anticipated first order rate indicating controlled behaviour. By studying the effects of copolymerisation components in isolation, further investigation established the Lewis acid's poor solubility and tendency for its chloride ligand to dissociate as responsible for an apparent lack of control. Additionally, the rate of polymerisation was found to be lower than the control where $ZnCl_2$ was absent (97% monomer conversion in 5 h). The solubility of the Lewis acid could be improved through future experiments by employing a THF salt of the metal halide. The latter is known to improve the solubility and give a controlled copolymerisation mediated by a metal halide based

Lewis pair as reported in research conducted by another group published during the course of this thesis' work.[1]

Chapter 3 aimed to improve the polymerisation rate of metal halide-based Lewis pair catalysts to give a higher catalytic activity than the organobase alone in the copolymerisation of PA and CHO through the aid of an alcohol CTA. Running the copolymerisation in neat epoxide rather than toluene helped to improve the solubility of a wider range of metal halides upon heating and a significantly faster polymerisation rate (53% monomer conversion after 15 min when $ZnCl_2$/PPNCl was employed) was lately observed. PPNCl performed the best among the Lewis bases screened with the fastest polymerisation rate detected in toluene and being the only Lewis base able to afford highly alternating polyester in neat epoxide (83% ester linkages). Subsequently, a range of Lewis acids were screened alongside PPNCl for the mediation of the copolymerisation with Lewis pairs $PdCl_2$/PPNCl (72% monomer conversion in 8 min, 94% ester linkages), YCl_3/PPNCl (65% monomer conversion in 8 min, 72% ester linkages) and $MgCl_2$/PPNCl (69% monomer conversion in 8 min, 85% ester linkages) all giving faster polymerisation rates than the control experiment conducted with PPNCl alone (52% monomer conversion in 8 min, 93% ester linkages). In all cases polyester chain lengths were short ($M_n \leq 3924$ g·mol^{-1}) due to the presence of multiple initiators and CTAs. Substituting chloride ligands for bromide and iodide ligands saw no significant difference in polymerisation rate or selectivity at the expense of a significant decrease in polyester chain length achieved (e.g. M_n = 1,859 g·mol^{-1} with $MgBr_2$ *vs.* M_n = 2994 g·mol^{-1} with $MgCl_2$) due to their greater likelihood to dissociate and therefore increase the number of initiators/CTAs available in the copolymerisation. Kinetic analysis showed accelerating polymerisation rates for copolymerisations mediated by

the $PdCl_2$/PPNCl, YCl_3/PPNCl, $MgCl_2$/PPNCl and the PPNCl control in the optimised reaction conditions. This reflected the accelerating rate seen with Chapter 2's model $ZnCl_2$/DMAP copolymerisation in toluene and therefore indicated that the solubility issues remained in neat epoxide with or without the Lewis acid. In future, both the Lewis base and Lewis acid could be pre-dissolved in CHO before PA monomer is added and a higher ratio of $[CHO]_0$ to $[PA]_0$ could be employed to ensure both Lewis pair components have dissolved before the copolymerisation has begun.

Finally, the Lewis pair catalyst which showed the best results from the optimisation, $PdCl_2$/PPNCl (72% monomer conversion in 8 min, 94% ester linkages) was employed to mediate the copolymerisation of a range of anhydrides and epoxides in Chapter 4. The monomers were chosen for the thermal properties they were likely to impart on the polyester and the ability to undergo post-polymerisation functionalisation. Additionally, the majority of monomers used had the potential to be sourced from biomass and thus could afford a biosourced polyester. 12 polyesters were successfully synthesised ($M_n \leq 6029$ g·mol^{-1}, $1.02 \leq Đ_M \leq 1.57$). The functionalised polyesters P(PA-*co*-ECH), P(PA-*co*-AGE) and P(CA-*co*-ECH) were afforded with significantly faster rates (94%, 94% and 91% monomer conversion in 8 min respectively) than P(PA-*co*-CHO) (72% monomer conversion in 8 min). However, the polymerisation rates for other polyesters were significantly slower (10-–39% monomer conversion in 8 min), thus proving that the choice of monomer had a significant impact on polymerisation rate. Where the alternating nature of the polyesters could be determined (P(PA-*co*-CHO), P(PA-*co*-ECH) and (P(PA-*co*-AGE)), it was found to be highly alternating (94-–98% ester linkages). Future work would include running the slower copolymerisations to higher monomer conversions and then analysing the thermal properties of resultant

polyesters from the entire monomer screen to determine how they compared with each other and related to polymer microstructure and catalyst control. Additionally, where appropriate, the polyesters could be functionalised to incorporate desired functionalities through click-chemistry reactions for example or through thiol-ene cross-linking.

In this work, it was discovered that using simple metal halides as commercially available, simple Lewis acids in an anhydride and epoxide ROCOP catalyst shows promise in delivering significant conversion of a range of anhydride and epoxide monomers into a variety of functionalised polyesters in competitive reaction times and conditions. This implies that metal halide-based catalysts demonstrate a potential cheaper and simpler pathway to produce potentially sustainable and biocompatible polyesters. The use of metal halides not only expands the scope of effective simple catalysts for ROCOP expanded but the variety of possible metal halides provide a higher degree of tunability to the Lewis acid component than many other simple catalyst systems in literature. It was learnt that the Lewis base is a more important component for controlling copolymerisation selectivity than the Lewis acid but that the introduction of the simple metal-halide Lewis acid has the potential to enhance the activity of the copolymerisation. It was also learnt that the presence of multiple potential initiators and CTAs in the ROCOP reaction led to a mechanism of copolymerisation that was not fully understood and that the immediate limitation for the system was the lack of controlled copolymerisation. Additionally, only short polymer chain lengths could be afforded from the copolymerisations. Therefore, work on this project could continue by investigating minimising the induction time in the copolymerisation and by carrying out in-depth studies of the copolymerisation mechanism aided by techniques

such as density functional theory (DFT) analysis. With this understanding, a more precise comparison of the metal-halide catalyst system with other simple catalysts could be made, and the copolymerisation conditions could be better used to optimise the production of polyester with higher molecular weight and/or using lower catalytic loadings.

References

1. Z. A. Wood, M. K. Assefa and M. E. Fieser, *Chem. Sci.*, 2022, **13**, 10437-10447.